# UNDERSTANDING THE FATE AND MOBILITY OF ZINC IN CONTAMINATED SHALLOW GROUNDWATER AND VADOSE ZONE WITH CLAY RICH SOILS

**C L Terrell**

Submitted in fulfilment of the academic requirements of

Master of Science
in Hydrology

College of Agriculture, Engineering and Science

University of KwaZulu-Natal

Pietermaritzburg

South Africa

October 2023

# PREFACE

The research contained in this dissertation was completed by the candidate while based in the Discipline of hydrology, College of Agriculture, Engineering and Science, University of KwaZulu-Natal, Pietermaritzburg, South Africa.

The contents of this work have not been submitted in any form to another university and, except where the work of others is acknowledged in the text, the results reported are due to investigations by the candidate.

Signed: Simon Lorentz

Date: 28-October-2023

# DECLARATION - PLAGIARISM

I, Christie Lynn Terrell, declare that:

(i) the research reported in this dissertation, except where otherwise indicated or acknowledged, is my original work;

(ii) this dissertation has not been submitted in full or in part for any degree or examination to any other university;

(iii) this dissertation does not contain other persons' data, pictures, graphs, or other information, unless specifically acknowledged as being sourced from other persons;

(iv) this dissertation does not contain other persons' writing, unless specifically acknowledged as being sourced from other researchers. Where other written sources have been quoted, then:

a) their words have been re-written but the general information attributed to them has been referenced;

b) where their exact words have been used, their writing has been placed inside quotation marks, and referenced;

(v) where I have used material for which publications followed, I have indicated in detail my role in the work;

(vi) this dissertation is primarily a collection of material, prepared by myself, published as journal articles, or presented as a poster and oral presentations at conferences. In some cases, additional material has been included;

(vii) this dissertation does not contain text, graphics or tables copied and pasted from the Internet, unless specifically acknowledged, and the source being detailed in the dissertation and in the References sections.

Signed: Christie L Terrell

Date: 03-November-2023

# CONFIDENTIALITY

The site selected for this project is on public land, however, as detailed in the South African legislation (RSA, 1998), the contamination remains the responsibility of the landowner at the time of the contamination in terms of their duty of care to the environment. I have been granted permission to utilise the existing site data for research purposes, with the understanding that the factory owner and associated parties are to remain anonymous. The information made available for the undertaking of this study includes the time series chemistry data of the groundwater quality, various site reports and site investigation data. I am bound by a confidentiality agreement with the concerned parties to refrain from referring to the specific site (name and location), current landowner or the previous landowners. Therefore, only general references regarding the nature of the site have been made in this document. For document references, the site name has been changed to Site A and no aerial maps have been included.

# ACKNOWLEDGMENTS

I would like to thank the following people for making this project a success:

Firstly, I would like to thank my family for their support, motivation, and patience during my studies. Thank you to my husband Graham for is continuing encouragement. My children, Daniella, and Jemma, for their understanding of my commitment to my studies as well as their interest in my explanations of the wonders of the world of water science.

My sincerest gratitude to my supervisor, Professor Simon Lorentz for his guidance and mentorship throughout this project.

I would also like to thank Mr Andrew Sibiya and Mr Nickson Mncube for their assistance in the field collecting the data for this project, as well as Mr Vivek Naiken and Joss Cahi for their assistance with the laboratory experiments.

My appreciation to my previous mentor, Diane Duthe, for her belief in me when I was starting out in the field of water science and for planting the seed which has grown into my passion today.

I would also like to extend my thanks to Mr Q Goveia for additional support in undertaking this research.

# ABSTRACT

This research thesis has focused on understanding the movement of zinc contamination within the shallow soils of a wetland hillslope, with the intent of gaining a better understanding of the potential future risks posed by the contamination. Soil classification was undertaken to identify the different soil types present within the hillslope: to create an in-depth conceptual site model (CSM) which identifies the main hydraulic flow paths within the shallow subsurface, as well as the potential chemical and physical interactions of the various soil types on the zinc contaminated pore water.

Soil characterisation included permeability testing (in-situ and in the laboratory), texture analysis, bulk density and particle density assessment, porosity, saturation, and residual water content. The samples were also submitted to an external laboratory for XRD analysis to identify mineral content, cation-exchange capacity, percentage organic carbon, major anions, cations, and metal content. Column leaching experiments were set up for five soil types to simulate the transport of zinc contaminated water through the soil profiles under aerobic and anaerobic conditions. Initially a bromide solution was leached through the columns to obtain the dispersion co-efficient of the soils, as bromide represented a conservative ion. This was then followed by leaching a solution of zinc chloride to simulate the contaminant flow conditions as measured on site. The experiment allowed for 2.5 to 3.5 pore volumes of solution to be leached through the column, which took between 22 to 26 days. The leachate breakthrough results were used to calculate zinc retardation for each soil type under aerobic and anaerobic conditions. Various correlations could then be drawn about the mobilisation of the zinc and the adsorption to soils under different environmental conditions.

The CSM was translated into a 2D mathematical model using the commercial software program Hydrus (2D/3D). This simulated the hydraulic flow conditions and contaminant transport within the vadose zone and groundwater along a 460 m length of the hillslope, extending from the historical contaminant source area to the downgradient wetland. The simulation considered historical rainfall records, evaporation data and soil characterisation information obtained from the site specific column data and was subsequently calibrated using historical site data of piezometer water levels and water chemistry. The model was then used to simulate potential future scenarios to determine zinc mobilisation within this

environment. The model demonstrated retardation of the zinc plume within the subsurface soils preventing contaminated seepage into the wetland.

This research highlighted the importance of having a good understanding of the physical and chemical behaviour of the soil-water-contaminant dynamic when assessing contamination migration in subsurface environments. It also emphasized that dynamics between physical and chemical parameters, such as pH, CEC, texture, mineralogy etc need to be considered when assessing zinc retardation. The difference in retardation dynamics emanating from anaerobic and aerobic column experiment also identified the importance of assessing environmental changes or conditions within the site. Further research could focus on the chemical interactions within the soil matrix which are responsible for the reduced mobilisation, such as the formation of zinc complexes vs the precipitation of solids under the changing environmental conditions. This could also progress to assessing the possible release mechanisms for the re-mobilisation of zinc from the soils into the pore water.

# TABLE OF CONTENTS

**Page**

# LIST OF TABLES

**Table** **Page**

# LIST OF FIGURES

**Figure** **Page**

# 1. INTRODUCTION

## 1.1 Rationale for the Research

Environmental contamination has become an ever-increasing concern on a global scale, as anthropogenic activities such as mining and heavy industry become more prevalent, and the demand for resources intensifies (Khan et al., 2008). For more than 50 years there has been a significant increase in the awareness of human impact on the environment, which has led to substantial governing and legislation changes, as well as industry goal setting with a key consideration for minimising environmental impacts and remediating contaminated resources to offset negative impacts (USEPA, 1987) (RSA, 1998).

To manage contaminated environments, many of the generally accepted remediation methods target specific contaminants without fully considering changes that can occur within the environment over the longer term, including site specific influences on contaminant chemistry, and shifts in contaminant mobility under changing environmental conditions (US Army Corps of Engineers, 2012). This has the potential to impact the success of remediation measures, as well as distorting the assessment of the actual risks posed by the contaminant over the long term. This research focuses on the above mentioned issue by assessing the movement of a contaminant, namely zinc, as it moves within a hillslope wetland environment, and assessing physical and environmental aspects which may have an impact on the plume migration within the vadose zone.

## 1.2 Justification

Remediation measures of contaminated land generally focus on the portion of plume that poses significant risks and is economically accessible (Critto et al., 2006). The type of remediation approach is often driven by the contamination concentration, toxicity, or perceived risks, as well as the material in which the contamination occurs i.e., surface and/or groundwater (generally mobile or dissolved phase contaminants), or soils (generally adsorbed or solid phase contaminants, but also mobile phase contamination within the soil pore water) (US Army Corps of Engineers, 2012) (Critto et al., 2006).

To assess the movement of a contaminant, the notable aspects of importance are brought together in a conceptual site model (CSM). The CSM is traditionally developed and refined

during site characterisation as site specific information becomes available and is used to assist decision making processes such as remediation actions and monitoring programs (US Army Corps of Engineers, 2012). Having a scientific foundation describing the mobility and behaviour of a contaminant is likely to improve the CSM and subsequent decision making.

## 1.3 Aims

This research was focused on undertaking a detailed study of a zinc contaminated site. The shallow groundwater and soils leading from a zinc galvanising factory were previously identified as having high acidity (above background levels), and elevated concentrations of metals (primarily zinc) which emanated from the historical facility operations. The historical source area (decommissioned acid dip baths and zinc galvanising) is located within an operating factory area, with hard standing extending around 200 m downgradient. After which, the land follows a gentle gradient for around 160 m along a hillslope which terminates at a valley bottom wetland.

The aim of this research was to ascertain a scientifically based understanding of the mobility of zinc in the vadose zone, by taking into consideration the dynamics of various environmental factors such changes in soil types, soil saturation, and chemical interactions within the hillslope.

## 1.4 Objectives

It is hypothesised that in the study site, the zinc present in the soil pore water will be transported down gradient towards the wetland within the soil pore water. Some of the zinc is expected to be sequestered within the soil matrix as it binds to the soil particles within the clay rich environment, thereby reducing the overall mobility of the zinc. This is anticipated to reduce the overall movement of the contaminant plume thereby reducing potential downgradient impacts. To assess this hypothesis, the following objectives have been outlined:

(a) Identify and characterise the main soils within the hillslope.
(b) Assess the soils retardation capacity in terms of mobility of zinc within the pore water.

(c) Determine the impact of variation in soil saturation from seasonal fluxes by establishing the zinc retardation capacity of the soils under aerobic as well as anaerobic conditions.
(d) Develop a detailed CSM which encompasses both flow attributes and chemical mobility.
(e) Quantify the flux of contaminants in the vadose zone through mathematic model simulations.
(f) Determine if the overall retardation capacity of the soils is sufficient to mitigate significant downstream impact of elevated zinc within the wetland.

## 1.5 Outline of Dissertation Structure

The chapters in this dissertation have been laid out to include the following information:

The introduction to the research topic, including the motivation for the research, aims and objectives have been outlined in Chapter 1 (this chapter).

Chapter 2 focuses on reviewing the existing literature on contaminated site assessments and highlighting the current assessment methods. This chapter comprises research into the movement of water and solutes within the vadose zone, including a review on methods for determining soil hydraulic conductivity and contaminant absorption to soils. It concludes by reviewing the chemistry of zinc and aspects which affect the mobility of zinc in the environment, as well as how the mobility of zinc is determined and options for predictive modelling of soil water physics and chemistry simulations.

Chapter 3 details the materials used for this research and details the methodology that was followed for the investigation, including: field work, laboratory work and assessment of the data in the form of calculations and modelling.

Chapter 4 presents the research results, including specific site parameters that were measured and calculated to characterize the different soils sampled from the hillslope wetland. This includes the quantification of zinc mobilisation retardation occurring within the soils.

Chapter 5 provides an interpretation of the collated data by constructing a conceptual site model, which was analysed using numerical software to simulate the movement of contaminated water within the soils of the research site.

The results are discussed further in Chapter 6, where the overall understanding of the current and likely future impacts of the contamination are presented. The merits of following the undertaken approach are also discussed and potential future work in this field/for this site are identified.

# 2. LITERATURE REVIEW

The impacts of environmental contamination have become a global issue, with the effects of man's impact on the environment becoming an increasing concern. Guidelines, best practices and limits addressing environmental issues are covered in a number of legislative documents in South Africa, including the National Environmental Management Act (RSA, 1998), the National Water Act (RSA, 1998), the Waste Act (RSA, 2009) and the Framework for the Management of Contaminated Land (RSA, 2010). These highlight the importance that the government has placed on managing natural resources and provide frameworks for assessing and remediating contaminated land.

A significant amount of research has been undertaken over the years into understanding contamination in our environment, and the range of factors that should be considered when assessing potentially contaminated sites. This chapter presents some of the research regarding understanding the movement of water and solutes within soils and porous media, while focusing on the physical and chemical interactions of soils and water with respect to zinc. This includes research on factors which may affect zinc mobility in the environment, as well as evaluating the various methods for determining contaminant mobility.

## 2.1 The Vadose Zone and Water Movement

The vadose zone is defined by Holden and Fierer (2005) as "the Earth's terrestrial subsurface that extends from the surface to the regional groundwater table". This includes the surface soils, the unsaturated subsurface materials, and the saturated capillary fringe where water from the regional groundwater table is under negative pore water pressure, as shown in Figure 2.1. Water occurring in porous subsurface material is termed pore-water. Water movement dynamics can be interpreted by using flow equations which have been adapted over time to include many varied factors, but source back to Darcy's Law which was published in 1856. The movement of water within this zone is primarily driven by hydraulic gradient and hydraulic conductivity (Freeze & Cherry, 1979). Hydraulic gradients are induced by gravity, or pressures. In

general, pore-water pressures are lower than atmospheric pressure, due to the tension caused by the capillary attraction of water to particle surfaces surrounding the pore space (Stephens, 2019). Pressure differentials can be caused by positive pressure exerted on pore water by adjacent more saturated zones, or by negative pressures. Hydraulic gradients and hydraulic conductivity are not viewed in isolation, but rather as a dynamic arrangement where one change in the system has a cascading effect on the movement of pore water.

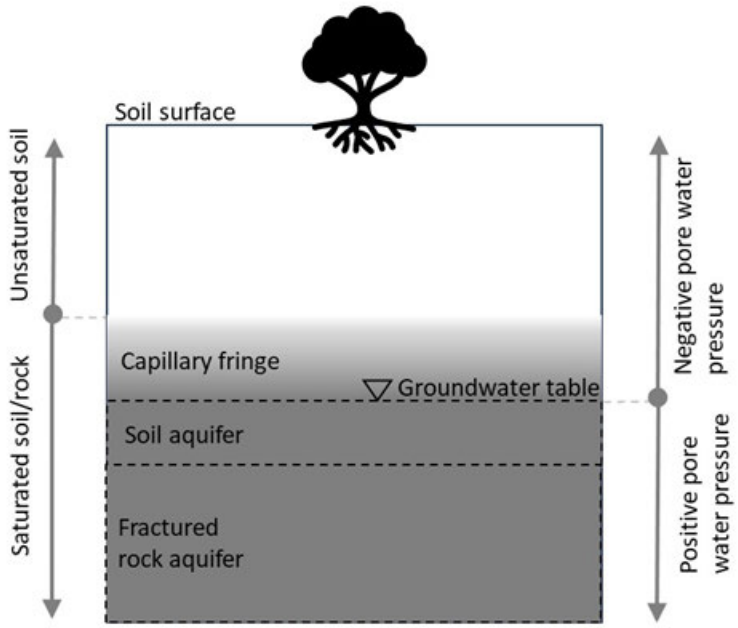


Figure 2.1 Schematic showing the location of water within the subsurface

Hydraulic conductivity refers to the volumetric rate of fluid flow within a material. There are a number of aspects which pertain to hydraulic conductivity, including, but not limited to, the electrostatic forces which hold water within the pore spaces, the air entry pressure at which water is released, the amount of water present, the connectedness of the water within the material pore spaces (pore water), and the compaction of the material which may change the material voids (both shape and size) (Stephens, 2019), (Dos Santos et al., 2013). The way in which water moves within unsaturated soils in response to a hydraulic gradient, can be described using the Richards Equation, a variation by Hillel (1980) is shown in equation 2.1.

$$\frac{\partial \theta}{\partial t} = \frac{\partial}{\partial z}\left[D\ \frac{\partial \theta}{\partial z}\right] - \frac{\partial K}{\partial z} \tag{2.1}$$

Where: z = vertical distance from soil surface,
t = time,
D = hydraulic diffusivity,
$\theta$ = water content, and
$K$ = hydraulic conductivity.

Several aspects can be measured in isolation, such as assessing physical soil properties of density, particle size, water content and porosity. However, hydraulic conductivity can also be directly measured in the field or in a laboratory by evaluating the soil matrix. The vadose zone in an area of land, such as a field or factory site, is not made up of homogenous material but rather of various soil horizons at different depths and spatial arrangements. It is assumed that the hydraulic conductivity of the vadose zone is also not homogenous throughout.

Various methods for measuring hydraulic conductivity have been noted in literature articles, these are summarised as follows: A study by Gallichand et al., (1990) compared the saturated hydraulic conductivity ($K_{sat}$) results from three different methods, including a Guelph permeameter (described by Renolds and Elrick (1984)), the falling head permeameter (Merva, 1987) and the auger hole method (Rogers & Carter, 1987), with the aim of assessing the accuracy of each method. This study concluded that calculations based on the Guelph permeameter method provided intermediate $K_{sat}$ values, which were values between the overestimation from the auger hole method (caused by disturbance of the soil), and underestimation from the falling head permeameter, conducted on an undisturbed sample. A further study by Noshadi et al., (2012) also confirmed the suitability of using the Guelph permeameter method for determining $K_{sat}$, when compared to three other methods including the auger hole method, Porchet and saturated Porchet methods, when the results were compared statistically.

For this study, the research site was noted to potentially have some soils which have a high clay content (see Section 3.2). Clay rich soils have a low $K_{sat}$ value due to the small grain size causing high electrostatic forces on the water particles within the small pore spaces. Typical $K_{sat}$ values for clay rich soils were presented by Garcia-Gutierrez

et al., (2018) and are shown in Table 2.1. These range from <2.78 x $10^{-8}$ to 1.17 x $10^{-3}$ m/s depending on the soil texture. The median values obtained in the abovementioned study, are comparable to those from Wischmeier et al., (1971) who noted that fine textured material (sandy clay, silty clay, and clay >60%).

Table 2.1 Typical $K_{sat}$ (m/s) value ranges for clay rich soils (after Gacia-Gutirrez et al., 2018)

| Sample | Min | Median | Max |
|---|---|---|---|
| Sandy clay | <2.78 x $10^{-8}$ | 1.14 x $10^{-6}$ | 1.68 x $10^{-4}$ |
| Sandy clay loam | <2.78 x $10^{-8}$ | 1.39 x $10^{-6}$ | 1.13 x $10^{-3}$ |
| Clay | <2.78 x $10^{-8}$ | 4.44 x $10^{-7}$ | 1.17 x $10^{-3}$ |
| Clay loam | 2.78 x $10^{-8}$ | 6.11 x $10^{-7}$ | 1.06 x $10^{-4}$ |
| Silty clay loam | <2.78 x $10^{-8}$ | 0.34 x $10^{-7}$ | 4.42 x $10^{-4}$ |

Rather than attempt to define each of these changes within an entire system or even some representative element of volume, it can be preferable to define typical characteristics, specific to the vadose zone profiles being studied, including the connectivity between these profiles. One approach to conceptualising subsurface flows is by conducting a hydropedology study. This is the study to generalise the interaction between the porous media and water, providing insights into the predominant interflow processes within the vadose zone environment. This is achieved by interpreting soil morphology relating to the hydrological behaviour of catchments, hillslope transects and soil horizons (Van Tol & Le Roux, 2019) The hydraulic behaviour of the soils can generally be classified into four main groups, namely recharge, interflow, responsive and stagnating (Van Tol & Le Roux, 2019). This has been described further by Job et al., (2018) as follows: the water movement in recharge soils is generally vertical, which moves water from the surface down the soil profile. With interflow soils, the predominant flow direction is lateral, with water moving along soil horizons and bedding planes. Responsive soils are dominated by upward moving water, which can result in overland surface flow, this is due either to their shallow profile or reaching saturation, such as in wetlands or hillslope seepages. Stagnating soils occur where the rate of water movement within the profile is negligible. By understanding the way in which water moves in the subsurface, we can

also gain better comprehension as to the movement of solutes, and hence contamination, within the subsurface. The hydropedology approach can therefore be used in constructing a conceptual model of the site which infers the dominant flow paths.

## 2.2 Soil Chemistry and Zinc

Coupled with understanding the flow regime of water within the vadose zone, is the recognition that various solutes are also present and being transported within the pore water. The porous media encompasses various minerals, metals and organic elements which can interact with the water and its solutes. The following section presents information on this soil-water chemistry relationship, with particular focus on zinc as this is the primary focus of the study site. It also considers the parameters described in the convection-dispersion equation (equation 2.2) which is used to understand the movement of solutes in unsaturated media.

$$\frac{\partial\, \theta\, R_f\, C}{\partial t} = \frac{\partial}{\partial z}\left[\theta D\, \left(\frac{\partial C}{\partial z}\right) - qC\right] - \phi \qquad (2.2)$$

Where: $\theta$ = water content,

$R_f$ = retardation factor (including absorption),

C = solute concentration,

t = time, z = the vertical co-ordinate positive upwards,

$D$ = dispersion coefficient (accounts for molecular and hydrodynamic diffusion),

$q$ = volumetric fluid flux density,

$\phi$ = sink or source term (accounts for zero and first order reactions).

### *2.2.1 Zinc in our environment*

Occurring naturally in the environment, zinc makes up around 0.0075% of the earth's crust. However anthropogenic activities, particularly mining and processing, have increased zinc concentrations on a local scale. Sphalerite (ZnS) is the usual form of zinc ore mineral, and around 90% of the zinc processed is mined from these deposits (Goodwin, 1989). Zinc has been used since the 18th century as an anti-corrosion

coating on steel and iron, galvanizing a thin layer to the surface of these metals to increase their longevity, as well as being used as an alloy to improve the properties of other metals. As human development grows, the demand for zinc has increased, resulting in a growing industry of mining, smelting, and galvanizing sites throughout the world. With this growing industry comes an increasing risk of environmental contamination from these activities, particularly regarding impacts on our natural resources.

Zinc is an essential micronutrient for all biological life and is involved in the functioning of many living systems, including the catalytic function of enzymes, protein folding, and regulation of ligand binding sites (Vallee & Falchuk, 1993). In comparison to other metals, zinc is considered innocuous to humans, and only high doses of >3 g/kg body weight are seen to have toxic effects on humans (Plum et al., 2010). However, the effects of zinc contamination can influence the environment even at low concentrations. For example, solubilized zinc in aquatic ecosystems can become toxic to fish at concentrations ranging between 0.24 – 13 mg/l (depending on fish species and water hardness), as zinc reacts with oxygen forming zinc compounds which precipitate in the mucus covering the gills (USEPA, 1987). In South Africa, the target water quality range for aquatic ecosystems has been set at 0.002 mg/l (DWAF, 1996). In agriculture, excessive zinc in soils and pore water may inhibit plant growth in terms of foliage health and root development (USEPA, 1987).

### *2.2.2 Zinc mobility*

In its soluble form, zinc occurs as a zinc ion with a positive 2 charge ($Zn^{2+}$), but in soils it can also be present as a colloidal fraction associated with clay particles, humic compounds, and hydroxides, or as an insoluble zinc complex (Lindsay, 1979). These bonds within the soil are described by Broadley et al. (2007), as being determined by soil-specific reactions, including precipitation, complexation, and adsorption, which are primarily controlled by pH. Kalbasi et al., (1978) further detailed these properties to include cation exchange capacity, redox potential, chemical species present in the soil and oxygen availability. By examining the potential bonding mechanisms of zinc occurring within contaminated soils, the mobility of zinc can be better quantified,

which is a key consideration when selecting appropriate remedial options (Wuana & Okeiemen, 2012).

The mobility of zinc in pore water is influenced both by chemical factors as well as physical properties of soils. This can include pH reactions, reduction-oxidation potential as well as complexing ligands, and organic content and the mineralogy of the media.

A study by Rutkowska et al., (2015) investigated the effective magnitude on zinc mobility that these aspects have. The study included assessing soil texture, soil pH, total soil zinc content and content of soil organic matter. The results presented indicate that statistically, soil pH is the strongest contributor to increasing the mobility of zinc, and that this outweighs the contribution of mobility reduction due to the presence of clay. Additionally, a study by Cappuyns and Rudy (2008) who undertook various leaching tests to identify the key factors influencing the mobilisation of metals, concluded that these key factors (such as pH or redox potential etc.) varied significantly, and rather depended on the soil properties itself. It has been noted that surface vegetation also tends to influence the mobilisation of metals within soils. This is due to the organic acids which plants produce around the rhizosphere which may cause chelating of surface trace metals, rendering them more mobile within the pore water (Cui et al., 2017). Rutkowski et al., (2015) reported that the presence of soil organic carbon showed the least degree of impact influencing the mobility of zinc. It is therefore understood that metal mobility is not governed by a set matrix, but rather by a composite of each individual soil or soil types within a study area. This should be assessed independently to obtain a better understanding as to the mobility of the various metals of concern.

### *2.2.3 pH and redox potential*

Zinc is amphoteric and can behave as an acid or a base depending on the pH conditions. The impact of pH on zinc mobility has been described by Deryse et al., (2009) as a near-linear relationship, however, as mentioned above, other factors impacting mobility should also be considered. As soil pH increases, the portion of mobile zinc decreases, due to several participating reactions, including adsorption onto the soils,

complexation reactions, multi nuclear reactions and precipitation of zinc in solid form. The adsorption of mobile zinc onto soil particles is due to the pH dependent negative charge on the soil surface attracting the positively charged zinc ion, forming hydrolysed compounds such as zinc carbonate, or precipitating with compounds such as iron oxides or calcites (Alloway, 2009).

Within a water environment at a pH <7, zinc will tend towards being present as a soluble $Zn^{2+}$ ion, whereas at a pH >7 it will tend to favour a solid ZnO precipitate. Pure elemental Zn would not form as this is out of the stable range of water (Degryse et al., 2009). The pH of the pore water will therefore be a factor in identifying which species of zinc is formed and potential reactions can then be presented.

Redox potential is another important aspect to be considered in assessing the mobility of zinc. Within a water environment, the states of zinc itself are not redox sensitive, as shown in the Pourbaix diagram Figure 2.2. This, however, does not reflect the effects of changing redox conditions on the environment (i.e., plant growth adding to the organic content of the soil) which could impact on bond formation and reactions with the zinc. An oxidizing environment with an Eh >0.8 V is considered as anaerobic soils, whereas an Eh <0.3 V is a reducing environment and considered to be aerobic soils (Pepper et al., 2014). In aerobic conditions, zinc tends to sorb onto hydrous iron oxides, manganese oxides and organic particles, as iron and manganese oxides can trap the zinc ions within their crystal lattice. Conversely, in anaerobic environments, zinc is released into solution through reductive dissolution from iron and manganese hydroxides. According to Bostic et al., (2001) zinc is often associated with sulphides and bicarbonates, in these wetter soil environments. The reactions with zinc will depend on the minerals present and available within the immediate environment.

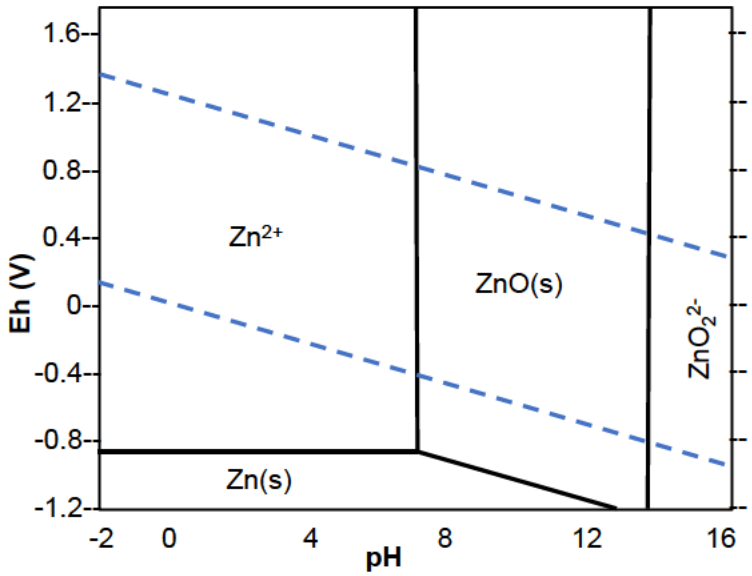


Figure 2.2 Pourbaix diagram showing states of zinc which varied pH and Eh conditions (after Pourbaix *(1974)*)

### *2.2.4 Soil texture*

The texture of soil is described in terms of particle size fractions. The international soil classification system (IUSS, 2002) defines particles which are <2 μm as clay, those between 2 – 50 μm as silt and particles >50 μm as sand. Within the context of this research, the clay soil texture is of interest. As noted previously in the study by Rutkowska et al., (2015) the mobility of zinc can be influenced by the presence of clay within the soil matrix.

A study by Cavallaro and McBride (1984) reports that the microcrystalline and non-crystalline oxides in the clay fraction provide the reactive surface for the sorption of zinc ions, observing this to be the dominant mechanism of reducing zinc mobility in low pH environments. This has been more clearly illustrated by Guinoiseau et al., (2016) who describes the mechanism in which the mobility of zinc decreases as it is adsorbed to the layered crystal structure of hydrated aluminosilicates (clay), as shown in Figure 2.3. This sorption can be quantified by measuring the cation exchange capacity of the soils.

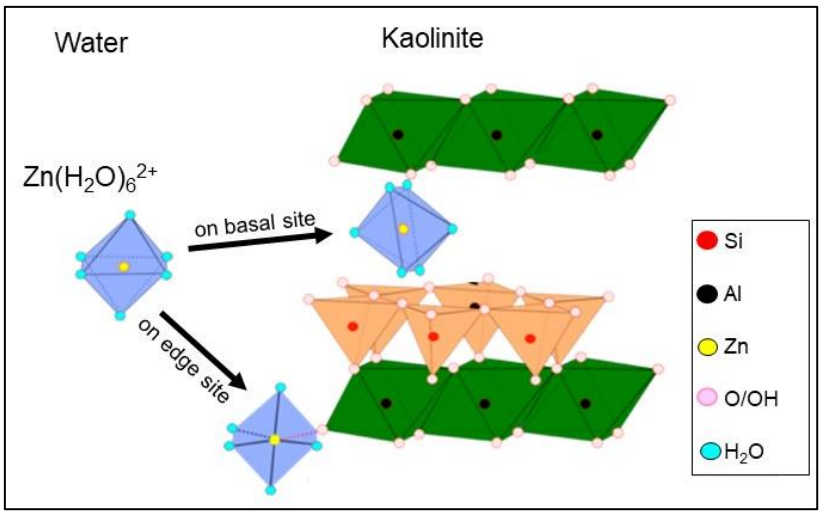


Figure 2.3 Representation of zinc sorption sites on kaolinite (after Guinoiseau et.al., 2016)

Along with the chemical impact of changes in soil texture, the particle size distribution of a soil also has a significant relationship to the hydraulic conductivity ($K_{sat}$) of a soil (Stephens, 2019). Garcia et al., (2018) reviewed methodologies for representing soil texture in relation to $K_{sat}$ values, which highlights the benefits of assessing soil texture on a site.

### *2.2.5 Soil organic content*

The organic matter in soil forms from decomposing material such as plants and organisms. Rieuwerts et al., (1998) summarised the dual impact on zinc mobility by organic matter, as reducing zinc in solution by adsorbing to the organic matter, but also increasing the zinc concentration in solution by forming complexes with the dissolved organic carbon compounds. Other studies have also found that soil organic content did not have as much of a significant effect in determining zinc mobility in soils, when compared to the extent of soil texture and pH (Stephan et al., 2008).

## 2.3 Quantifying Zinc Mobility

Contaminant movement in soils between soluble and non-soluble fractions is measured by the equilibrium partition coefficient (known as $K_d$ values), which broadly quantifies the relationship of concentrations bound to soil particles (immobile mass

per mass of solid (soil)) versus the soluble concentrations (mass in solution per volume of solvent (soil water)) (USEPA, 1999).

The $K_d$ for compounds and metals are not listed within the South African Framework for Contaminated Land (RSA, 2010) as insufficient information is available to define $K_d$ values for the specific soil types nationally. However, several studies have noted varying $K_d$ values for zinc according to site specific conditions based on soil types and local environments, including increasing $K_d$ with increasing vegetation growth (Cui et al., 2017), lower $K_d$ from fallout in neutral soil environments (Dos Santos et al., 2013), lower $K_d$ in soils with a high humic contents (Svendsen et al., 2011). Reported values range from 0.1 L/kg at the lower end, to greater than 4 orders of magnitude larger (Baes & Sharp, 1983) (Bunzel et al., 1999). This highlights the importance of understanding the specific conditions at individual sites. $K_d$ is commonly assessed by following two main methodologies for leaching of soils, namely batch tests and column tests, although these tests are noted to yield varying results (Tanchuling et al., 2003).

Batch tests require a specified amount of soil to be mixed with a leaching solution for a time, till equilibrium is assumed to be reached. This is a quick simple test, requiring minimal equipment and can be done in a few hours. However, studies by Naka et al., (2016) and Tanchuling et al., (2003) found that batch tests tended to generate an overestimation of the sorption capacity due to the greater reaction surface area available in the dispersed soil particles, while column tests more closely resemble field conditions. These conclusions were reiterated by Antoniadis and McKinley (2003) who also concluded that the retardation factor derived from testing had a direct relationship to the interaction time of leachate with the soil, particularly with regards to metals in clay rich, low permeable soils. Burglsser et al., (1993) also noted that during agitation of the soil during testing, particles tended to break into finer fragments, thereby also impacting the absorption results.

In comparison, column tests require more equipment and a longer time duration. A column test requires a specified amount of soil to be placed in a column and a leaching solution percolated through the medium, continually supplying new leachate solution.

This is usually done over an extended period of several days or weeks. A study by Cappuyns and Rudy (2008) reported that the column test method was representative of natural conditions, due to control of the flow rate of leachate to simulate equilibrium conditions. A report issued by the EPA (USEPA, 1999) on understanding $K_d$ factors, also supported the conclusion that flow through column experiments are more accurate in simulating field conditions than batch experiments.

By varying the test conditions such as pH or degree of saturation, different environmental circumstances can be simulated to assess the impact of the environmental changes on the capacity of the soil to reduce the mobility of the zinc. An absorption isotherm can then be calculated for a particular solution by graphing the concentration of solute in the leachate at set time periods or input concentrations. Many zinc retention isotherms have been produced as the result of laboratory investigations, a typical one is shown in illustrating Figure 2.4, the variation in adsorbed zinc for clay textured soil types ( (Casagranade et al., 2008).

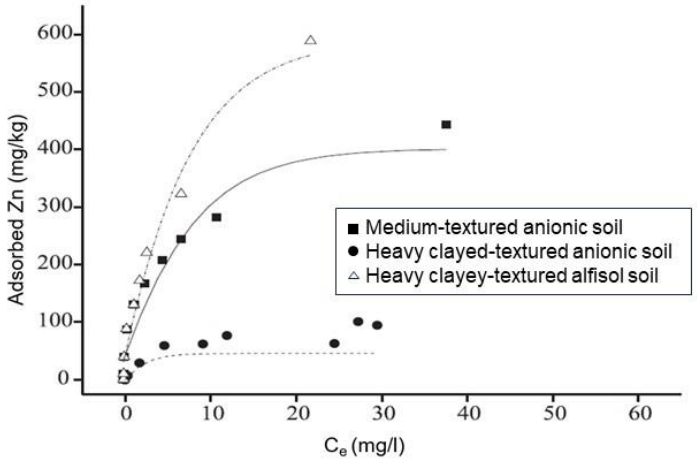


Figure 2.4 Typical zinc adsorption isotherm in different soil types (after Casagrande et al., 2008)

MacDonald et al., (2004) compared the results of different laboratory methods together with site data, to determine a method for estimating the mobile phase of soil solutions, which is consistent and accurate to the results obtained in the field. In their assessment, $K_d$ from literature based on laboratory abstractions was overestimated by

an order of magnitude. This study further highlighted the variation in $K_d$ values obtained for zinc from three methods undertaken on soils, namely field lysimeters, column test leachate and calculation from regression, this data is shown in Table 2.2. The $K_d$ calculated using regression equations was argued to be orders of magnitude over estimation of potential mobile zinc. Their results from column leachate aligned with the values measured in the field lysimeters, which increases the confidence in data when using column leach tests to obtain site specific parameters to assess the retention and mobility of zinc.

Table 2.2 Range of $K_d$ values calculated using different analytical methods (after MacDonald et al., 2004)

| Sample | Calculated log $K_d$ values for zinc | | |
|---|---|---|---|
| | Lysimeters | Column leachate | Regression equation |
| Soil 1 | 3.34 | 3.46 | 1.89 |
| Soil 2 | 3.64 | 3.49 | 1.38 |
| Soil 3 | 2.86 | 3.19 | 2.17 |
| Soil 4 | 2.83 | 3.28 | 1.74 |
| Soil 5 | 3.36 | 3.48 | 1.88 |
| Soil 6 | 2.93 | 3.53 | 1.79 |

Together with understanding the soil adsorption of a metal, one should also review the various solutes within the pore water as multiple reactions are possible within a system resulting in soluble ion and metal complexes which affect reaction kinetics. When assessing metal concentrations adsorbed directly to the soils, the standard method is via EDTA extraction, however, this often results in inaccurate results due to effects of dilution of metal-complexing ligands such as dissolved organic matter, which results in an underestimation of metal concentration within the actual soils. It is therefore assumed to be more accurate to measure metal concentrations within the soil pore water (Degryse et al., 2009).

## 2.4 Chemical and Flow Modelling

Modelling of a site or scenarios entails creating an image, document, or utilising software to mimic the measured or expected environmental conditions. A Conceptual

Site Model (CSM) provides a description of a site, based on existing knowledge or knowledge that is easily obtained. This usually includes a description of the source, potential exposure pathways and key features within the area of study (US Army Corps of Engineers, 2012). It is also used as a tool in assisting visualisation and identifying potential knowledge gaps that can then be filled by more in-depth work such as solute transport modelling and can be refined as more information becomes available. A CSM can also be used as the base data when undertaking more complex analytical or numerical flow modelling scenarios, which is usually undertaken to either confirm assumptions that have been made, or as an assessment tool for predictive scenarios. When modelling the mobility of a solute, empirical parameters such as adsorption isotherms are used to determine the sorption and desorption of the solute (Cherry et al., 1984).

Several studies have used modelling to assess the potential future impacts of zinc contamination within the subsurface environment. These highlight considerations that should be assessed when undertaking flow and chemical modelling of subsurface environments. Kent et al., (2000) modelled the influence of pH on the transport of zinc through a semiempirical surface complexation model, instead of utilising distribution coefficients or adsorption isotherms. However, the study noted that the complexity of the model will increase substantially when multi-component solutes are to be considered. A study by Molina et al., (2010) found that metals in multi-component solutions compete simultaneously for the sorption sites on the soil particles, with the soil having a much higher affinity to adsorb to other metals rather than zinc. The study cited the order of soil sorption preference in equilibrating solutions as follows: lead > copper > zinc > cadmium > nickel. Therefore, when modelling the transport of zinc, the impact of possible competing metals for sorption may need to be considered. Cernik et al., (1995) also was able to model a zinc plume emanating from a foundry by utilising input parameters from laboratory experiments. He found that modelling higher concentration within a source area to be more effective, whereas lower concentration areas were more difficult to model as the factors influencing contaminant transport become more pronounced (i.e., preferential flow paths, biological activity).

### *2.4.1 Modelling software*

Several software packages are available for modelling flows within the vadose zone, including HYDRUS (Simunek et al., 2008), MODFLOW-SURFACT (Panday & Huyakorn, 2008), STOMP (White et al., 2008), SWAMP (van Dam et al., 2008), and TOUGH2 (Finsterle et al., 2008) a number of these have been detailed by Simunek and Bradford (2008) to outline their capabilities. This included a review of the analytical models for solute transport, the multi-dimensional saturated flow and transport models as well as various databases and tools. One of the most frequently used software packages is HYDRUS (including HYDRUS-1D, HYDRUS-2D and HYDRUS-2D/3D. HYDRUS software was developed by using the Richards flow equation to solve for variably saturated water flow conditions. The software also used a convection-dispersion equation to solve for the solute transport aspect (Simunek et al., 2013).

Chemical equilibrium modelling software such as PHREEQC accounts for solutes which are multi-component. This is an ion-association aqueous model which accounts for many of the chemical reaction pathways (Parkhurst & Appello, 2013). The modelling of soil-water physics within the vadose zone includes both the saturated and unsaturated porous media flow, accounting for how the water is held (water retention), as well as how it moves within the soil matrix (hydraulic conductivity).

A recent software development is the coupling of HYDRUS with PHREEQC which has been named HP2, to simulate transient water flow and transport of multiple components (Jacques et al., 2003). Successful models for zinc transport have been simulated using HP2, such as the simulation presented by Dos Santos et al., (2013) who used this coupled software to predict the long term movement of zinc and lead in soil and Mallmann et al. (2012), where the vertical movement of zinc in soil was simulated. Both studies used a two-site sorption model for the best calibration simulation.

The use of HP2 for modelling was compared to similar established geochemical modelling software by Jacques et al., (2003), where outputs from HP2, CRUNCH-GIMRT and CRUNCH-SNIA (Steefel & Yabusaki, 1996) where compared, and near identical results were reported from all three methods, as shown in Figure 2.5. This

confirms the confidence value with using HYDRUS as a vadose zone modelling software.

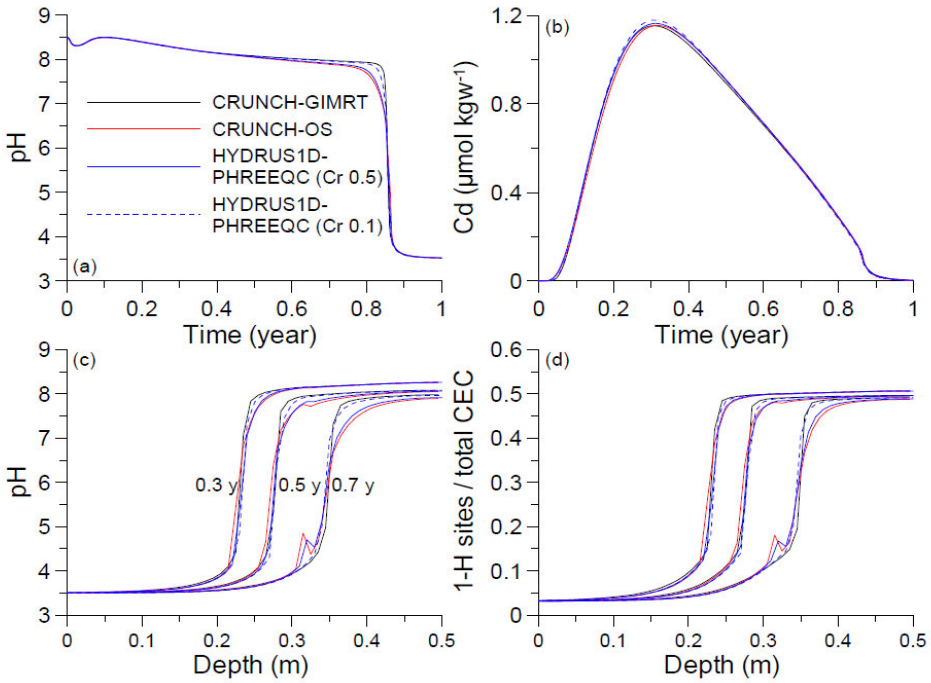


Figure 2.5 Comparison of outflow curves and distributions of infiltration of high pH solution in clay soils, as solved using different analytical software (after Steffell and Yabusaki *(1996)*)

## 2.5 Literature Review Summary

Extensive research has been undertaken into understanding the migration of contamination within groundwater and soils, with this study focusing on zinc as the main chemical of concern. Various methods and aspects of testing soils have been reviewed, including hydraulic conductivity, soil classifications, chemical reactions, and physical attributes, which have the potential to impact the migration of zinc within the shallow surface soils.

The hydraulic conductivity of a soil and residence time that soil water is contact with the soil matrix is linked to physical characteristics such as particle density and particle size distribution of the matrix. Chemical attributes such as CEC, redox

potential, and bonding mechanisms are also integral in assessing zinc movement. These attributes are better understood by analysing pH (with zinc ionisation occurring in acidic or highly basic solutions), soil mineralogy (availability of possible zinc bonding sites on soil matrix or presence of preferred order bonding elements (a study noted soil sorption preference of Pb > Cu > Zn > Cd > Ni in equilibrating solutions), and soil organic content (decaying material producing humic acids and acidic conditions or the possibility of complex ligands bonding with zinc). In conclusion, the research indicates that zinc mobility in the vadose zone is not predetermined by any single aspect or defined matrixes (as listed above), but rather by the dynamic composite of these factors for each of the soils encountered on a site.

Various software packages allow for predictive modelling, to assess the potential future impact of a contaminant plume within the vadose zone. Numerous peer reviewed articles used HYDRUS to simulated vadose zone conditions, which has been demonstrated to be a robust and multifaceted package the capability of simulating water and solute transport through materials of varying properties within a single model.

# 3. MATERIALS AND METHODS

An initial collation of existing information was used to identify potential knowledge gaps regarding understanding the migration of zinc contamination within the shallow subsurface environment. These gaps were then examined within the scope of this research. This chapter details the methods and material used for this research, including a summary of existing information on the site, site work undertaken, and methods and procedures followed in subsequent laboratory analysis and modelling.

## 3.1 The Study Site and Existing Hydrogeological Information

The site considered for this study is located downgradient from a zinc galvanising factory which has been in operation since the 1960's. The old facility infrastructure included HCl tanks and large acid dip baths, which were decommissioned in 1992. Location data has been excluded from this report (see page iv) and therefore a site map has not been provided. For this dissertation, the area is referred to as Site A. Analysis of the downgradient groundwater and shallow soils indicated acidic conditions with elevated metal concentrations, mainly zinc, which has been attributed to historical impacts from standard factory operations, no significant spillage incidents were noted. Subsurface water movement follows the hydraulic gradient and flows down-slope, feeding into a nearby wetland. Various studies have previously been undertaken on the site to characterize and monitor the extent of the zinc plume. The previous studies have focused on the concentration of zinc within the groundwater, as this is the primary medium for the contamination movement from the source area to off-site receptors. However, the mechanisms of zinc movement within the hillslope wetland which affect its mobility, has not been fully considered.

The water quality records available for the site over the last 10+ years have monitored the extent of the zinc plume within the shallow groundwater (<10 meters below ground level (mbgl)), which extends from the source area (zinc galvanising baths which have been decommissioned and removed from the site), and into the hillslope wetland located some 300 m downslope. Within the wetland itself, the area impacted by the plume remains localised (extending <100 m downstream) and seasonal monitoring of the water quality, through shallow piezometers located at 100 m intervals along the wetland, has confirmed that the impact has remained localised.

A hydropedology study undertaken on the site (DSA, 2015) identified the main water flow regime within the subsurface towards the wetland: this also showed a significant component of flow within the soils above the fractured rock interface (Figure 3.1). Hillslope seeps are observed on the site as the soil pore water accumulates behind clay rich horizons which have lower permeability, creating a restriction point for water moving within the matrix and driving it to surface. DSA reported saturated hydraulic conductivity values (Ksat), soil density and maximum absorption capacity for zinc ($q_m$) as derived from Langmuir isotherms from batch test results, these are summarised in Table 3.1.

Table 3.1 Soil characteristics ($K_{sat}$, density and Zn absorption capacity) for Site A as reported by DSA (2015)

| Sample | $K_{sat}$ m/d | Density $g/m^3$ | $q_m$ mg Zn/kg |
|---|---|---|---|
| Soft plinthic | $6.50 \times 10^{-1}$ | $1.45 \times 10^{-6.}$ | 625.0 |
| G-horizon | $1.20 \times 10^{-2}$ | $1.35 \times 10^{-6.}$ | 1666.7 |
| Orthic A | 1.92 | $1.38 \times 10^{-6.}$ | 666.7 |
| Hard plinthic | $6.86 \times 10^{-1}$ | - | 434.0 |

Note: $q_m$ denotes the maximum absorption capacity for zinc, as derived from Langmuir isotherms, with datapoints obtained from batch tests.

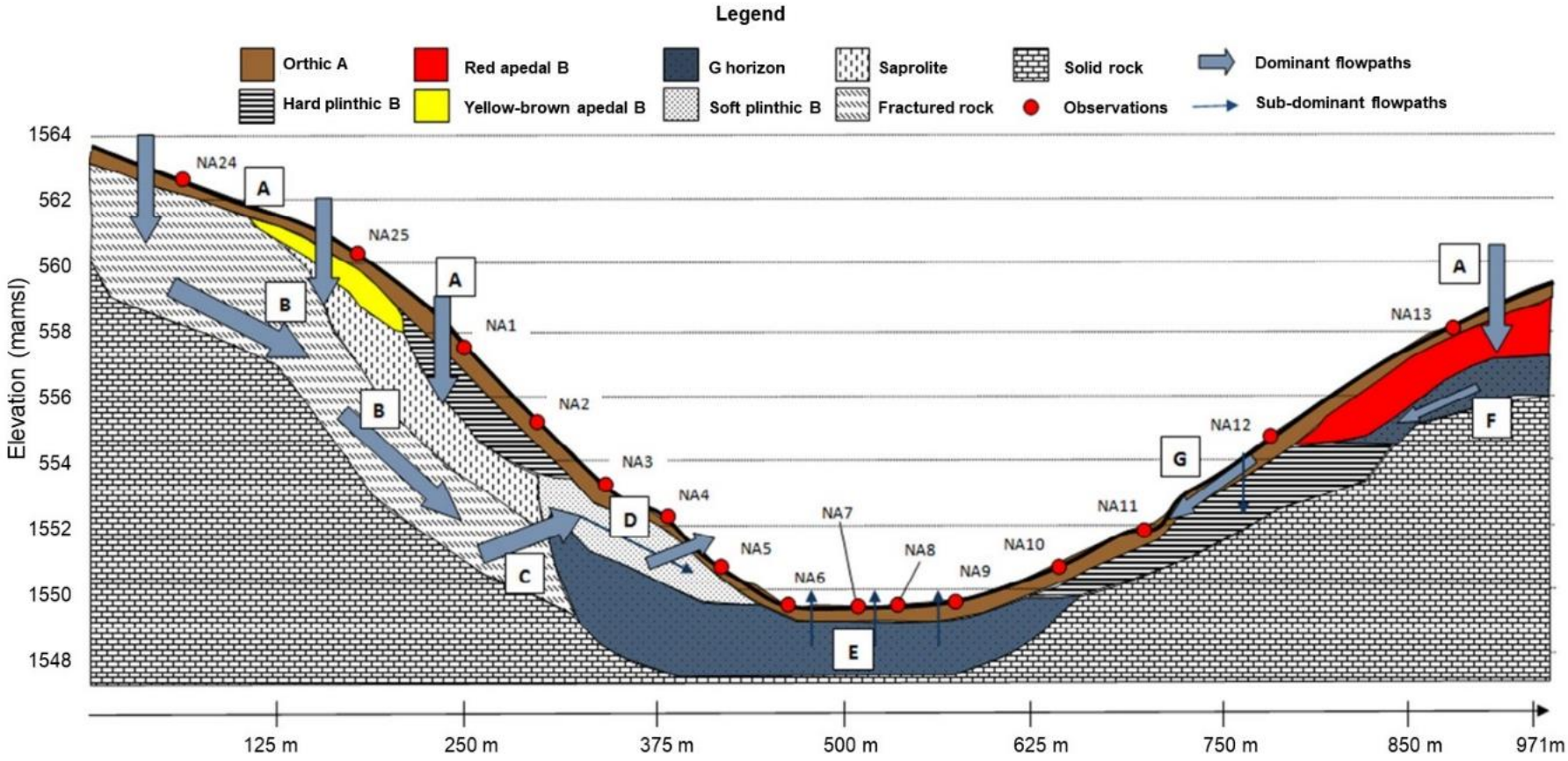


Figure 3.1 Schematic showing soil distribution pattern and conceptual hydrogeological flow paths at Site A (from DSA, 2015)

A report on the site groundwater monitoring (SRK, 2018) confirmed the groundwater level to be shallow (between 0.5-3 mbgl), with seasonal fluctuations of up to 0.8 m. By comparing chemistry data over a 10-year period, the groundwater plume was noted to spread from the source area into the adjacent hillslope wetland (SRK, 2018).

The source of the water within the wetland was determined to be mostly from recently recharged sources (rainwater), thus confirming the importance of understanding the contributing flows from the vadose zone. This was done through assessment of the concentration of stable isotopes deuterium ($^{2}H$) and oxygen-18 ($^{18}O$) in the various potential wetland contributors of water, namely deep groundwater (>30 mbgl), shallow groundwater (2-6 mbgl), rainwater, water from seepage within the vadose zone and upstream water sources (SRK, 2016).

The hillslope and wetland soils consist of deposited materials, with fine grain soils such as silt and clay, as well as a high quantity of soil organic matter from decaying wetland plants. Based on the literature (see Section 2.3.5), metal contaminants such as zinc have been shown in previous studies to adsorb onto soil surfaces, with a particular affinity for soils which are rich in organic matter and clays (Antoniadis & McKinley, 2003), (Guinoiseau et al., 2016) (Jalali & Hemati, 2013).

Following this review of the site reports and data, this research project aimed at refining the CSM within the hillslope wetland by conducting additional soil assessments to better understand the movements of zinc and expanding this into a detailed numerical model with a focus on the vadose zone contributions into the wetland.

## 3.2 Sample Collection

The location of sampling positions was selected based on the slope direction in which water within the vadose zone would flow from source of contamination towards the wetland with gravity. It also followed a similar transect to that of the existing hydropedological study, with this data guiding the locations for sampling the dominant soil types which were previously identified within the hillslope and wetland area, namely recharge soils, interflow soils and responsive soils. The sample positions were located along a transect from the upper slopes to the midpoint of the saturated soil at the base. The samples are named UHS (upper

hillslope), MHS (mid hillslope) WET1 (saturated valley bottom) and WET-UP (saturated soils, upgradient of site). A schematic of the site and sample locations is shown in Figure 3.2.

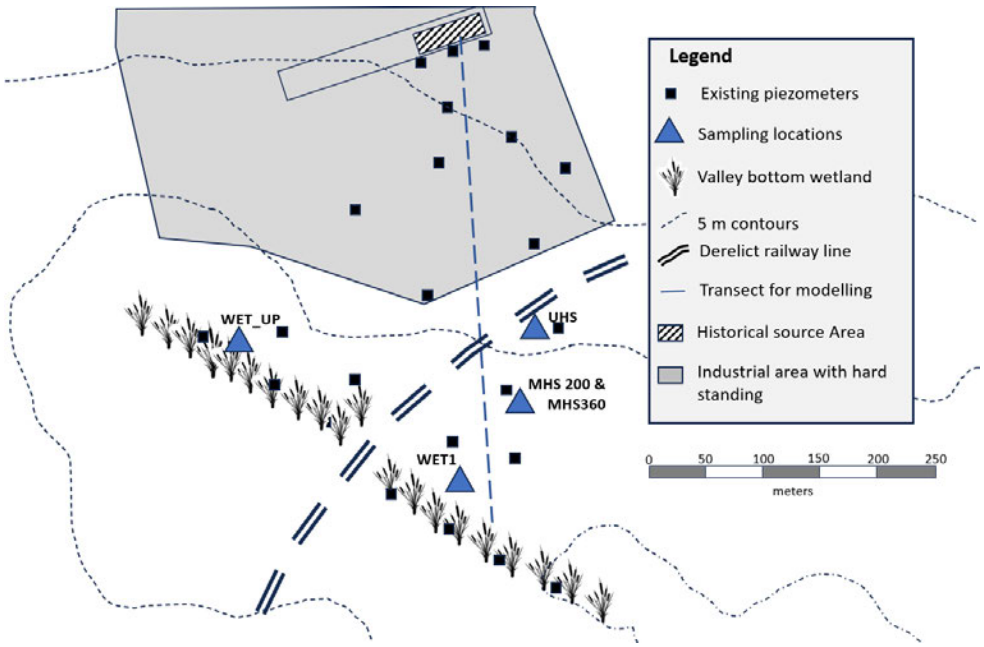


Figure 3.2 Schematic showing relative location of sampling positions, existing monitoring points and infrastructure

The soil sample collection was undertaken, together with the aid of Mr Nickson Mnube, on the 25th of November 2019. On completion of sampling at each point, the hole was backfilled with the residual material. The samples were packaged and transported to the laboratory at the University of KZN (Pietermaritzburg campus) for further analysis as described in Section 3.4 and 3.5. Site photos and sampling locations were recorded using a smartphone (Samsung A6+ equipped with a 16 megapixel camera and using Google Maps V5.29 for recording of sample locations).

### *3.2.1 Soil sampling and logging*

The sites for soil sampling were cleared of surface vegetation using a spade, followed by vertical excavation using a hand auger (Johnsons Soil Auger, equipped with 75mm open auger bucket) until refusal depth or repeated collapsing of the hole. The vertical soil profile was logged at each sample point, guided by the methodology described in the guidelines for soil and rock logging (Brink & Bruin, 2001). This includes a description of the soil in terms of moisture, colour, consistency, structure, soil texture and origins.

The main observations included the distinction in soils between the topsoil and lower layers, noting changes in relative water content and texture that would indicate a notable change in hydraulic characteristics. Representative soil samples of the profile were collected in the following manner.

- Disturbed soil samples were collected from the excavated material with a spade, and placed in sealed plastic bags which were kept cool in a portable cooler-box. Approximately 2.5 kg of material was collected for each sample.
- A bulk quantity disturbed sample was collected in a 25 l plastic container with sealing lid.
- Undisturbed soil samples were collected using a uPVC tube segment (70 mm internal diameter, approximately 100 mm in length). The tube was pushed into the soil and excavated out using a spade, the ends of the sample were smoothed level and the sample wrapped with plastic wrap and packing tape for stability during transport.

## 3.3 Observations and Soil Characterisation

The soils for the site were characterised using data collected on site, and through laboratory analysis of the samples collected. On site, observations were made on the vertical soil profile and the in-situ saturated hydraulic conductivity was assessed. In the laboratory, soil samples were assessed/analysed for bulk density, moisture content, soil texture, porosity, specific gravity, and water retention characteristics. Samples were also submitted to an external laboratory for analysis of pH, electrical conductivity, selected anions, cations, and metals as well as organic content and mineralogy. Details have been provided below.

### *3.3.1 Density and porosity*

The dry bulk density ($\rho_b$) of the samples was assessed by measuring the dimensions of the bulk density uPVC sample pipe segment (described in Section 3.3) to obtain the sample volume (V). The undisturbed soil sample was then removed from the pipe segment and dried in an oven for 24 hours at 105°C. The dry sample was weighed using a laboratory scale (Adam, Model LAB 254e, this scale was used throughout the laboratory experiments) to obtain the mass ($m$), which was used to calculate the dry bulk density ($\rho_b$) of the sample using equation 3.1.

$$\rho_b = \frac{m}{V} \tag{3.1}$$

The particle density ($\rho_s$) of the samples was calculated by adding a measured mass of soil to a volumetric flask of distilled water of known density (mass and volume at specific temperature). The flask was re-weighed to calculate the $\rho_s$ using equation 3.2. Unlike bulk density, this considers the solid material (soil) only and excludes pore spaces in the sample volume.

$$\rho_s = \left(\frac{m_s}{m_{fw} - m_{fsw} + m_s}\right)\rho_{wt} \tag{3.2}$$

Where $m_s$ is the mass of the sample (soil); $m_{fw}$ is the mass of the flask and distilled water; $m_{fsw}$ is the mass of the flask, sample, and water; $m_s$ is the mass of the sample; and $\rho_{wt}$ is the density of water at the temperature measured at the time of the experiment. This experiment was repeated twice to provide a median value.

Bulk density and particle density were then used to calculate the porosity (φ) of the sample by using equation 3.3, where $\rho_s$ is the particle density, and $\rho_b$ is the bulk density.

$$\varphi = \left(1 - \left(\frac{\rho_b}{\rho_s}\right)\right) \times 100 \tag{3.3}$$

### *3.3.2 Hydraulic conductivity*

The hydraulic conductivity (*K*) of the soils on the site was measured both in-situ and in the laboratory. On the site, saturated hydraulic conductivity ($K_{sat}$) was measured using a Guelf Permeameter, following the principles of design described by Reynolds and Elrick (1985). This method considers the combined horizontal and vertical $K_{sat}$. Hydraulic conductivity measurements were taken in each of the auger holes where soil samples were obtained. The Guelf Permeameter field setup is shown in Figure *3.3* (photo a).

In the laboratory, $K_{sat}$ was measured using the constant head method described by Reynolds (1993) where a tube segment of known dimension was filled with the sample material and repacked to the required density. The ends of the tube segment were packed with washed silica sand and separated from the soil sample by filter paper. Water was gravity fed through the sample from a height of 1930 mm. The experiment setup is shown in Figure *3.3* (photo b). The rate at which the water collected after passing through the

sample was then calculated based on the volume of sample collected per time unit. Four separate readings were obtained for this experiment, to provide four datapoints per sample. The median value of the data points was then used for further calculations.

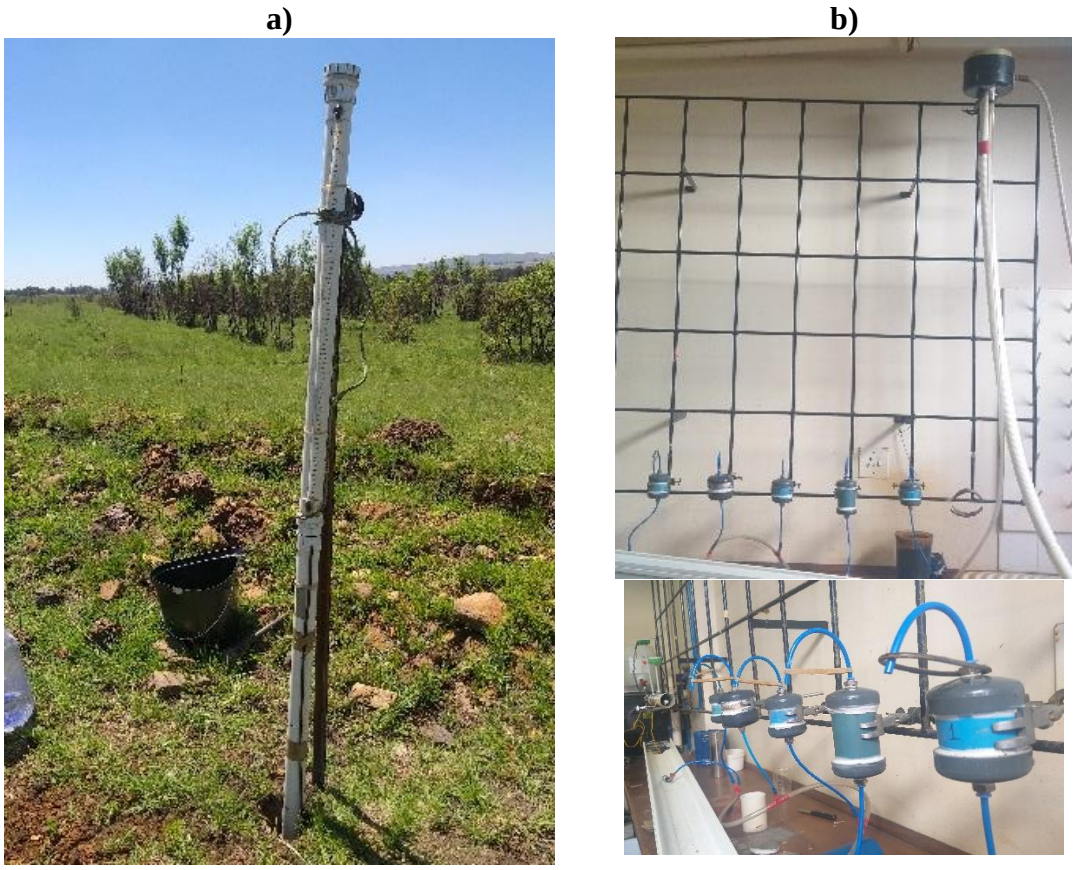


Figure 3.3 Equipment and setup used for measuring hydraulic conductivity: a) in situ measurements using a Guelf Permeameter, and b) constant head method as set up in the laboratory

### *3.3.3 Water retention*

The water between the soil pore spaces in saturated conditions ($\theta_s$) and the residual water content ($\theta_r$) was determined by using an outflow cell method described by Han et al., (2008). Each sample was packed into metal sample rings at a density to mimic the undisturbed sample, with porous ceramic disks on each end. These were saturated for 24 hours in a water bath by increasing the water level in the tank from the bottom, thereby minimising trapped air pockets (Figure 3.4, photo a). The samples were transferred to the outflow cell cylinder with the top end fitted to a pressure controlled airline, and the bottom to a burette (Figure

3.3, photo b). The system was pressurised at the following steps: 18.75 cmHg, 37.5 cmHg, 75.0 cmHg, 187.5 cmHg, 375 cmHg and 735.75 cmHg. The water displaced during pressurisation of the sample was pushed into the burette and measured (Figure 3.4 photo b).

The data was graphed to show the water retention curves for each sample. The $\theta_s$ (saturated water content) was calculated based on the gravimetric water content and bulk density of the saturated sample and $K_{sat}$ calculated from field measurements. The residual water content ($\theta_r$) was calculated using the software RETC (van Genuchten et al., 1991) using the van Genuchten-Burdine model to solve for the unknown coefficients, with the solution solving optimised using the nonlinear least-square parameter method.

**a)** **b)**

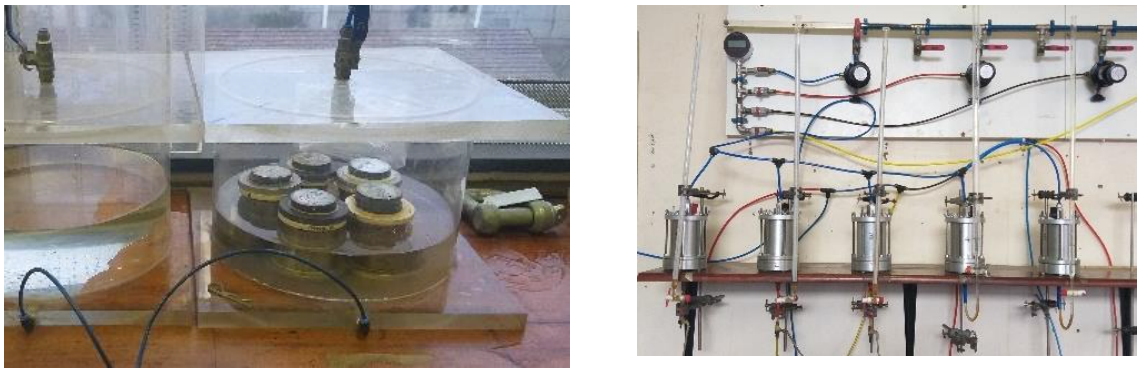

Figure 3.4 Laboratory equipment used for water retention experiment: a) saturation of samples and b) pressure cells

### *3.3.4 Soil texture*

The soils texture was assessed using the standard test method for particle-size distribution of fine grained soils using sedimentation analysis (ASTM, 2000) which utilises a hydrometer to measure density changes in solution with time as the soil sediments settle. Dispersion of the soil used 4% sodium hexametaphosphate, buffered in 1% sodium carbonate (Calgon solution) (Tan, 2005). This was used to identify the clay (0.002 mm) and silt (0.05 mm) fractions, and sieve separation was used for the larger sand (2.0 mm) and gravel (>2.0 mm) fractions.

Following the sedimentation assessment, the samples were separated into further fractions using standard brass sieves (sizes: 2 mm, 0.85 mm, 0.3 mm, 0.18 mm, 0.09 mm, and 0.053 mm). The mass passed through the sieves was then weighed to ascertain the percentage of material within each texture range. The soils were classified according to the USDA texture classification system (USDA, 1987) (Garcia-Gaines & Frankenstein, 2015), using the specific gravity (SG) calculated per soil type. Photographs of both soil texture assessment experiments are shown in Figure 3.5.

**a)** **b)**


Figure 3.5 Laboratory setup and equipment for soil texture analysis: a) Samples prepared for analysis with hydrometer and b) sieved fractions of soil samples

## 3.4 Soil Chemistry

The soil chemistry was determined for each of the samples, this included identifying the mineral content of the soils through XRD analysis, as well as various chemical properties such as organic content and cation exchange capacity. Laboratory simulations were also run using column tests to assess the zinc absorption capacity (section 3.5).

### *3.4.1 Mineralogy*

The mineral content of the soils was determined using X-ray diffraction (XRD). This was undertaken by an external laboratory, XRD Analytica and Consulting in Pretoria.

Dried samples were sieved to obtain the -75 micron fraction and the samples analysed using a Malvern Panalytical Aeris diffractometer with PIXcel detector and fixed slits with

Fe filtered Co-Ka radiation. The software used by the laboratory for the phase identification was X'Pert Highscore plus, followed by relative phase amount estimation using the Rietveld method.

### *3.4.2 Chemical properties*

The soil samples were analysed by Vans Laboratory in Bloemfontein for the following:

- Cation Exchange Capacity (CEC): 5 step extractable CEC (based on Page (1983)).
- % Organic Carbon (TOC) using the Walkley Black Method (The Non-affiliated Soil Analysis Work Committee, 1990). Organic matter % content calculated from organic carbon assessment.
- pH (KCl): using the method described by The Non-Affiliated Soils Analysis Work Committee (1990).

Samples were also submitted to Talbot and Talbot laboratory in Pietermaritzburg for analysis as per the methodology detailed[1] ( (Naiker, 2023)

- EC: EC probe with error not exceeding 1% or 0.1 mS/m, whichever is the greater, graduated in millisiemens per metre (mS/m) and calibrated using a standard reference solution.
- pH: pH instrument with a sensitive glass electrode to measure the potential exchange of hydrogen ions.
- Sulphate, chloride and total alkalinity[1]: Colorimetric assay.
- Sodium, calcium, magnesium, dissolved metals (aluminium, copper, iron, manganese, lead, zinc): ICP Analysis - The sample was filtered through a 0.45 µm syringe filter and acidified with 2 drops of Nitric Acid. A nebulizer and spray chamber generated the sample into an aerosol and injected into and ICP machine for analysis. The plasma elevated temperature (6 000 to 8 000°K) excites the atoms, with ionization producing an ionic emission spectrum.
- Metals in soils: ICP-OES Analysis - Samples are homogenised using cone and quartering method and sieve using 2 000 µm sieve. 0.5 g of the sample (dry weight) is digested to 50 ml volume using acids and a Microwave digester. The sample was filtered and analysed using an ICP-OES machine as described above.

[1] The laboratory provided a broad description of the methodology followed, was unable to provide additional details on the instrumentation utilised for analysis.

- Bromide in water: Colorimetric assay using phenol red, as described in the Standard Methods for the examination of water and wastewater (Rice et al., 2012).

## 3.5 Zinc Absorption

Zinc absorption to the porous media was assessed by analysing the breakthrough curve data obtained from column leaching experiments, which were undertaken between 17 January – 16 March 2020 at the University of Kwa-Zulu Natal soils laboratory in Pietermaritzburg. A total of ten columns were set up in pairs, to simulate both aerobic and anaerobic leaching conditions for all five soils, as detailed by USEPA (1999). The twin columns, demonstrating aerobic vs anaerobic conditions were set up to compare the impact of seasonal water table fluxes on the migration of zinc.

The columns were constructed using a length of 40 cm PVC piping, with an internal diameter of 13.6 cm. The soil samples were dried for 24 hours in a laboratory oven at 105°C. The mass of soil required for each column was calculated based on the volume of the column and the density of the soil to mimic natural conditions. The soils were then mixed with a solution of 2000 mg/l potassium bromide (KBr) to a saturation of 50% before packing into the columns. This was to assess the dispersity of the soils as described later in this section. The details of soil volumes and rate of solution addition has been tabulated in Appendix A.

Aerobic columns were fed with solution from the top, with gravity pulling the solution through the soil sample and the leachate collected via an outlet valve at the base of the column. The top of the column of soil was packed with washed silica sand to allow for better distribution of the incoming solution water fed from the top of the column, with minimal evaporation. The base of the soil sample was packed with diatomaceous earth, separated from the outlet by filter paper, and 1 mm stainless steel mesh over the valve outlet of the bottom cap.

The anaerobic columns were fed with solution from the bottom, allowing a longer contact time as the soils became saturated without the presence of oxygen. The base and top of the anaerobic columns were packed with washed silica sand separated from the soil sample by filter paper, again with 1 mm stainless steel mesh over the inlet valve at the bottom, and outlet valve at the top of the column. A diagram of the setup for both columns is shown in Figure 3.6.

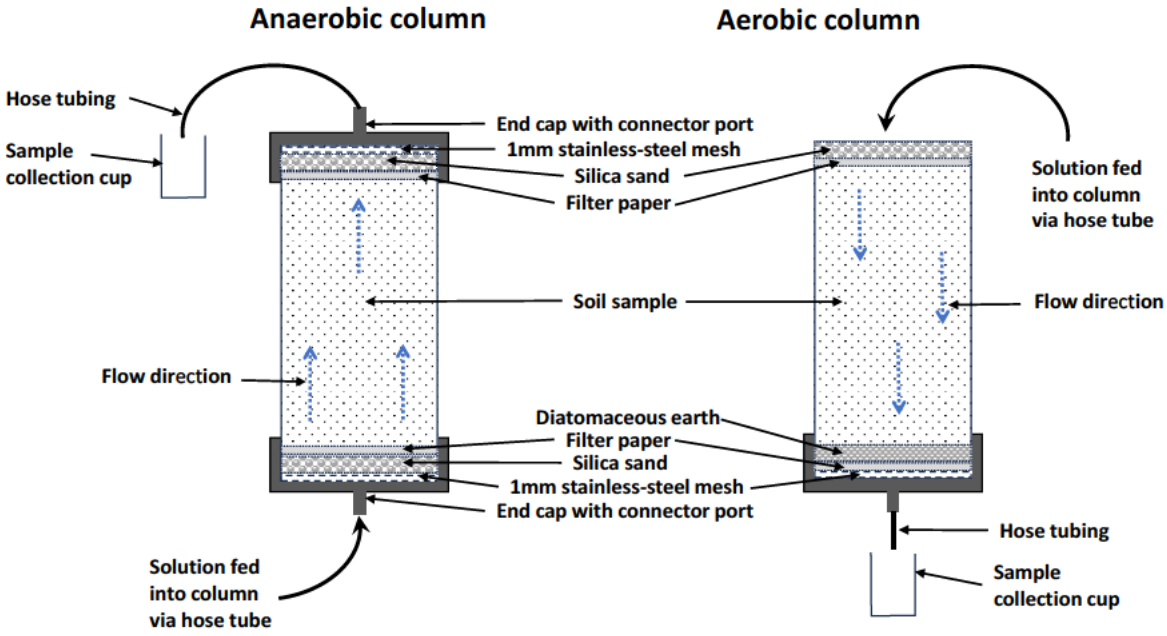


Figure 3.6 Schematic of column setup showing aerobic and anaerobic columns

The columns were fitted to a wall mount and inlet valves connected to the solution pump (Watson Marlow 520DuN IP66/NEMA 4X) with 3.0 mm ID PVC manifold pump tube or 1.5 mm ID marprene manifold tube, depending on flow rate required for each column. The larger tube delivered a flow rate of 4.4 ml/min and the small tube delivered 1.9 ml/min. The setup of the columns is shown in Figure 3.7.

Figure 3.7 Photograph of laboratory setup of the 10 columns on wall mount

The data collected from the column leach experiments included measuring the rate of KBr leaching from the soil with deionised water as a leaching solution and was used to calculate the dispersion coefficient (*D*) of the material. KBr is a non-reactive solute, with minimal interactions assumed between the Br ions and the soil matrix (Stephens, 2019), therefore making it a suitable tracer to assess water movement. The leachate was sampled periodically, with a total leachate volume >2.5 pore volumes (pV), which was calculated using the porosity of each soil and the volume of the column. Each incremental volume of leachate was measured by weight and analysed using a portable meter (Hanna Instruments HI-98121 probe) for pH, Eh and electrical conductivity (EC). The pV vs EC data was graphed, and samples selected for additional analysis based on EC inflection points. These were submitted to Talbot and Talbot laboratory for analysis of Br concentrations (see section 3.3.1 for method). The dispersion coefficient (*D*) was calculated by fitting the breakthrough curve using the computer software STANMOD (STudio of ANalytical MODels) (Simunek et al., The STANMOD computer software for evaluating solute transport in porous media using analytical solutions of convection-dispersion equation. Versions 1.0 and 2.0 IGWMC-TPS-71, 1999) which uses the convection-dispersion solute equation (section 2.3, equation 2.2). Inputs for the model included the time series leachate concentration data from the column tests, and a retardation factor ($R_f$) of 1 (assumed Br is a conservative tracer). The model package within STANMOD was CXTFIT, to solve inverse problems using a nonlinear least-squares parameter optimization method to provide best fit values for unknown variables, namely dispersion coefficient (*D*) and first order decay coefficient (μ) (Toride et al., 1995).

After the Br breakthrough curves were complete the columns were further used to assess the absorptivity of zinc by mimicking the contamination present on the study site within the hillslope. A solution of 530 mg/l zinc chloride (ZnCl) was fed to the columns to achieve leaching of 2.5 to 3 pore volumes[2]. The concentration of ZnCl solution was selected based on water quality data from monitoring points on the study site, to mimic the current pore water conditions at the top of the hillslope. Incremental leachate volumes were measured by weight and analysed using the portable meter (detailed above), measuring pH, EC,

[2] Note: The column tests took around 46 days to complete, over which time the national electricity grid was unstable with power outages occurring, resulting in occasional pump shutoff for a few hours.

temperature, and oxygen reduction potential (ORP electrode, Ag/AgCl reference with 3.5 mol/L KCl). ORP readings (Eh) were calculated relative to the standard hydrogen electrode using the Nerst-Equation (equation 3.4), with α = 50301 and b = 297 which are specific constants relating to the ORP electrode specifications. The collected leachate was immediately sealed with a plastic top and refrigerated.

$$E_{0(25°C)} = E_t - 0.198 \times (T - 25) + \sqrt{(a - b \times T)} \quad (3.4)$$

A selection of four to six leachate samples per column were selected for further detailed analysis, this selection was based on the pV and measured EC inflection points to represent key data sets. These selected samples were analysed by Talbot and Talbot laboratory for pH, EC, major anions (nitrate, sulphate, chloride), major cations (calcium, magnesium, sodium) alkalinity as $CaCO_3$, and selected metals (zinc, copper, lead, aluminium, iron, manganese). The methodology for analysis is detailed above. The data was graphed and analysed further to better understand potential chemical interactions and movements. Zn breakthrough curve data was further analysed using the program STANMOD to ascertain the retardation factor for zinc in each of the columns. The dispersion coefficient (*D*) previously derived from the KBr column leach test was used, thus the software solved for the retardation factor ($R_f$), and first order decay coefficient (μ).

The distribution coefficient ($K_d$) of zinc for each soil was then calculated from $R_f$ by using equation 3.5. Where, $\rho_d$ = bulk density and $\theta_s$ = saturated water content.

$$K_d = \left(\frac{R_f - 1}{\rho_d}\right) \theta_s \quad (3.5)$$

## 3.6 Modelling

The parameters obtained in the soil characterisation and chemistry analysis were used to construct a hydrological model of the study site. This was done in two main phases, namely refinement of the conceptual site model (CSM), followed by numerical modelling using Hydrus (2D/3D) software.

### *3.6.1 Conceptual site model*

The existing CSM (see section 3.2) for the site was reviewed, and areas identified for information to be refined identified. The understanding of the hydraulic flow regime in each

of the soil types (recharge, interflow and responsive) was confirmed by assessing the revised hydraulic conductivity and water retention measurements. The absorption of zinc within the soil profile was also explored, as this study provided a more detailed assessment of $K_d$ than previous studies.

A graphical representation of the CSM for a transect stretching from the source area (historical factory operations) to the wetland was illustrated. The topographical profile was extracted from Google Earth Pro (Google Maps, (n.d)) and the underlying pedology inferred from previous data logs of test pits, auger hole observations, refusal depths and soil characterisation.

### *3.6.2 Flow and contaminant transport modelling*

A combined solute flow and contaminant transport model was created using the HYDRUS (2D/3D) software (PC Progress, 2006). The CSM provided the framework for the HYDRUS model, which was set up as follows:

- Geometry: 2-dimentional transect representing 460 m (X-axis), with a depth of 23 m (1 544 – 1 567 m, Y-axis). The base of the model was a contact boundary between the solid rock and fractured rock interface.
- Mesh: A finite element model consisting of 50 953 nodes (to represent approximately 0.3 m on X-axis, and 0.5 m on Y-axis), with finer nodes generated around boundaries of material property changes. The refined grid created a mesh representing 0.15 m on X-axis, and 0.01 m on Y-axis).
- Soil hydraulic model: Run as a single porosity model (van Genuchten-Mualem) with no hysteresis (van Genuchten, 1980).
- Domain properties: The porous media profile was simplified to the six key domains identified in the field investigations. Properties assigned to these domains included:
    - Residual water content ($\theta_r$).
    - Saturated water content ($\theta_s$).
    - Alpha, parameter $\alpha$ in the soil water retention function.
    - N, parameter $n$ in the soil water retention function.
    - Saturated hydraulic conductivity ($K_{sat}$).
- Boundary conditions:
    - Constant head boundary along left and right sides of model to mimic median groundwater level.

    - No flow boundary along bottom contact with rock interface and along top surface where hard standing is located.
    - Seepage face boundary along hillslope.
- Time Series data:
    - No atmospheric boundary was applied; however, a variable head boundary value was used. This was achieved by running a single layer Hydrus-1D simulation, utilising topsoil properties (MHS200) for the model. A 60 year time series daily rainfall record was constructed from a consolidation of three local weather stations. The daily evaporation time series data was tabulated from the S-pan datasets from these weather stations, this was then converted to A-pan values (Bosman, 1990) for the model input. The net-flux of precipitation-evapotranspiration varied between -1.3 and -0.4 m/d. Due to the complexity of the Hydrus-2D model domains, this was simplified to the median value of -0.1 m/d and applied to the surface boundary of the model.
- Solute transport parameters: Soil specific parameters were assigned to each domain, including:
    - Bulk density ($\rho_b$).
    - Longitudinal and transverse dispersivity ($D_L$ and $D_T$).
    - Distribution coefficient ($K_d$).
- Initial pressure head conditions:
    - -1.0 m head at the source area, as per measurements from groundwater piezometer.
    - 0 m head along the seepage face of the hillslope.
    - 0 m head at the valley bottom.
- Initial concentration conditions:
    - 0 m head at the source area, with concentration of 2 500 mg/l zinc.

The model was initially run as a water flow model only to obtain steady state conditions and calibrated against piezometer data for water levels. The water level data from 8 piezometers located near the modelled transect were used for this purpose, with time series data available for a 23 year period. These piezometers were added to the model as observation nodes (Appendix D, Figure D.1).

Solute transport modelling was added to simulate leakages from the factory area. A constant contaminant head with a length of 5 m was applied for a simulated period of 40 years (1950-1990), after which the source of zinc contamination was removed, and the model continued to run for a further 30 years (1990 - 2020). The model concentrations were compared with observed data and the model refined to align with the groundwater and seepage water chemistry data for the site which covers the years 2008 - 2018. Future simulations were run for a further 30 years to assess potential future contamination plumes (2020-2050).

### 3.7 Materials and Methods Summary

The location for this study is a hillslope wetland, positioned down gradient from a zinc galvanising plant that has been in operation for over 80 years. This project commenced by reviewing existing reports relating to the groundwater contamination at the site and collating water quality data from various groundwater and surface water monitoring points. Soil samples were then collected at varying depths, extending along an inferred subsurface flow pathway from the factory to a valley bottom wetland. At each sampling point, observations were made, soil media collected, and field testing for saturated hydraulic conductivity undertaken.

Collected soil samples were analysed in a laboratory to obtain various soil parameters, including density, porosity, saturated hydraulic conductivity, water retention and soil texture. Zinc absorption to the different soils was assessed through column tests, as ZnCl solution was leached through the soils under both aerobic and anaerobic conditions. The soil samples were also analysed by an external laboratory to determine mineralogy, pH, cation exchange capacity and organic carbon content.

Based on the collected data, a conceptual site model was drafted, and transposed into an analytical model using Hydrus-2D. Modelled simulations were adjusted to align with the available timeseries water quality datasets, thus leading to predictive future modelling scenarios of zinc plume migration.

# 4. ASSESSMENT OF SOILS AND EVALUATION OF THE RETARDATION CAPACITY FOR ZINC MOBILISATION

The study site for this research project was investigated by examining existing site reports, as well as through site observations, and soil characterisation. The results of the soil characterisation are presented in this chapter, detailing the physical and chemical characteristics of the hillslope soils. The results of the column leaching tests provide insight into the capacity of the soils to retard the movement of zinc within the pore water of the hillslope as well as the potential impact of seasonal variations in soil saturation of the vadose zone.

## 4.1 Soil Characterisation

Five locations were selected for soil sampling along a transect which followed the topographic slope from the historical source area to the valley bottom wetland. The soil sampling locations included one sample on the upper hillslope (sample UHS, classified as Orthic A soil), two samples in the middle hillslope (MHS200 and MHS360, classified as hard plinthic and soft plinthic soils respectively), and two samples within the near saturated soils of the wetland (WET1 and WET_UP, classified as G-horizon soils). The observations recorded during excavation of the material are detailed in Table 4.1.

Table 4.1 Locations and observations on collected soil samples

| Soil ID & soil type | Location | Sample depth (mm) | Observations (MCCSSSO)[1] |
|---|---|---|---|
| UHS: Orthic A | Upper hillslope | 0-200 | Slightly moist, dark reddish brown with red and yellow mottles. Soft fine loamy sand with large matrix supported subrounded smooth hard boulders of various sizes. Transported soil. |
| MHS200: hard plinthic | Middle hillslope | 100-300 | Slightly moist, medium brown with reddish yellow mottles. Medium dense sandy loam with matrix supported subrounded smooth hard boulders. Transported soil. |
| MHS360: soft plinthic | Middle hillslope | 300-700 | Slightly moist, light orange-brown with red mottles. Loose silt with matrix supported subrounded hard boulders. Transported soil with residual material. |
| WET1 G-horizon | Valley bottom | 0-200 | Moist, deep brown, with yellow and red mottles. Loose sandy clay with a high content of root matter. Combination of decomposed matter and transported material. Alluvium origin. |
| WET_UP G-horizon | Valley bottom: up-stream | 0-200 | Very moist, becoming wet at 200mm, soft brown silt. High content of roots, organic matter and hard ferricrete nodules. Combination of decomposed matter and transported material. Alluvium origin. |

Note (1): MCCSSSO abbreviates soil description for soil and rock logging, namely moisture, colour, consistency, structure, soil texture and origins.

The factory footprint and parking area consists of hard standing; this extends around 200 m along the transect. The soils beneath the hard standing consist of a topsoil layer (UHS) ranging between 200-350 mm deep, this is underlain by saprolite and fractured rock, with more competent bedrock encountered at around 3-7 mbgl. The hillslope leading from

the factory towards the valley bottom consist of alluvial and transported material, as noted by the fine grain matrix with rounded and sub-rounded boulders. At the middle of the hillslope, the near surface soil layers consist of sandy loam material, supporting residual sandstone boulders. (MHS200). Below this layer, as well as further down gradient, the material becomes finer grained with an increasing silty-clay matrix which surfaces at the lower end of the hillslope (MHS360). At the bottom of the valley the topography flattens out and the clay content becomes significantly higher, with roots from wetland vegetation contributing to a high organic content (WET1). In some area within the hillslope, the upper soils have been eroded to expose areas of ferricrete, with scattered ferricrete boulder noted throughout the site.

### *4.1.1 Physical parameters*

The physical parameters measured for the five soil samples has been summarised in Table.4.2.

Table.4.2 Physical parameters ($\rho_s$, $\rho_b$ and φ) of soil samples as determined in the laboratory

| Parameter measured | UHS | MHS200 | MHS360 | WET1 | WET_UP |
|---|---|---|---|---|---|
| Particle density ($\rho_s$) (g/cm$^3$) | 2.35 | 2.41 | 2.08 | 2.46 | 2.53 |
| Dry bulk density ($\rho_b$) (g/cm$^3$) | 1.44 | 1.53 | 1.58 | 0.87 | 1.87 |
| Porosity (φ) (%) | 38.4 | 36.6 | 35.6 | 58.4 | 26.0 |

The particle size distribution assessment undertaken in the laboratory showed three distinct soils in terms of texture analysis, including sandy loam (UHS and MHS_200 samples), sandy loam (MHS360) and sandy clay loam (WET_UP) and clay (WET1). The data has been graphed from the hydrometer and sieve analysis and shown in Figure 4.1. Two of the samples contained gravel and therefore the % passing did not reach 100%. The percentage of silt, clay, sand, and gravel is shown in Table 4.3.

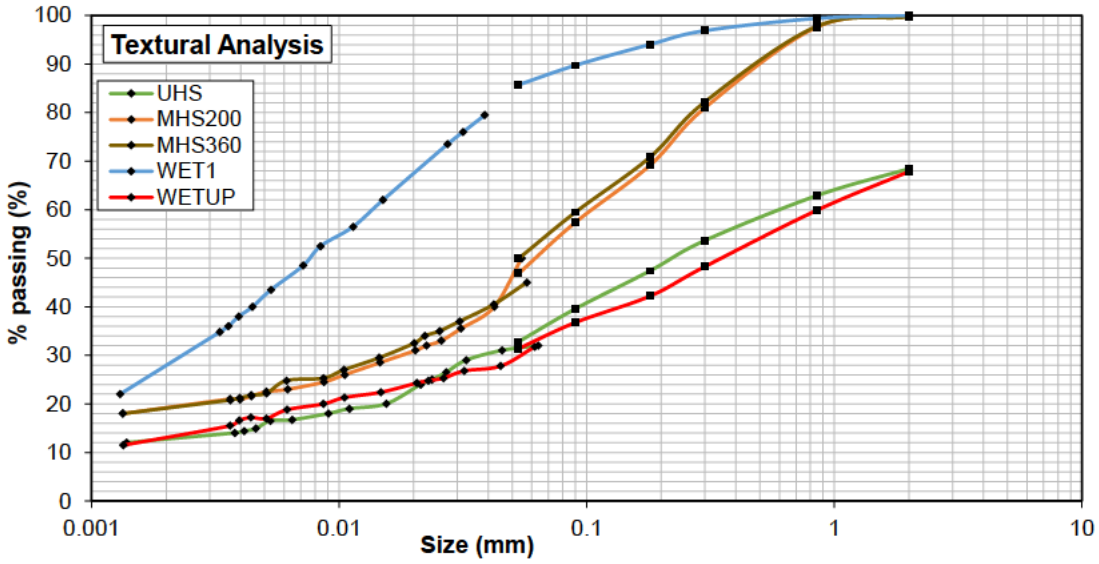


Figure 4.1 Graph of hydrometer and sieve analysis data showing particle size and percent passing

Table 4.3 Soil texture analyses percentage data for the collected soil samples

| Sample ID | % Gravel | % Sand | % Silt | % Clay | Texture Classification (1) |
|---|---|---|---|---|---|
| UHS | 31.6 | 36.9 | 18.5 | 13.0 | Sandy loam |
| MHS200 | 0 | 54.5 | 26.5 | 19.0 | Sandy loam |
| MHS360 | 0.3 | 56.2 | 24.5 | 19.0 | Clay |
| WET1 | 0 | 15.4 | 56.6 | 28.0 | Sandy loam |
| WET_UP | 32 | 39.0 | 15.0 | 14.0 | Sandy clay loam |

Note: (1) Soil texture classification was referenced using the USDA soil classification triangle for the sand, silt, and clay percentage of the soil. This excludes the gravel component.

The fitted water retention curves are displayed in Figure 4.2, from this, the calculated residual water content, alpha and n parameters for the 5 samples are shown in Table 4.4. The saturated water content in the hillslope samples ranged between 0.42 to 0.52, however, this increases to 0.73 at the valley bottom (WET1), thus highlighting the high water holding capacity of the wetland soil matrix. The fitted curve for each of the tests had a statistical $R^2$ value of >0.97, inferring a good data fit.

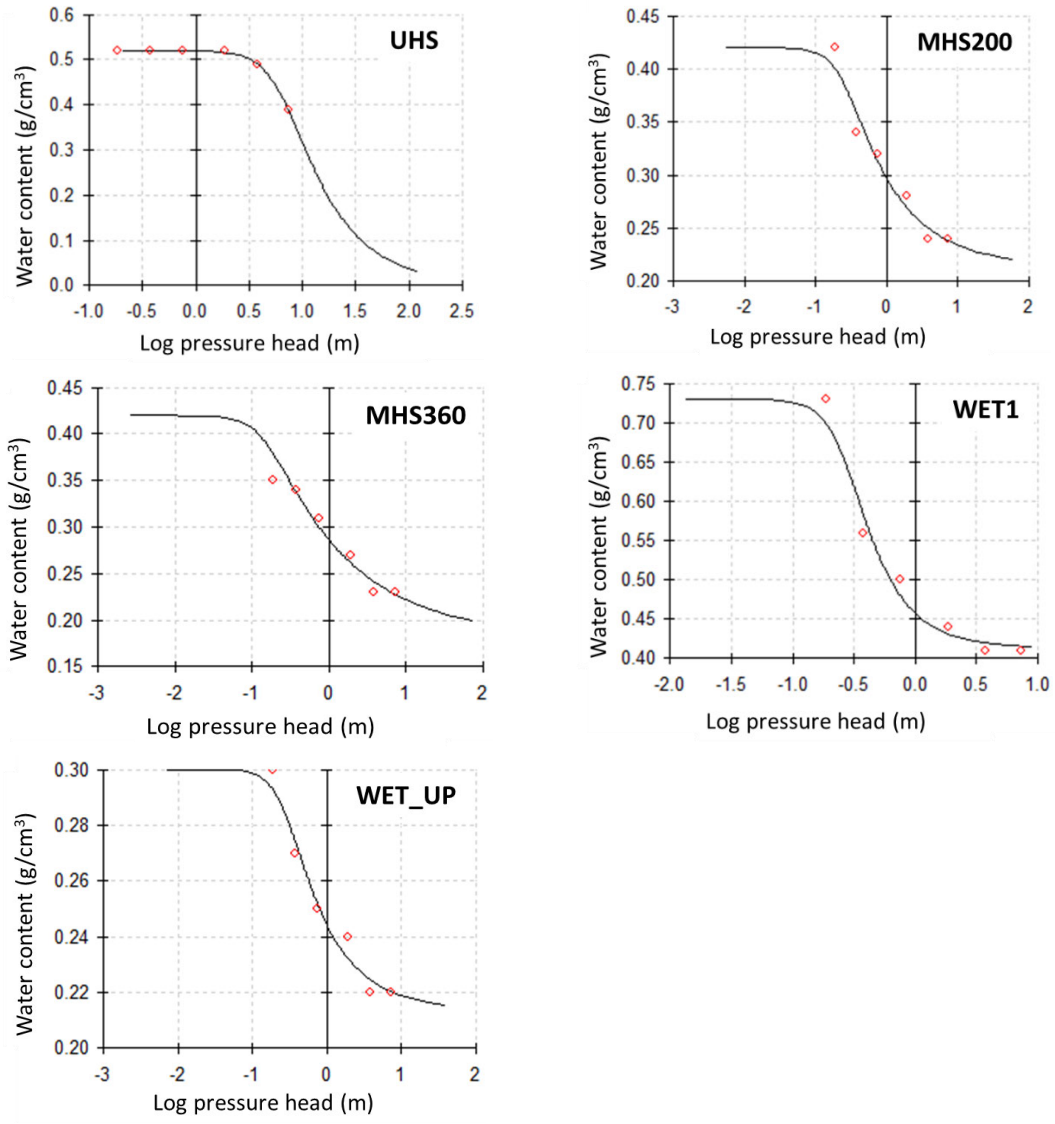


Figure 4.2 Graphical display of water retention data showing log pressure head vs water content for soil samples

Table 4.4 Calculated water retention parameters ($\theta r$, $\theta s$, $\alpha$ and n) for soil samples

| Water Content ($\theta$) g/cm$^3$ | UHS | MHS200 | MHS360 | WET1 | WET_UP |
|---|---|---|---|---|---|
| Residual water content ($\theta_r$) | 0.000 | 0.215 | 0.205 | 0.414 | 0.214 |
| Saturated water content ($\theta_s$) | 0.524 | 0.425 | 0.428 | 0.738 | 0.298 |
| $\alpha$ (1) | 0.153 | 4.175 | 1.879 | 3.695 | 3.177 |
| n (2) | 2.971 | 2.639 | 2.620 | 3.513 | 2.789 |
| Curve fit: $R^2$ (3) | 0.998 | 0.970 | 0.984 | 0.981 | 0.978 |

Note: (1) $\alpha$ is related to the inverse of the air entry suction. (2) n is a measure of the pore-size distribution. (3) Curve fit of $R^2$ is a statistical measure of the proportion of variation from the predicted value.

The saturated hydraulic conductivity ($K_{sat}$) had significant variability in the soils assessed in-situ using a Guelf Permeameter, as can be seen in the data graph Figure 4.3. The upper slope soils (UHS and MHS200) had the highest $K_{sat}$ values of 2.14 and 1.4 m/d respectively. Further downslope, the $K_{sat}$ rate decreased by an order of magnitude to around 0.14 m/d (MHS360 and WET1). The lowest hydraulic conductivity was measured at the WET_UP site, however this soil was already oversaturated and therefore the permeameter measurements may not reflect the actual $K_{sat}$ of the soil. In terms of the hydropedology classification to describe pore water movement noted in Section 2.1 (Job et al., 2018), soils which can drain recharge and inflows are known as recharge or interflow soils, whereas soils that are either fully saturated or result in upward movement of water are responsive soils. Water would move quicker in the upper slope, where the $K_{sat}$ values are highest, but would accumulate around the materials with a lower $K_{sat}$ as the water cannot migrate fast enough through these soils. As observed on the site, surface seepages have resulted in the accumulation of water around these areas and the higher $K_{sat}$ topsoils have become responsive soils in some areas.

In comparison to the in-situ testing noted above, similar $K_{sat}$ measurements were observed in the laboratory testing, as shown in Table 4.5. However, the $K_{sat}$ measured in-situ for the upper slope soils (UHS and MHS200) were an order of magnitude lower compared to the laboratory testing. This is expected as the laboratory testing is limited horizontally and therefore assesses the vertical $K_{sat}$ component, whereas the field measurement method accounts for both the horizontal and vertical movement of water. In the literature review, field measurements are preferred over laboratory measurements, due to the inevitable disturbance of the soil from its natural condition (MacDonald et al., 2004). Therefore, the in-situ measurements have been used in the model for the site (Chapter 5).

By comparing the literature values presented earlier in Table 2.1 (Garcia-Gutierrez et al., 2018), to the measured $K_{sat}$ for clay soils (WET1) and sandy clay loam soils (WET_UP), the measured values of 0.1 and 0.02 m/d for these soils respectively are within the median expected range.

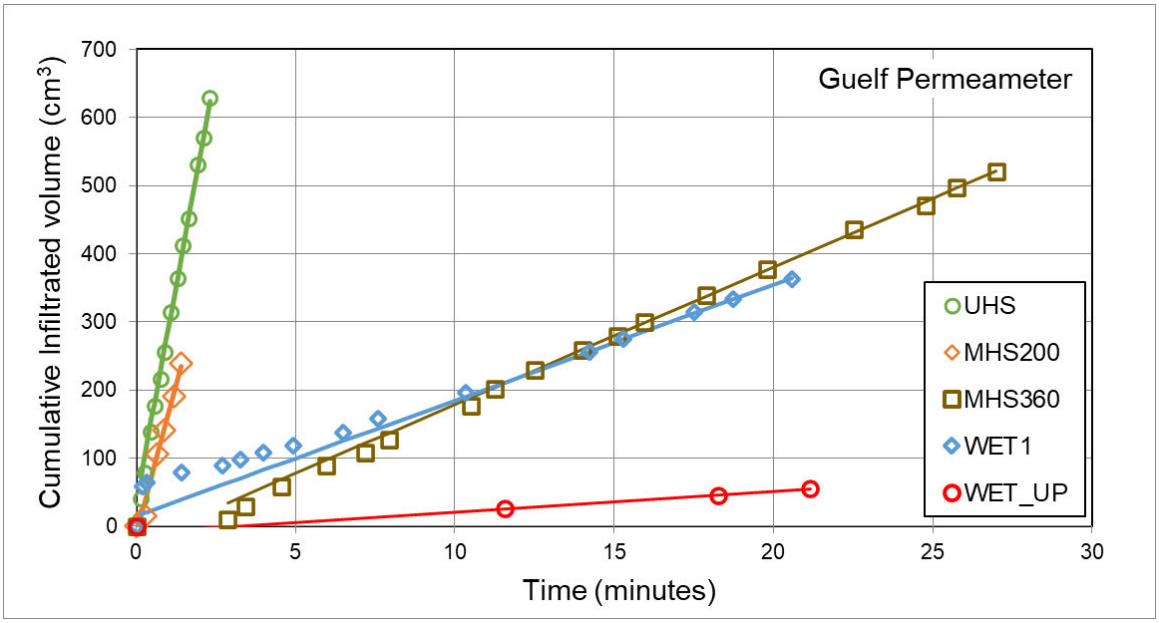


Figure 4.3 Graph showing infiltration volumes with time, as taken during Guelf Permeameter testing of site soils

Table 4.5 Saturated hydraulic conductivity measurements of soils from laboratory and field testing

| Measurement method (m/d) | UHS | MHS200 | MHS360 | WET1 | WET_UP |
|---|---|---|---|---|---|
| $K_{sat}$ Constant Head (1) | 0.162 | 0.042 | 0.147 | 0.117 | 0.045 |
| $K_{sat}$ Guelf Permeameter (2) | 2.135 | 1.389 | 0.138 | 0.141 | 0.020 |

Note: (1) The constant head $K_{sat}$ measurement was undertaken in the laboratory on a reconstituted sample, (2) in-situ measurements were taken on site using a Guelf Permeameter

## 4.2 Soil Chemistry

As with the physical characterisation, the soil chemistry also showed significant variability throughout the study area. The soils within the drier near-surface hillslope have a mineralogy dominated by quartz (80 – 85% for UHS200 and MHS200), which reduces with depth (74% at MHS360). These hillslope soils have a clay content of around 13 to 25%. Within the wetter valley bottom, the soils have a much higher clay content (42 to 47% kaolinite for WET1 and WET_UP). These alluvial soils are deposits of fine sediments within the wetland. The mineralogy analysis has been shown in Table 4.6, and elements are discussed further in the paragraphs below.

The pH of the soils is above 5, except for the mid-slope soils, which have a pH between 3.4 to 3.9. This acidic environment is noted to be an identifying characteristic of the plume as hydrochloric acid storage tanks and acidic wash baths were components from the decommissioned factory.

The cation exchange capacity (CEC) of soils ranged between 5.6 and 15.3 cmol/kg, with the highest capacity in the valley bottom soils (WET1). The clay content is the highest within the valley bottom (28%), aligning with the literature study that clay content increases the CEC of a soil; inferring the wetland soils capacity for zinc adsorption. The organic carbon content was also highest in the valley bottom (4.1% in WET1), where fine roots were present, binding the soil together. Unlike the findings by Rutkowska et al., (2015) and Stephan et al., (2008) in the Section 2, the analysis of the five site soils does not indicate a direct correlation between clay content, organic matter, organic carbon, and cations exchange capacity. Highlighting the need to look at the physical as well as the chemical properties of the soils in unison, to understand the possible interactions, rather than relying on a single determinant as linear correlations to soil characteristics and $K_d$ are unlikely.

Table 4.6 Soil mineralogy analysis of soil samples (mineralogy, pH, CEC, and organic carbon)

| Mineralogy (%) | UHS200 | MHS200 | MHS360 | WET1 | WET_UP |
|---|---|---|---|---|---|
| Quartz | 84.7 | 79.8 | 74.1 | 42.6 | 50 |
| Kaolinite | 13.4 | 18.2 | 25.2 | 46.8 | 42.4 |
| Anatase | 0.2 | 0.4 | 0.6 | 0.6 | 0.3 |
| Muscovite | 1.4 | 1.6 | 0 | 6.7 | 5.8 |
| Goethite | 0.3 | 0 | 0.1 | 1.3 | 0.6 |
| Microcline | 0 | 0 | 0 | 2 | 0.9 |
| pH | 5.33 | 3.85 | 3.39 | 5.28 | 6.78 |
| CEC cmol/kg (1) | 12.92 | 5.57 | 6.20 | 15.25 | 5.99 |
| % organic carbon | 0.52 | 0.61 | 0.68 | 4.06 | 0.66 |
| % organic matter | 0.90 | 1.06 | 7.01 | 1.17 | 1.14 |

Note: (1) CEC refers to cation exchange capacity of soils

## 4.3 Zinc Adsorption

The first soil columns tests involved pumping deionised water to the columns, to leach out the non-reactive solute (potassium bromide) from the soil. The bromide concentrations were measured in the leachate to ascertain the dispersion coefficient for the soil, by determining the breakthrough curves (BTC) Figure 4.4.

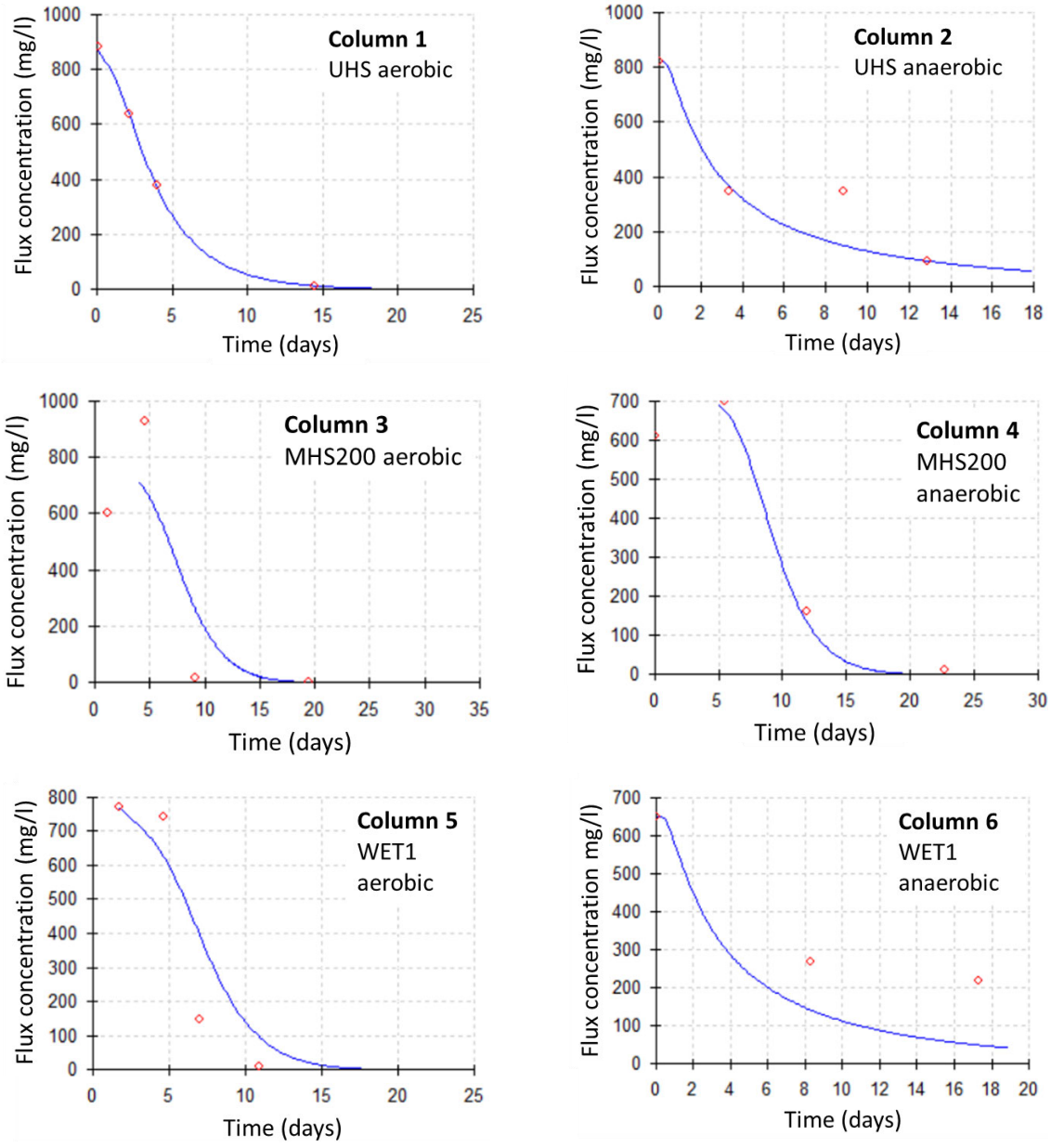


(Continued on next page)

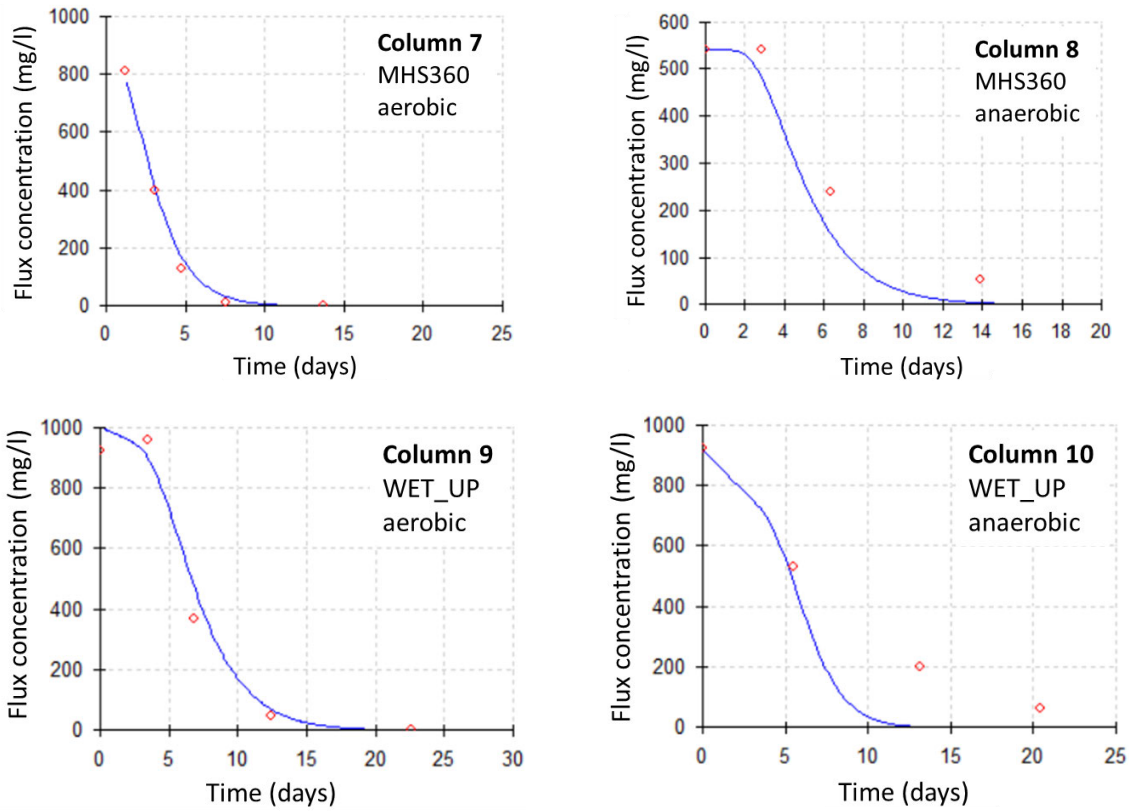


Figure 4.4 Soil column breakthrough curves showing bromide flux concentration with time in the collected leachate

The input and solved variables using the BTCs has been given in Table 4.7. The calculated dispersion coefficients (*D*) ranged between 0.0007 (WET_UP aerobic column), to 0.0181 (WET1 anaerobic column). Although the D varied between the aerobic and anaerobic column pairs, no identified trends were obvious to link to the changing environmental conditions. Statistically, the BTCs calculated had an $R^2$ fit of >0.92, except for WET1 anaerobic and MHS360 aerobic columns which had a $R^2$ fit of >0.88.

Table 4.7 Parameters derived (D, μ) and measured (***v***) from column leach test with KBr solution

| Column identification | Velocity (m/d) | *D* | μ | $R^2$ | MSE |
|---|---|---|---|---|---|
| Col1: UHS ae | 0.0553 | 0.0153 | 0.1438 | 0.980 | 0.010 |
| Col2: UHS an | 0.0617 | 0.0118 | 0.0129 | 0.963 | 0.002 |
| Col3: MHS200 ae | 0.0302 | 0.0024 | 0.0214 | 0.923 | 0.112 |
| Col4: MHS200 an | 0.0347 | 0.0080 | 0.0222 | 0.983 | 0.017 |
| Col5: WET1 ae | 0.0381 | 0.0034 | 0.0465 | 0.924 | 0.186 |
| Col6: WET1 an | 0.0515 | 0.0181 | 0.0198 | 0.880 | 0.016 |
| Col7: MHS360 ae | 0.0639 | 0.0039 | 0.0258 | 0.893 | 0.073 |
| Col8: MHS360 an | 0.0660 | 0.0272 | 0.0340 | 0.947 | 0.012 |
| Col9: WET_UP ae | 0.0430 | 0.0007 | 0.0425 | 0.994 | 0.054 |
| Col10: WET_UP an | 0.0464 | 0.0151 | 0.0144 | 0.973 | 0.077 |

Note: 'ae' denotes aerobic column, 'an' denotes anaerobic column. Flow velocity (measured) and retardation factor ($R_f$=1) are input parameters. D denotes dispersion coefficient, μ denotes first order decay coefficient, $R^2$ and Mean Square Error (MSE) are statistical parameters.

In the second set of column tests, a solution of ZnCl replaced the deionised water used to infiltrate the soils. The leachate was collected and analysed to ascertain the soils retardation of zinc under aerobic and anaerobic conditions. The zinc BTCs for each column is shown in Figure 4.5.

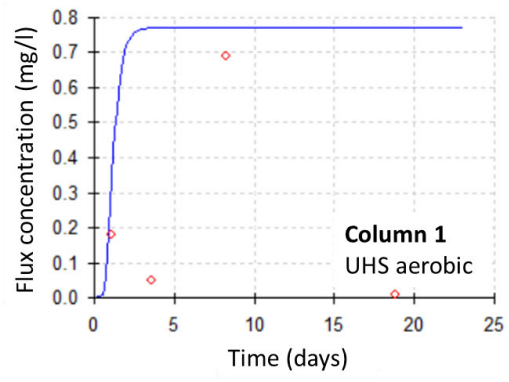


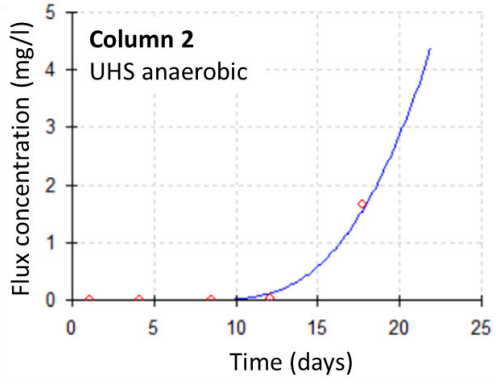


(Continued on next page)

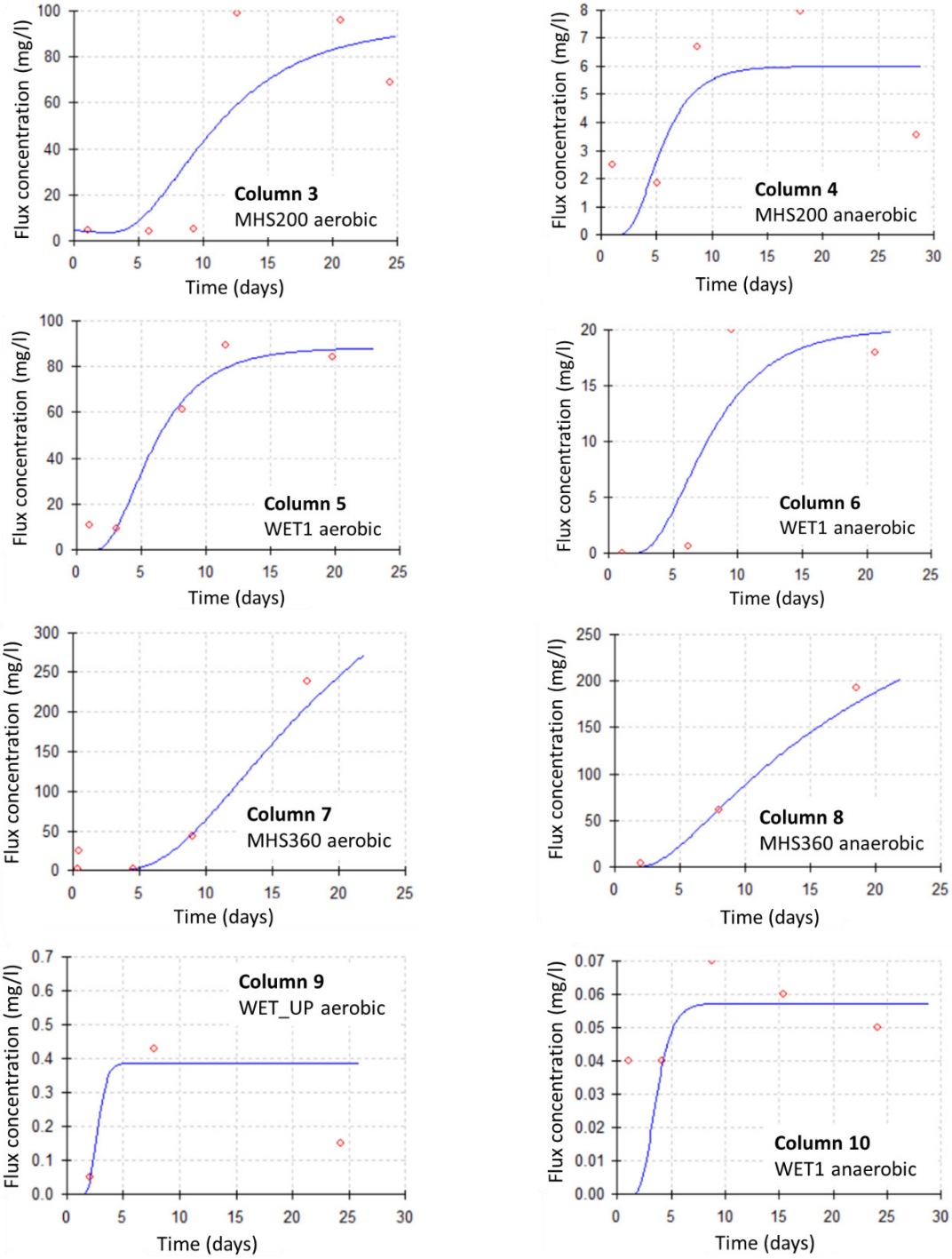


Figure 4.5 Graphs showing the zinc concentration flux curves vs time for the soil column experiments

The calculated retardation factor ($R_f$) and first order decay coefficient (μ) of zinc are shown in Table 4.8. The flow velocity for these tests was the same as for the KBr column leaching experiment. Statistically, the curve fitting ($R^2$) showed less correlation to the ZnCl column experiment data than with the KBr column data, with $R^2$ ranging from 0.33 to 0.99. This could be due the nature of the experiments: with the KBr column experiment, water was used to leach $Br^-$ out of soil, this occurred at a steady rate. Whereas with the ZnCl column experiment the $Zn^{+2}$ reacted with the soils as it was introduced to the column in solution, with reactions occurring at different rates (absorption, complexation, precipitation etc.), resulting in slightly erratic concentration spikes.

The retardation factor ($R_f$)was higher in the anaerobic columns than the aerobic columns, the difference ranging between an $R_f$ of 2.8 to 34.6. The literature has indicated that spatial and temporal factors play an important part in the adsorption of solutes to soil surfaces. It is likely that the more saturated flow through the anaerobic columns provides more soil surface contact with the solution for reactions to occur. In the aerobic columns the flow rate is slightly faster due to gravity, thus reducing the contact time of the solution with soil material, as well as the possibility of preferential flow paths to develop, reducing the probability of contact reactions with the soils surfaces with this more direct flow path. The environments of aerobic and anaerobic conditions will have a different impact on the amount of zinc sorbed to the soils. On the study site, the more easily drained and drier soils are likely to have a lower zinc absorption than the more saturated and wetter soils. This may impact zinc absorption on a seasonal level, beneath the factory site, the water table has a seasonal fluctuation of around 0.8 m, resulting in aerobic conditions in the upper soils. Within the downgradient hillslope, the groundwater level is closer to surface, with little seasonal variation. At the upper slopes, it occurs at 0.8 meters below ground level (mbgl), this decreases to 0.4 mbgl at the mid-hillslope, and a further decrease to 0 mbgl with seepage faces near the valley bottom. Thus, anaerobic conditions are likely to be present in the lower hillslope and valley bottom soils.

The distribution coefficient ($K_d$) was calculated from the retardation factor, as this is the term used in the Hydrus model (elaborated in the next section). Comparing the $K_d$ in the anaerobic samples, as this is the dominant condition within the wetland environment, the highest zinc absorption was noted in the UHS and MHS360 soils ($K_d$ of 13.06 and 10.59 respectively). These are in the upper soil layers of the hillslope and are likely to adsorb zinc

in solution that flows through these materials from either spillages or seeps. The UHS soil has a high cation exchange capacity (CEC) (Table 4.6), which is the likely factor influencing the absorption of zinc. The MHS360 soil has a lower CEC, however the large $K_d$ could be attributed to the high organic matter component (7%) as well as percentage of clay present (25% Kaolinite).

Table 4.8 Absorption parameters ($R_f$ , μ) derived for soil column tests during leaching of ZnCl from the soils

| Column Identification | $R_f$ | μ | $R^2$ | $K_d$ |
|---|---|---|---|---|
| Col1: UHS ae | 2.354 | 6.5000 | 0.423 | 0.491 |
| Col2: UHS an | 36.97 | 0.0001 | 0.993 | 13.056 |
| Col3: MHS200 ae | 2.238 | 0.213 | 0.703 | 0.344 |
| Col4: MHS200 an | 5.041 | 2.035 | 0.328 | 1.122 |
| Col5: WET1 ae | 1.325 | 0.243 | 0.961 | 0.273 |
| Col6: WET1 an | 6.316 | 1.333 | 0.767 | 4.473 |
| Col7: MHS360 ae | 3.754 | 0.001 | 0.960 | 3.754 |
| Col8: MHS360 an | 10.59 | 0.001 | 0.985 | 10.59 |
| Col9: WET_UP ae | 0.625 | 1.251 | 0.436 | 0.000 |
| Col10: WET_UP an | 9.704 | 12.000 | 0.380 | 1.386 |

Note: 'ae' denotes aerobic column, 'an' denotes anaerobic column. $R_f$ denotes retardation factor. μ denotes first order decay coefficient. $R^2$ indicates statistical parameters for curve fitting. $K_d$ is the calculated distribution coefficient for zinc

Another factor considered in terms of accessing the zinc concentration within the leachate, was the impact of pH on the mobility of the zinc. The ZnCl solution for the column leach tests had a median pH of 3.3 (see Appendix B). Within the columns, the soils neutralising ability increased the pH of the leached solution, and therefore had the potential to contribute to the reduced mobility of zinc. The median dataset of pH measurements and calculated Kd are displayed in Table 4.9 below and the data graphed in Figure 4.6. This shows the large buffering capacity of the soils, which increased the pH of the leached solution to >5, except for MHS360 which showed a minimal pH increase to 3.8 - 4.0. As both the MHS360 and UHS samples had the highest $K_d$ value for zinc, no obvious correlation is drawn within the test parameters, to the relationship between pH and the amount of zinc adsorbed by the soils and/or precipitated out of solution.

Table 4.9 Measured pH and derived Zn $K_d$ from column test leachate

| Sample ID | Median pH | pH Range | $K_d$ |
|---|---|---|---|
| UHS ae | 6.66 | 6.22 - 7.26 | 0.491 |
| UHS an | 6.42 | 6.06 - 6.92 | 13.056 |
| MHS200 ae | 5.26 | 4.92 - 6.21 | 0.344 |
| MHS200 an | 5.44 | 5.16 - 5.79 | 1.122 |
| WET1 ae | 6.19 | 5.86 - 6.75 | 0.273 |
| WET1 an | 6.34 | 6.13 - 6.6 | 4.473 |
| MHS360 ae | 4.02 | 3.79 - 5.72 | 3.754 |
| MHS360 an | 3.83 | 3.77 - 4.11 | 10.590 |
| WET_UP ae | 7.00 | 6.35 - 7.51 | 0.000 |
| WET_UP an | 7.52 | 7.09 - 8.04 | 1.386 |
| ZnCl Solution | 3.33 | 3.12 – 3.89 | - |

Note: 'ae' denotes aerobic column, 'an' denotes anaerobic column. $K_d$ is the calculated distribution coefficient for zinc

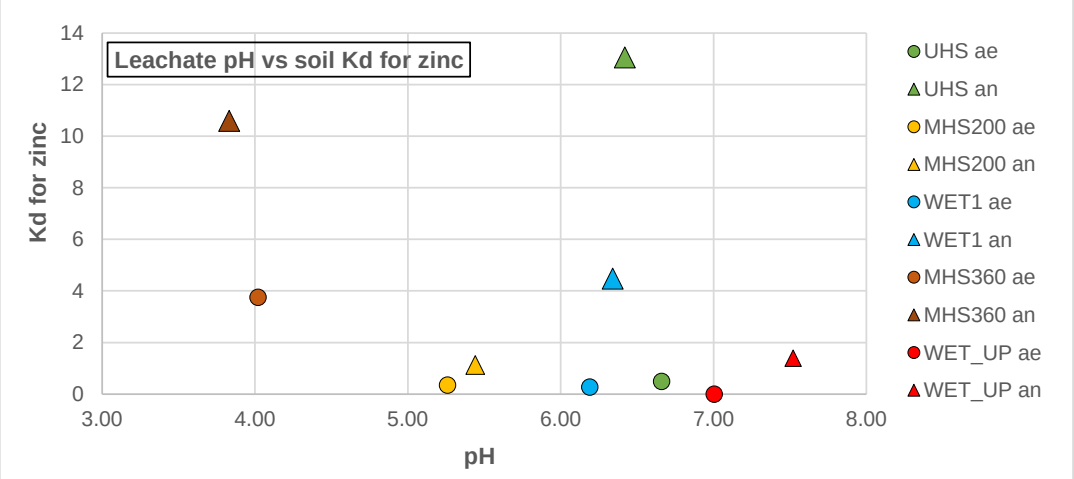


Figure 4.6 Graph showing pH of leachate for column tests vs the calculated Zn $K_d$

This data has been assessed further by discussing the relationship between zinc precipitation and redox measurements. Redox measurements (Eh) taken of the leachate during the experiment show a variation between the aerobic and anaerobic column pairs, confirming that a difference in reduction-oxidation potential was maintained during the experiment. Graphs of the individual Eh measurements taken during the experiment are

shown in Appendix C, Figure C.1. The leachate of the aerobic columns often shows more erratic readings in the start of the breakthrough, which reduced as the breakthrough progressed. This was due to turbulent flow conditions within the soil matrix as preferential flow paths were yet to be achieved along saturated routes within the soil matrix. The redox measurements for these columns ranged between 0.4 - 0.5 V, except for WET1 aerobic, which ranged between 0.3 - 0.4 V. In the anaerobic columns the redox ranged between 0.2 - 0.45 V and remained stable throughout the experiment. The readings for the WET1 column pair showed the least variation, with only 0.5 V difference between the anaerobic vs the aerobic samples. The low permeability of this material meant that the flow velocities were close to saturation in the aerobic system, resulting in near-anaerobic conditions. By comparing the median pH and redox measurements with the anticipated states of zinc as per the Pourbaix diagram (Figure 4.7), we can see that for most of the column tests, the zinc should typically remain as a dissolved ion ($Zn^{2+}$, with only one of the columns (WET_UP anaerobic) falling just within zinc range to bond with oxygen and form zinc oxide precipitate (ZnO).

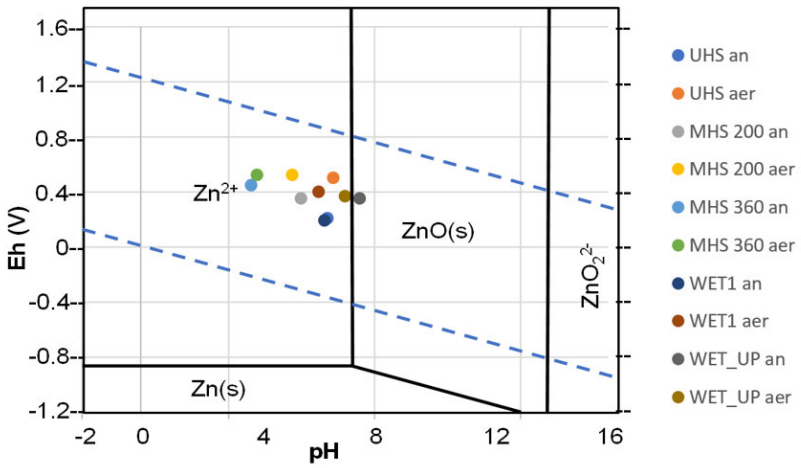


Figure 4.7 Pourbaix diagram superimposed with graph showing median redox measurements taken of leachate from column experiment

## 4.4 Additional Parameters Measured

Other parameters measured during the column leach test included EC, anions (Cl, Ca, Mg, Na), cations (Ca, Mg, Na), and metals (Zn, Cu, Al, Fe, Mn). As these components do not form the core focus of the research objectives, the data has been included in graphs under

Appendix C and a general observation summary provided below, as well as these aspects discussed under the discussion and summery section of this study (Section 4.5)

A slight disagreement was noted between the pH and EC measurements taken during the testing on leachate collection, and the measurements reported by the laboratory on the samples submitted for analysis. EC measurements are shown in Appendix C, Figure C.2. This is due to the lag time between sample collection and measurements by the laboratory, during which various chemical reactions could have occurred.

The concentration of the major ions (Ca, Mg, Cl, $NO_3$, $SO_4$, Na) and EC are graphed in Appendix C, Figure C.3. The major ions leached in both anaerobic and aerobic column pairs were similar in concentration, all at low levels. The exception to this was Cl at ±500 mg/l, as this is the contribution from the added contaminant solution of ZnCl. Cl is also a conservative tracer and therefore expected to move with the pore water rather than be adsorbed by the soils. The EC readings show a good correlation to Cl concentrations, as can be seen on the graphs (Figure C.3). In general, the initial Cl concentrations were low as the residual soil moisture in the soil matrix was leached through, this was followed by an increase at around 0.25 pV, as Cl from the source contaminant (added solution) leached through the soil.

Analysis data of selected metals is displayed in Appendix C, Figure C.4. Fe and Zn were the main metals present in the leachate, however, Zn from the source solution was immobilised to varying degrees within the soil matrix. The geology and mineralogy confirmed the iron rich environment of the research site, as evident with the observed ferricrete boulders and mineralogy analysis results indicating the presence of goethite, (1.3% in WET1, see analysis Table 4.6). To a lesser extent, aluminium and manganese were also leached from the soils, sourced from the muscovite and kaolinite containing soil material, consisting of aluminium.

The literature indicated possible preferential absorption of lead, and copper to soils, before zinc absorption, following which, absorption of cadmium and nickel proceed (section 2.3). The historical datasets of groundwater chemistry did not show significant concentrations of these metals (<5 mg/l). This aspect of preferential absorption was therefore not relevant to the study site.

## 4.5 Soil Assessment Discussion and Summary

Five soil samples were collected from various locations within the study site hillslope, including the upper hillslope, middle hillslope (at depths of 200 and 360 mm below surface), and within the valley bottom wetland. The various soil parameters were assessed to assist in characterizing the soils and understanding the flow pathways and zinc absorption capacity of the soils.

The upper hillslope soils had the largest gravel component, whereas the middle hillslope soils had a greater portion of sand and silt. At the valley bottom, the soils were dominated by silt and clay. This textural distribution was anticipated as the valley bottom alluvial soils were deposited as the land slope changed and finer sediments accumulated among the wetland vegetation.

This soil texture change was also reflected in the range of hydraulic conductivities measured within the hillslope. With the upper and mid slope topsoil having a higher Ksat than the valley bottom wetland soils. The deeper mid-slope and valley bottom soils also had a lower saturated water content. These factors infer that water would flow quickly through the upper and mid-slope topsoil, and would saturate the wetland soils, with excess water impound along the contact boundary of the soils. This has resulted in surface seepage areas, inducing anaerobic conditions within these areas.

The soil retardation capacity for zinc was assessed through column experiments. This showed a significant variation between the soil types assessed, and the environmental conditions induced (aerobic vs anaerobic). A perspective from the literature review on factors impacting zinc absorption, was that zinc mobility in soils was predominantly controlled by pH (Broadley et al., 2007) (Rutkowska et al., 2015). However, this was not observed in the collected data from the column experiments, as no correlation could be drawn between pH variations in leachate, vs zinc absorption. Further insight, the pH range for this study remained between 3 and 7, within these conditions minimal precipitation of zinc is anticipated. Therefore, the pH variation range for this study was not a significant impacting variable on zinc mobility.

The two soil samples collected in the valley bottom wetland (WET1 and WET_UP) were identified on a textural bases as clay and sandy clay loam, consisting of 46 and 42% kaolinite,

respectively. Many research articles identified clays as having a significant role in reducing zinc mobility through absorption of zinc ions onto these negatively charged soil particles (Alloway, 2009), where microcrystalline and non-crystalline oxides in the clays provide a reactive surface for zinc ions (Cavallaro & McBride, 1984), particularly with regards to the presence of kaolinite, muscovite and microcline due to the structure of these aluminosilicates (Guinoiseau et al., 2016). Again, no correlation between zinc absorption ($K_d$) and clay content could be made. Under anaerobic conditions where most zinc absorption occurs, the valley bottom wetland soils had $K_d$ values of 1.4 (WET _UP) and 4.5 (WET1). In comparison, the upper slope soil (UHS) was calculated to have a higher zinc $K_d$ value of 13, and consisted predominantly of quartz (84%), with only a 13% kaolinite content.

The redox measurements taken during the column experiments indicated that the zinc in the pore water was likely to remain as a zinc ion ($Zn^{2+}$), with only one column (WET_UP anaerobic) having precipitation of zinc oxide as a mechanism for reducing the mobility of zinc. However, for all ten column experiments, the zinc absorption capacities were greatest for the induced anaerobic conditions, with reduced zinc absorption occurring or the aerobic conditions.

As a linear relationship could not be established between zinc absorption capacity, and any single soil characteristic (e.g. texture, pH, CEC, organic carbon content etc.). This study findings agree with that of Cappuyns and Rudy (2008), that soil and environmental conditions vary, even within a single study area, and can result in significant differences in the mobility of metals within pore water.

# 5. MODELLING AND SIMULATIONS OF ZINC MOVEMENT WITHIN THE VADOSE ZONE

The soil characterisation identified the spatial, physical, and chemical aspects of the various soils within the study area. These aspects are viewed holistically within the site, with the water and chemical interactions of the various soils examined. This data is displayed graphically in the form of a CSM, which follows a 2D transect reaching from the contamination source area to the down gradient wetland, providing a simplified graphic of the subsurface stratigraphy profile. This was translated to a numerical model to simulate historical, current, and potential future scenarios of the plume migration.

## 5.1 Conceptual Site Model

The site has a gentle slope towards the south where surface and subsurface flows generally follow the topography, spatially the factory is at the top of the slope and the valley bottom wetland is around 460 m to the south. Flows following this transect along its trajectory has been described below, including classification in terms of recharge, interflow, responsive or stagnation as described in Section 2.1 (Job et al., 2018), (Van Tol & Le Roux, 2019).

The factory area, although currently under hard standing, had areas of exposed soil. Spillage of chemicals from the acid baths or tanks would have entered the subsurface through this exposed soil or through areas of deteriorated concrete. The topsoil throughout the site occurs at varying in depths of between 200 to 350 mm below surface (as represented by the sample UHS). The composition of this soil has a significant sand and gravel component, dominated by quartz. These large particles have resulted in a higher saturated hydraulic conductivity compared to other soils on the site ($K_{sat}$ of 2.1 m/d). Water in this area quickly filters through the soil (recharge soil) and is not retained within the matrix (residual water content: 0). The large potential for zinc absorption ($K_d$ 13.056) in anaerobic conditions is attributed to the CEC of this soil (12.92 cmol/kg). Within the factory footprint, the environment is more conducive to aerobic conditions, as the water table sits >1.5 mbgl, whereas within the hillslope wetland, the conditions are anaerobic, as noted by the seep areas and elevated piezometer water levels.

On the upper slopes of the site (beneath the factory footprint), the topsoil is underlain by saprolite which has a much lower hydraulic conductivity ($K_{sat}$ of 0.514 m/d). This interflow soil would conduct water slower than in the topsoil, with flows directed horizontally along the interface with the underlying fractured rock at a depth of 3-10 mbgl.

In the middle of the hillslope transect (represented by MHS200 sample), the soils are classified as sandy loam (54% sand) with a high quartz component and small fractions of silt and clay. As with the topsoil (UHS), the sandy loam has a high hydraulic conductivity ($K_{sat}$ of 1.389 m/d). Water in these soils will tend to infiltrate through the profile, provided the underlying layer is receptive to the flows (recharge/responsive soil). Zinc absorption is anticipated by these soils ($K_d$ of 1.12), although the absorption capacity is low. In comparison to the other site soils, there are no obvious soil properties which reduce zinc migration (low content of organic carbon, organic matter, and clays as well as a low CEC). This hard plinthic layer is around 1 m at its thickest, pinching out towards the valley bottom.

Underneath and down gradient of MHS200, the soils retain similar physical characteristics, as represented by the MHS360 sample, with a high sand component (56%), consisting of quartz (74%). These soft plinthic soils have a larger organic matter content (7%) compared to the overlying MHS200 soil. The low hydraulic conductivity ($K_{sat}$ of 0.141 m/d) indicates soil water would move slowly within these soils, and water filtering through from more permeable layers (such as MHS200), may back up along this contact (interflow/stagnating soil). This is confirmed by piezometer water level data around the area of contact between the overlying hard plinthic and underlying soft plinthic horizons, this is slightly up gradient to the G-horizon soils. Figure 5.1 shows a time series plot of the above mentioned piezometer water levels.

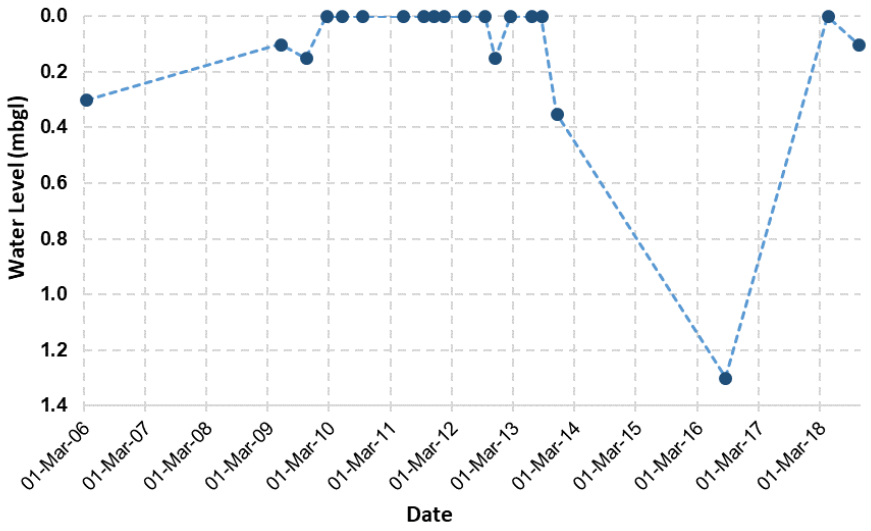


Figure 5.1 Groundwater level data from shallow piezometer located on lower hillslope (hard plinthic overlying soft plinthic horizon)

Zinc dissolved within contaminated pore water would adsorb to the mid-slope soils, as indicated by the high $K_d$ value (10.59 for MHS360). This reduction in zinc mobility could be impacted by the organic matter component, as well as the presence of clays (25% kaolinite) within this soil horizon.

Within the valley bottom the soil texture changes to have high silt (56.6%) and clay (28%) component, of which kaolinite is a considerable portion (46.8%) (represented by WET1 sample). This fine material has a low hydraulic conductivity ($K_{sat}$ 0.138 m/d) however, the clay component also impacts the cation exchange capacity, which is the highest within the site transect (15.25 cmol/kg). These are G horizon soils as evident by their gleying from continued saturation. The valley bottom soils also have a large organic component (4.06%) from the presence of alive and decaying wetland vegetation. The potential for zinc absorption is high ($K_d$ of 4.473), due to the clay and organics within the soil creating a high CEC. Contamination reaching this point within the pore water would be adsorbed to the soils under anaerobic conditions, as the water is transmitted slowly within the soil matrix (almost stagnating soil).

Up gradient from the transect, the soils (represented by sample WET_UP) contained significant gravel component (32%), however the hydraulic conductivity remained low ($K_{sat}$

of 0.02 m/d) from the finer clay matrix (kaolinite at 42.4%). Despite the clay content, these soils had a low zinc absorption ($K_d$ of 1.386). The CEC, organic carbon and organic matter content were also measured on the lower range for the site. Zinc contaminated water, should it reach this area, would move slowly, with only a small amount of zinc adsorbed to the soils, therefore any surface discharges from pipework would likely move within the wetland surface flow.

The site conceptual model described has been graphically represented in Figure 5.2 to show the soil characteristics and anticipated flow regime.

| Sample | Soil Type | Ksat m/d | Kd | CEC | pH | % Organic matter | % Clay |
|---|---|---|---|---|---|---|---|
| UHS | Orthic A | 2.135 | 13.056 | 12.92 | 5.33 | 0.90 | 13.00 |
| MHS200 | Hard plinthic | 1.389 | 1.122 | 5.57 | 3.86 | 1.06 | 19.00 |
| MHS360 | Soft plinthic | 0.138 | 2.533 | 6.20 | 3.39 | 1.17 | 19.00 |
| WET1 | G Horizon | 0.141 | 4.473 | 15.25 | 5.28 | 7.01 | 28.00 |
| | Saprolite | 0.514 | 0 | | | | |
| | Fractured Rock | 0.010 | 0 | | | | |

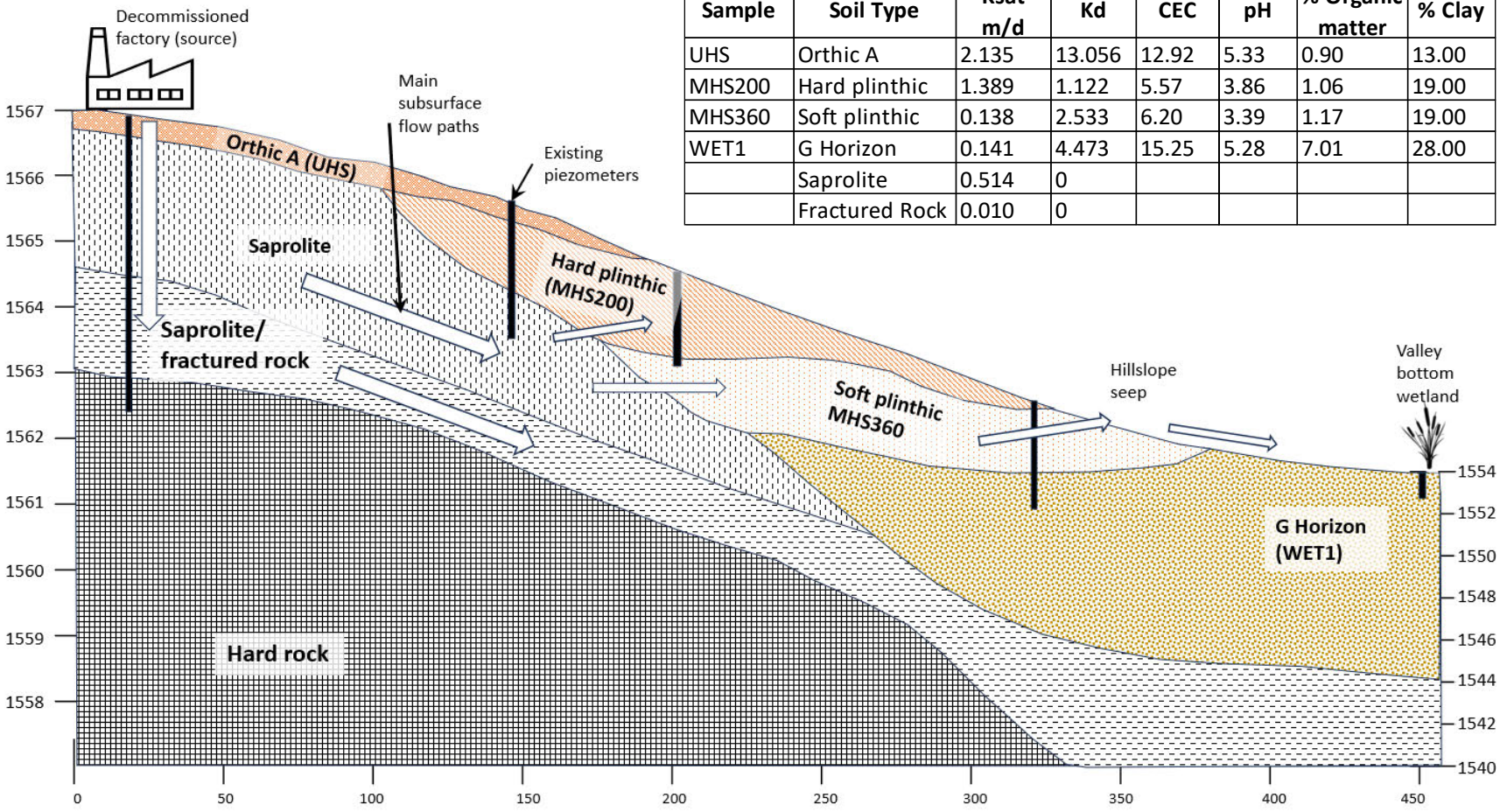


Figure 5.2 Schematic transect CSM showing main water flow paths within the vadose zone

## 5.2 Numerical Modelling

The CSM was translated into a numerical model for further simulation testing. The model setup and domain properties have been included in Appendix D, Figures D.1 and D.2. respectively. The equilibrated pressure head assigned to the model grid is shown in Figure 5.3. This was calibrated to piezometer water levels, saturated conditions at the valley bottom wetland, and the observed seepage face on the hillslope. The locations of various piezometers have been shown as observation points on the model (Figure D.1). The steady state modelled pressure heads compared to the median water levels at each of the observation points has been included in Appendix D (Figure D.2). This showed that modelled water levels were between 0.1 to 0.8 m within the median water levels for the observation points.

The model results were provided in concentration units of $kg/m^3$, however the existing site data reports concentrations in mg/l. These two terms have therefore been used interchangeably when discussing the model results.

The solute transport model shows the migration of the zinc plume from the old factory operations at the top of the hillslope. The contamination source was assumed to be present from the start of operations in 1950, up until 1990 when the old factory was decommissioned. The contaminant plume moves both vertically and horizontally from the source area, with a predominant horizontal extension above the fractured rock-saprolite interface. Figure 5.4 shows the model scenario after 20 years of factory operations, with the concentration of Zn in the pore water at >1 000 mg/l (or 1.0 $kg/m^3$ as indicated on the model) extending 50 m down gradient from the source area. At 200 m distance, the plume reduces to 250 mg/l, tapering off within 50 m.

After 40 years of operations (year 1990) the zinc concentration within the pore water reaches its highest as shown in Figure 5.5, with concentrations of >2 000 mg/l extending from the source area to 140 m down gradient. This decreases with distance to 1 000 mg/l at 215 m, 600 mg/l at 250 m and 0 mg/l at 300 m from the source. The absorption of zinc from the pore water as it flows through the topsoil (UHS) and plinthic layer (MHS200) is shown as a lower zinc concentration within the upper soils of the hillslope.

In 1992, after 40 years of operation, the old factory was decommissioned, and the source of contamination was removed. Figure 5.6 shows this next 20-year scenario model run with the removal of the contamination source and subsequent reduction in zinc concentrations throughout the site. The highest concentration of zinc noted at the end of this timestep (year 2010) was 100 m down gradient from the source within the topsoil (UHS). Minimal movement of incoming water reaches this layer as it is above the general water table and beneath the factory footprint hard stand. Incoming clean water replaces the contaminated water beneath the source area as the plume continues to be pushed horizontally through the site.

Figure 5.7 and Figure 5.8 show the modelled zinc concentrations in pore-water at each of the key monitoring points, versus the site monitoring data. The location of observation points in the model is shown in Appendix D, Figure D.1. Existing water chemistry data at 70 m downgradient from the source area showed a good comparison between the modelled Zn concentrations (Obs 1) and the actual site data (BH1 and AH1) in terms of general concentration and trends. It is likely that areas of contaminated soil were not removed/remediated during the factory decommissioning, and therefore remain as a secondary source on site, which continues to contribute to the contamination in this area. This could be a plausible explanation for the erratic zinc concentrations (0.025 to 2.4 $kg/m^3$) reported at the source area site monitoring points. At 150 m downgradient from the source, the modelled Zn concentrations (Obs 2) are elevated compared to the site data (AH6). A trend which continued 200 m downgradient, as seen with the modelled data (Obs 3) and site data (BH4). This could be due to zinc retardation reactions occurring which have not yet been considered, or that the monitoring points are not located directly in the path of the main plume body preferred flow path.

The modelled plume did not extend to the wetland area (400 m downgradient) but was withheld within the subsurface fringes of the Saprolite / G horizon and soft plinthic contact area. The lower permeability of the G horizon and soft plinthic materials causes mounding behind these layers, with excess water pushed to surface to develop a seepage face. No significant concentration of zinc was noted within this seep, as confirmed by both on-site monitoring data and modelling outputs.

Future scenarios were modelled to ascertain the potential risks posed by the contamination on the wetland. The model showed that 80 years after factory operations (year 2030), the plume would be retained within the subsurface soils of the hillslope, and not reach the valley bottom soils or seepage point Figure 5.9. The main body of the zinc plume continued to reduce in size and concentration, with only a relatively small area of top hillslope soils (UHS) having a concentration of around 1 800 mg/l. A further 20-year prediction (year 2050, Figure 5.10) showed a continued reduction in the plume width and concentration, with the highest concentration reported at 1 650 mg/l (1.65 kg/$m^3$).

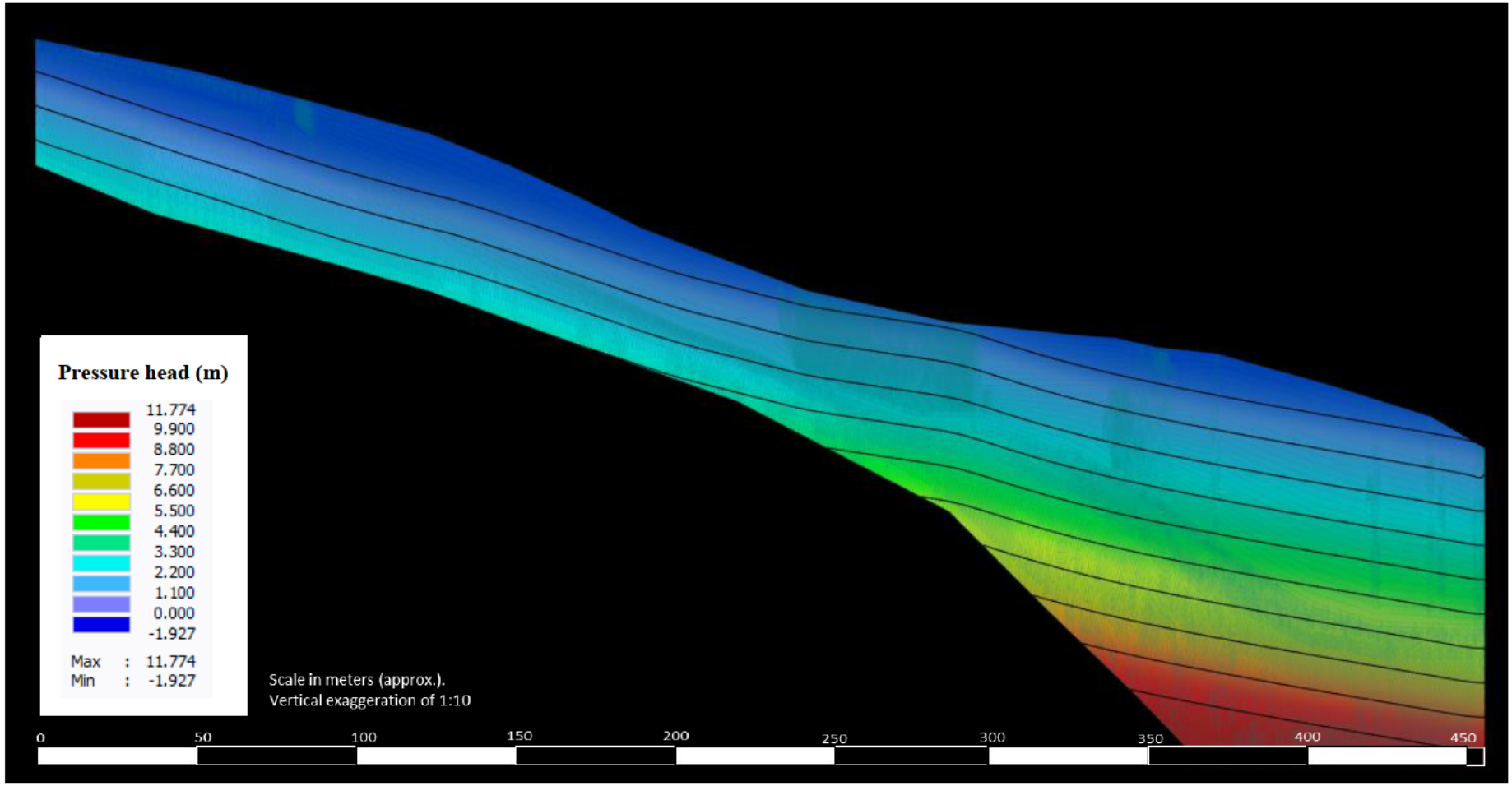


Figure 5.3 Hydrus water flow model illustrating isolines of equilibrated water pressure heads

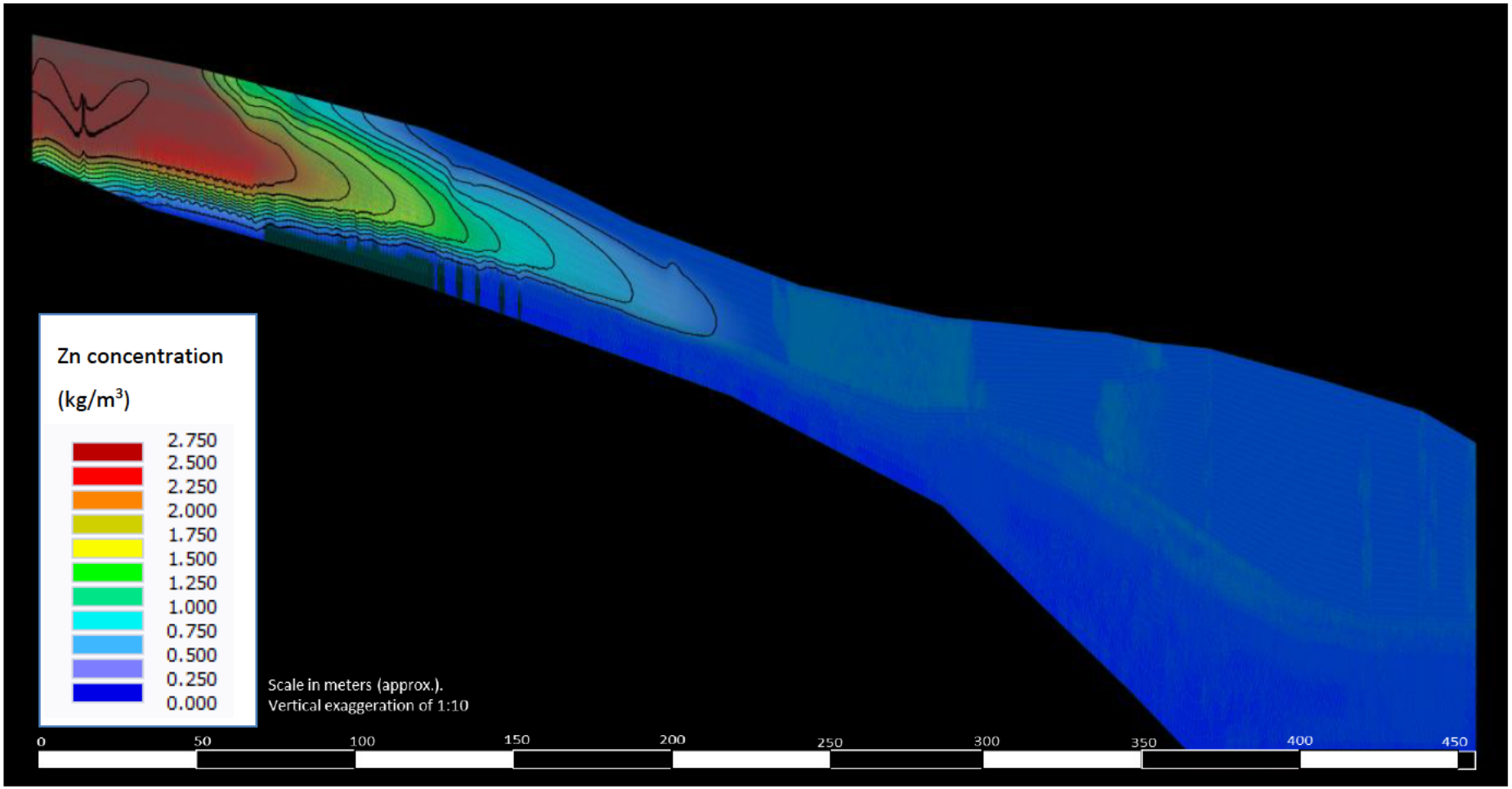


Figure 5.4 Hydrus model illustrating the extent of zinc plume migration at the year 1980 (20 years after operations commenced)

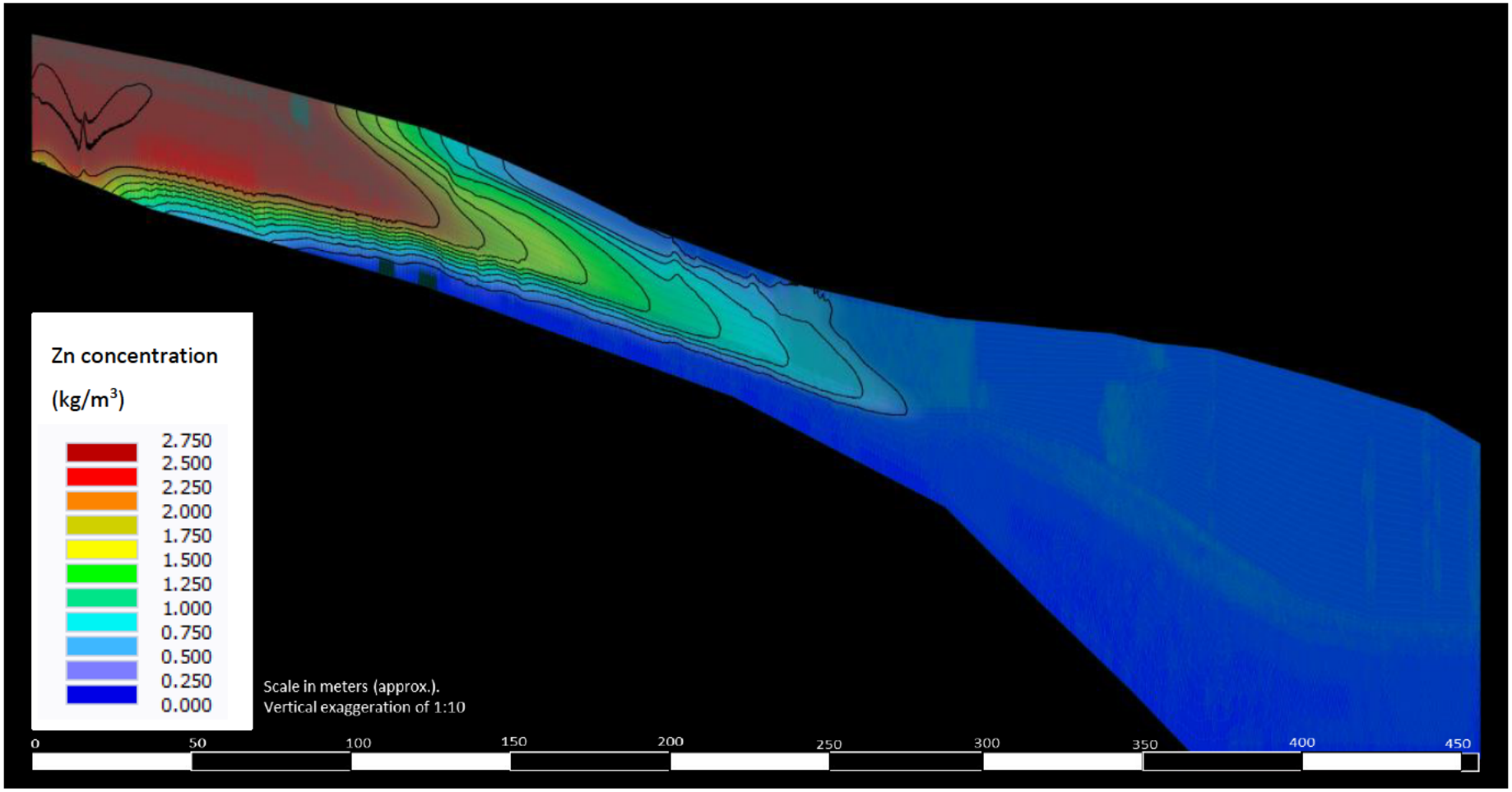


Figure 5.5 Hydrus model illustrating the extent of zinc plume migration at the year 1990 (40 years after operations commenced)

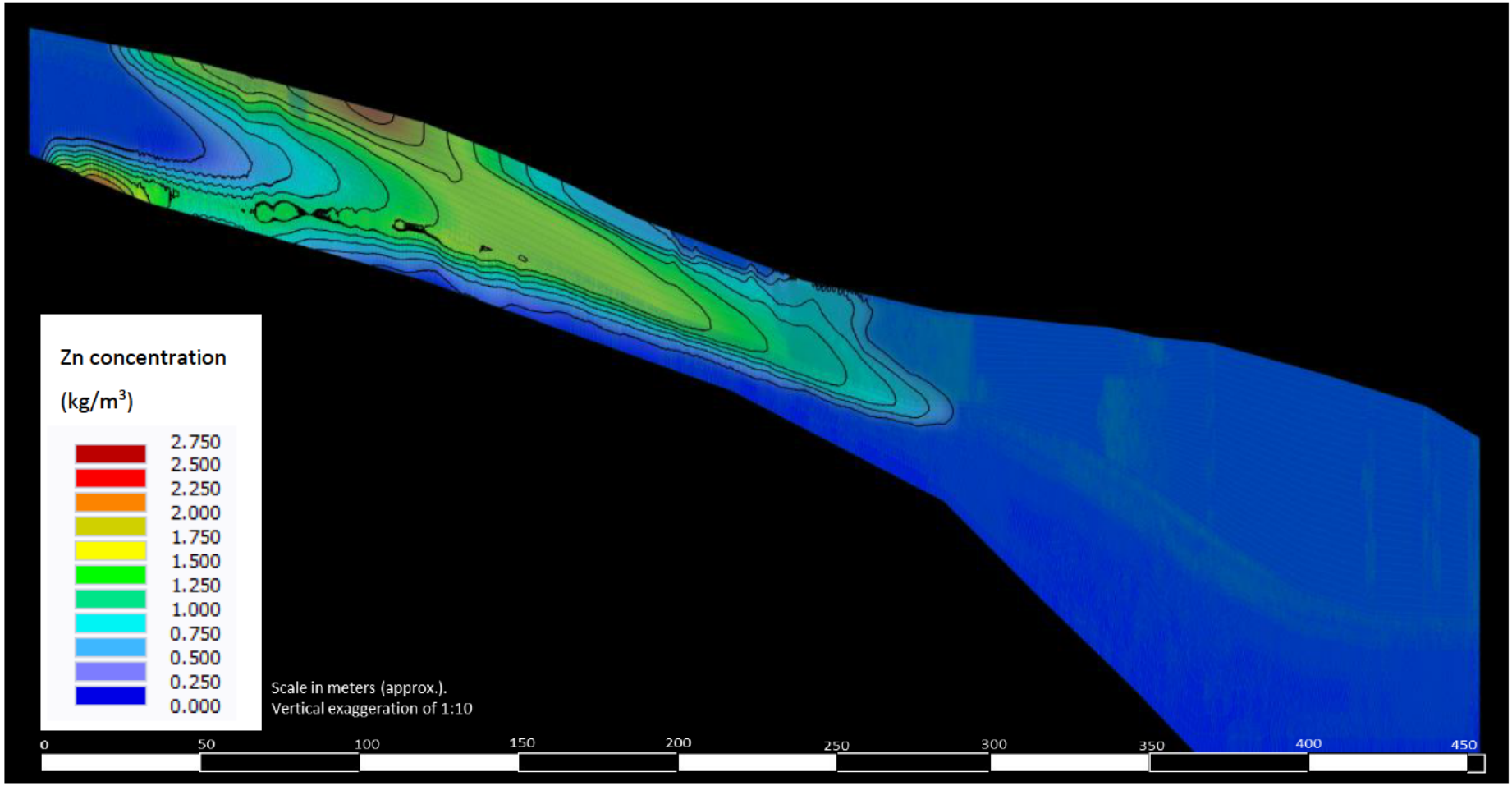


Figure 5.6 Hydrus model illustrating the extent of zinc plume migration at the year 2010 (60 years after operations commenced), following source removal

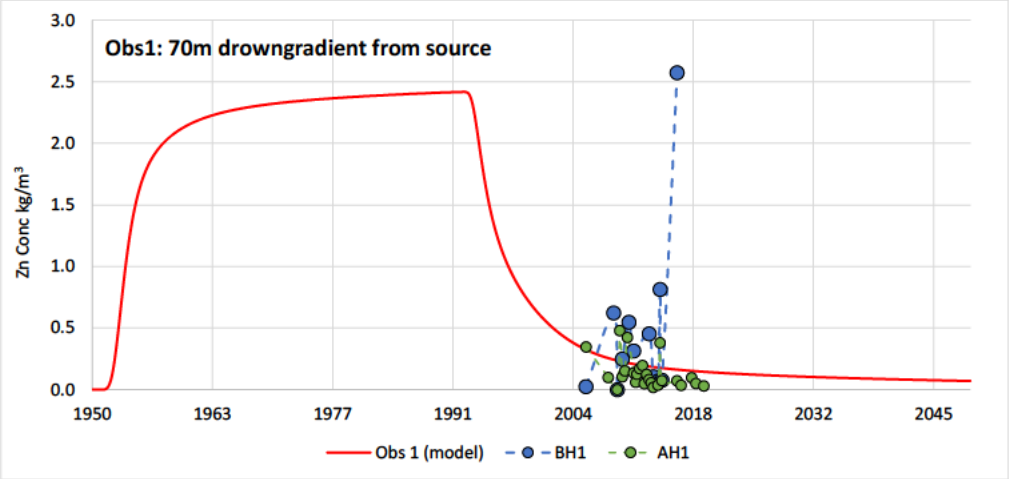


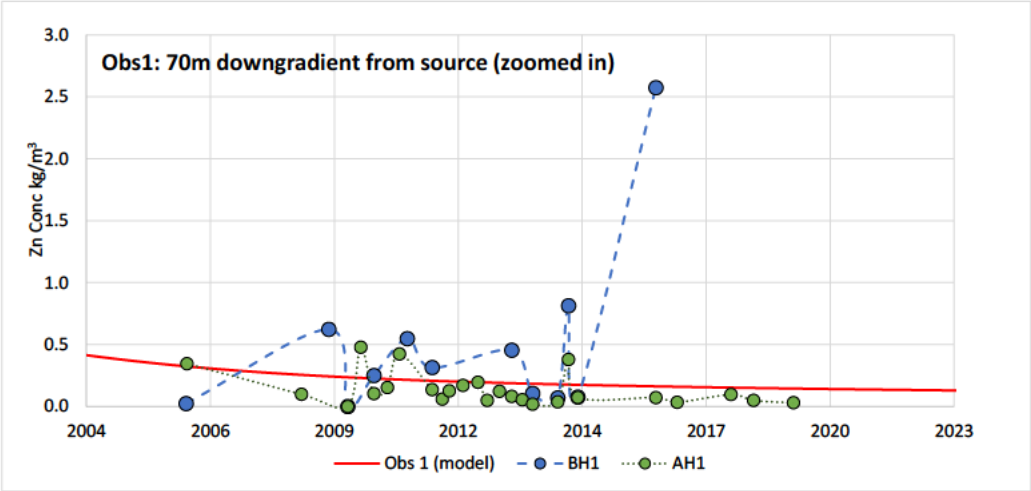


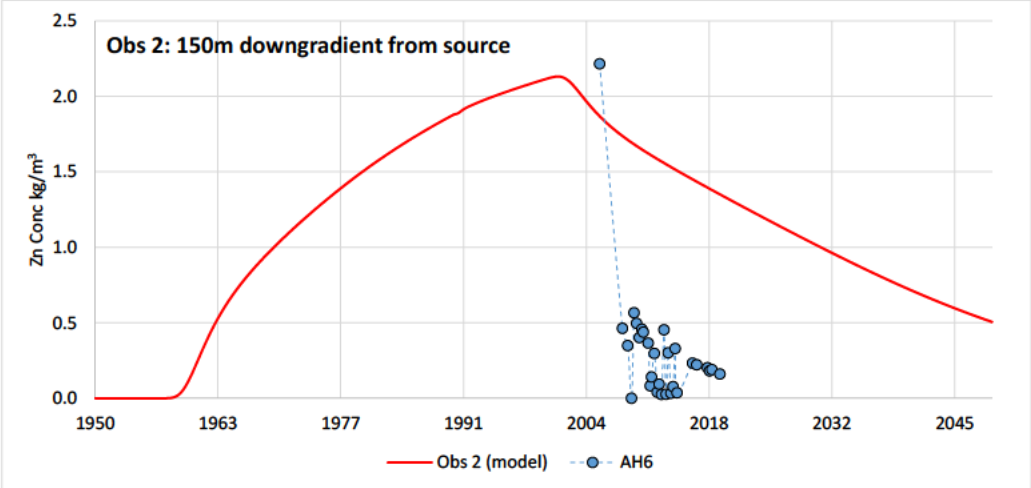


Figure 5.7 Zinc concentrations comparison between modelled observation points (Obs 1 and Obs 2) vs on-site water monitoring points

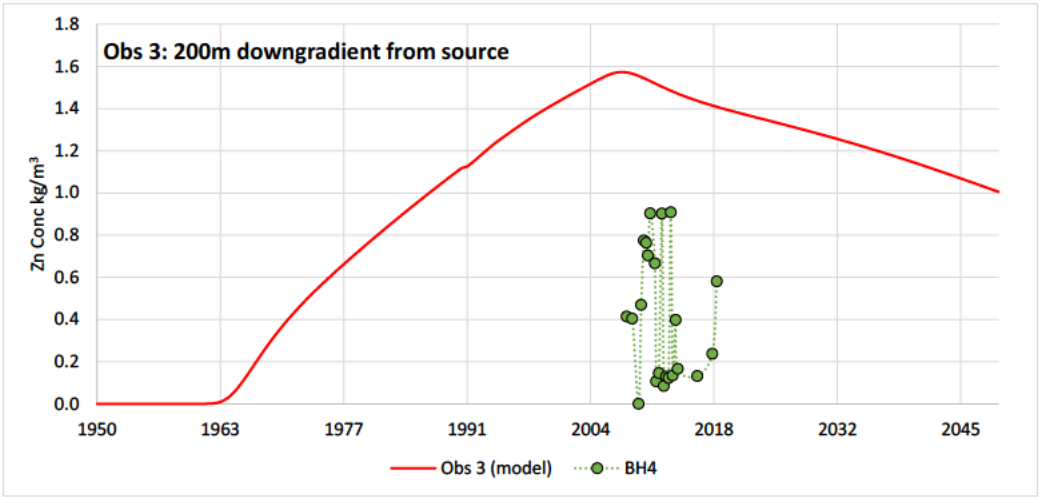


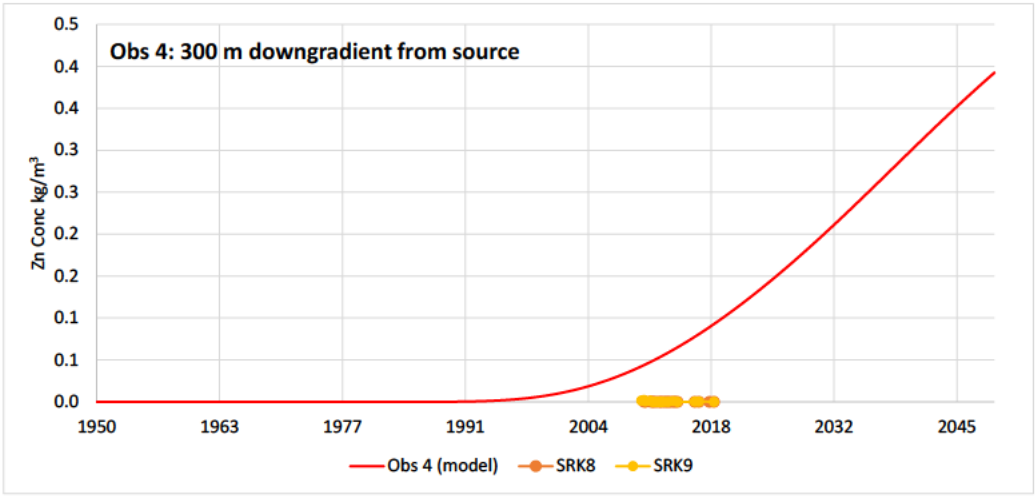


Figure 5.8 Zinc concentrations comparison between modelled observation points (Obs 3 and Obs 4) vs downgradient site water monitoring points

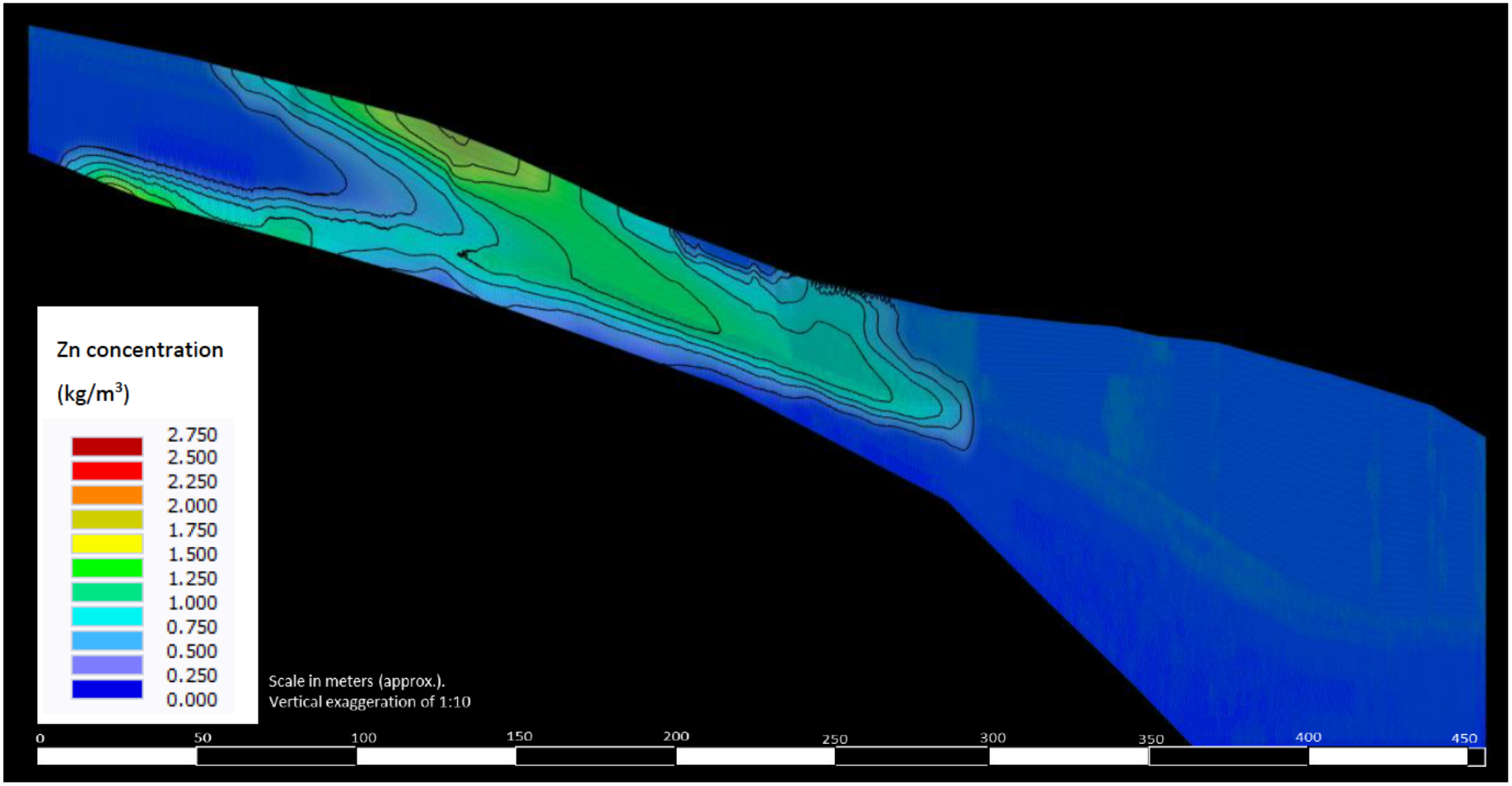


Figure 5.9 Hydrus model illustrating the predicted extent of zinc plume migration at the year 2030 (80 years after operations commenced)

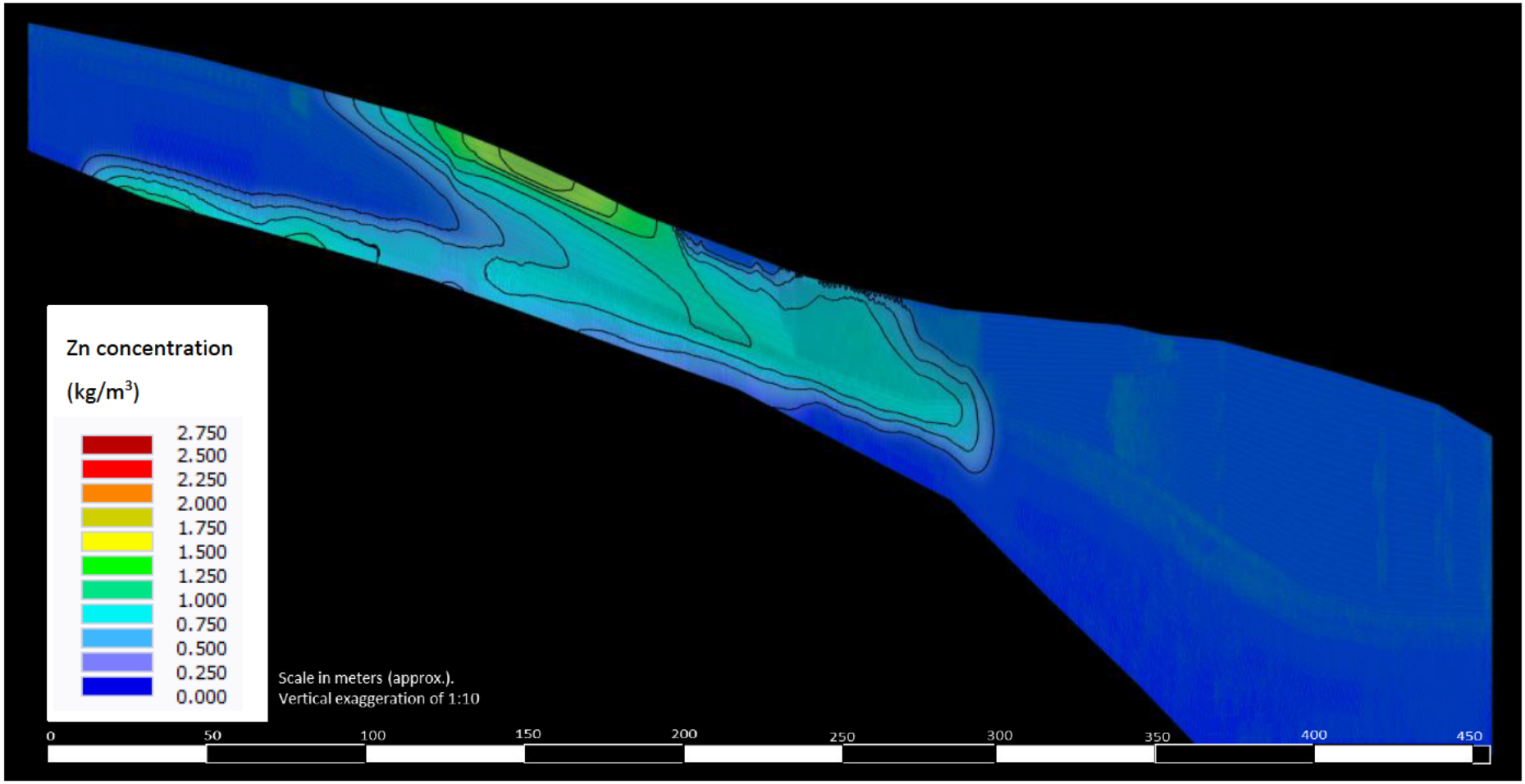


Figure 5.10 Hydrus model illustrating the predicted extent of zinc plume migration at the year 2050 (100 years after operations commenced)

### 5.2.1 Modelling assumptions and limitations

The model was based on available data for the site, either from historical water quality or water level records, observations and collected site data with regards to soil locations and properties. However, where data was unavailable, various assumptions were made. Particularly with regards to the characteristics of the soils underlying the factory area, as well as the area, duration, and concentration of the initial contamination source. The soil horizons and stratigraphy of the hillslope was also simplified due to the large extent of the study area, accessibility, and shallow soil refusal depths during soil sampling.

## 5.3 Modelling Summary

The numerical model of the site was able to simulate contaminant water flow conditions within the hillslope. It showed reasonable alignment with the available historical groundwater quality and water level data. The model demonstrated the zinc plume migration through the subsurface soils, with the main plume body remaining within the saprolite and plinthic soils of the middle hillslope. Simulations of future scenarios (20 years) showed the continued reduction of the extent and concentration of the plume, with minimal penetration into the soils of the valley bottom wetland. The soil water which was pushed to the surface along the seepage face near the wetland, was also determined to have a minimal zinc concentration.

It was therefore concluded from the model, that the hillslope soils have sufficient zinc absorption capacity for the residual plume, as to result in minimal impact to the wetland and further downstream areas.

# 6. CONCLUSIONS AND RECOMMENDATIONS FOR FURTHER RESEARCH

## 6.1 General Discussion, Outcomes, and Contributions

Soil characterisation identified physical and chemical aspects within the soils that have the potential to reduce the mobility of zinc within a contaminated site. These included elevated pH conditions, high clay content potentially leading to elevated CEC, and organic content within the soils which have the potential to form metal complexes. The results from the column leach tests to determine the equilibrium partition coefficient for zinc, showed that the relationship is not linear between zinc $K_d$ and any single physical or chemical parameter. Instead, the capacity of each soil should be assessed by taking all factors into account, including physical, chemical, and environmental parameters, followed by actual capability assessment. This can be demonstrated by comparing two soils of the site soils which were assessed to have the highest $K_d$ on the site (UHS and MHS360); the first soil had an elevated CEC, but no significant clay or organic content to attribute to this characteristic, in contrast, the second soil did not have any of the physical or chemical aspects which would identify the potential to retard zinc mobility in contaminated pore water (texture, CEC, clay mineralogy, organic matter etc). This highlights that physical and chemical characteristics identified as potential contributors to zinc retardation, my not necessarily translate to actual zinc absorption.

The column leach tests also identified the variance in $K_d$ from changes in environmental settings, namely anaerobic vs aerobic conditions. The columns leached under anaerobic conditions had a significantly higher zinc retardation capacity, either attributable to the longer contact time or soil surface area exposed to the contaminant solution, and/or due to more complex redox reactions reducing the zinc mobility.

Site data viewed holistically takes dynamic interactions between the different soils into consideration. This was emphasized in the modelling of the site, as the difference in the hydraulic conductivity of the soils determined which soils the contaminated water would flow through vs impounding behind less permeable layers, resulting in surface seepage and changes in anaerobic/aerobic conditions.

## 6.2 Challenges

A few challenges were encountered during this study. These included:

- Electricity failures during the column tests which interrupted the pump operations for constant solution flow to the columns. This was overcome by assistance with regular checks by persons assisting in the laboratory with sample collection and testing and installation of a UPS unit.
- Learning new software to undertake the modelling. This required additional time as well as the model runs were initially slow, with many changes required.
- Unconfirmed contaminant source in terms of dates of leakages, volumes, and concentrations. The old factory was decommissioned more than 30 years previously, and the contamination pre-dated this, with no paper records available. This was overcome by calibration of the model with piezometer water quality records, however some uncertainty as to the accuracy of source contamination details remains.
- As with any model, the site stratigraphy was simplified and sampling limited to the open hillslope and wetland. No detailed characterisation was undertaken of the soils beneath the factory footprint, relying on data from existing reports.

## 6.3 Future Opportunities

This project assessed the zinc retardation capacity of the soils through column testing. The $K_d$ derived using this method does not detail the adsorption reactions. This leaves room for further research to be done to assess the chemical interactions taking place within the soil matrix, focusing on the geochemical processes. It is not yet understood what fraction of the demobilised zinc has been adsorbed to the soils, complexed with organics, or precipitated through interactions with oxygen at neutral pH conditions created by the acid neutralising capacity of the soils.

This could also progress to assessing the possible release mechanisms for the re-mobilisation of zinc from the soils into the pore water, as could occur from acid spills from the current operating factory or neighbouring industrial facilities. The current HYDRUS (2D/3D) model could be extended to include the HP2 module which incorporates the geochemical modelling program PHREEQC into this domain.

## 6.4 Final Comments and Conclusions

The aim of this research was to undertake a detailed study of a zinc contaminated site to ascertain a scientifically based understanding of the mobility of zinc in the vadose zone which comprises clay-rich soils. The research results imply that the retardation capacity of the soils within the study site have sufficient potential to retard the mobility of the zinc contaminated groundwater from impacting significantly on the surface water within the wetland. The clay content of the wetland soils was thought to be a significant parameter in determining the retardation ability, however, this study highlighted the importance of holistic consideration of the site data with integration of the various physical, chemical, and environmental aspects.

# REFERENCES


Alloway, B. J. (2009). Soil factors assocaited with zinc deficiency in crops and humans. *Environmental Geochemistry and Health, 31*(5), 537-648.

Antoniadis, V., & McKinley, J. D. (2003). Measuring heavy metal migration rates in a low-permeability soil. *Environmental Chemistry Letters*(1), 103-106. https://doi.org/10.1007/s10311-002-0019-y

ASTM. (2000). *Standard test methods for determining the particle-size analysis of soils. D 422-63. Annual Book of ASTM Standards 04 08:518-520.* Philadelphia, PA: American Socieity of Testing and Materials.

Baes, C., & Sharp, R. (1983). Proposal for estimation of soil leaching and leaching constants for use in assessment models. *Journal of Environmental Quality, 12*(1), 17-28.

Bosman, H. H. (1990). Methods to convert American Class A-pan and Symon's tank evaporation to that of a representative environment. *Water SA, 16*(4).

Bostick, B., Hansel, C., La Force, M. J., & Fendorf, S. (2001, November). Seasonal fluctuations in zinc speciation within a contaminated wetland. *Environmental Science and Technology, 35*(19), 3823-3829. https://doi.org/10.1021/es010549d

Brink, A. B., & Bruin, R. M. (2001). Guidelines for soil and rock logging in South Africa, (2nd Impression). *Geoterminology Workshop organised by AEG, SAICE and SAIEG, 1990.*

Broadley, M. R., White, P. J., Hammond, J. P., Zelko, I., & Lux, A. (2007). Zinc in plants. *New Phytologist, 173*(4), 677-702.

Bunzel, K., Trautmannsheimer, M., & Schramel, P. (1999). Partitioning of heavy metals in a soil contaminated by slag: A redistribution study. *Journal of Environmental Quality*, 1168-1173.

Burglsser, C. S., Cernik, M., Borkovec, M., & Sticher, H. (1993). Determination of nonlinear adsorption isotherms from column experiments: An alternative to batch studies. *Envrionment Science and Technology, 27*(5), 943-948.

Cappuyns, V., & Rudy, S. (2008). The use of leaching tests to study the potential mobilization of heavy metals from soils and sediments: a comparison. *Water Air and Soil Pollution*, 95-111.

Casagranade, J. C., Soares, M. R., & Mouta, E. R. (2008). Zinc adsorption in highly weathered soils. *Pesquisa Agropecuária Brasileira, 43*(1), 131-139.

Cavallaro, N., & McBride, M. (1984). Zinc and copper sorption and fixation by an acid soil clay: effects of selective dissolutions. *Soil Science Socieity of Ameria Journal, 45*(5), 1050-1054.

Cernik, M., Federer, P., Borkovec, M., & Sticher, H. (1995). Calculation of zinc transport in a soil contaminated by a brass foundry. *Groundwater Quality: Remediation and Protection. Proceedings of the Prague Conference, IAHS Publ. No.225*, (pp. 239-246).

Cherry, J., Gillham, R., & Barker, J. (1984). Contaminants in groundwater: chemical processes. *Groundwater Contamination*, 46-64.

Critto, A., Cantarella, L., Carlon, C., Giove, S., Petruzzelli, G., & Marcomimi, A. (2006). Decision support-oriented selection of remediatino technologies to rehabilitate contaminated sites. *Integrated Environmental Assessment and Management, 2*(3), 273-285.

Cui, J., Luo, C., & Li, X. (2017). Speciation and leaching of trace metal contaminants from e-waste contaminated soils. *Journal of hazardous Materials*, 150-158. https://doi.org/10.1016/j.jhazmat.2016.12.060

Degryse, F., Smolders, E., & Parker, D. R. (2009). Partitioning of metals (Cd, Co, Ni, Pb, Zn) in soils: concepts, methodologies, prediction and applications - a review. *European Journal of Soil Science, 60*, 590-612.

Dos Santos, D. R., Cambier, P., Mallmann, F. J., Labanowski, J., Lamy, I., Tessier, D., & van Oort, F. (2013). Prospective modeling with Hydrus-2D of 50 years Zn and Pb movements in low and moderately metal-contaminated agricultural soils. *Journal of Contaminant Hydrology, 145*, 54-66. https://doi.org/10.1016/j.jconhyd.2012.12.001

DSA. (2015). *Hydropedological Survey Report - Site A.* Bloemfontein: Digital Soils Africa.

DWAF. (1996). *South African Water Quality Guidelines. Volume 7 Aquatic Ecosystems.* Pretoria: Department of Water Affairs and Forestry.

Finsterle, S., Doughty, C., Kowalsky, M. B., Moridis, G. J., Pan, L., Xu, T., . . . Pruess, K. (2008). Advanced vadose zine simulations using TOUGH. *Vadose Zone Journal, 7*, 601-609.

Freeze, R. A., & Cherry, J. A. (1979). *Groundwater.* New Jersey: Prentice-Hall Inc.

Gallichand, J., Madramootoo, C., Emight, P., & Barrington, S. (1990). An evaluation of the Guelph Permeameter for measureing saturated hydraulic conductivity. *American Society of Agricultural and Biological Engineers, 33*(4), 1179-1184. https://doi.org/10.13031/2013.31455

Garcia-Gaines, R. A., & Frankenstein, S. (2015). *USCS and the USDA Soil Classification System. ERDC/CRREL TR-15-4.* Vicksburg: U.S. army Engineer Research and Development Centre.

Garcia-Gutierrez, C., Pachepsky, Y., & Martin, M. A. (2018). Technical note: Saturated hydraulic conductivity and textural heterogeneity of soils. *Hydrology and Earth System Sciences*(22), 3923-3932. Retrieved from https://doi.org/10.5194/hes-22-3923-2018

Goodwin, F. (1989). Zinc Compounds. In J. Kroshwitz, M. Howe-Grant, & eds, *Kirk-Othmer Encyclopedia of Chemical Technology* (pp. 840-853). New York: Wiley. Retrieved from https://doi.org/10.1002/0471238961.2609140307151504.a02.pub2

Google Maps. ((n.d)). South Africa. Retrieved June 6, 2019. Google Earth. Maxar Technologies.

Guinoiseau, D., Gelabert, A., Moureau, J., Louvat, P., & Benedetti, M. F. (2016). Zn isotope fractionation during sorption onto kaolite. *Environmental Science and Technology, 50*, 1844-1852. https://doi.org/10.1021/acs.est.5b05347

Han, K. H., Ro, H. M., Cho, H. J., Hwang, S. W., Cho, H. R., & Song, K. C. (2008). Unsaturated hydraulic conductivity functions of van Genuchten's and Campbell's medels tested by one-step outflow methods through Tempe pressure cell. *Korean Journal of Soil Science and Fertilisation, 41*(4), 273-278.

Hillel, D. (1980). *Applications of Soil Physics.* New York: Academic Press.

Holden, P. A., & Fierer, N. (2005). Vadose Zone: Microbial Ecology. In D. Hillel (Ed.), *Encyclopedia of Soils in the Environment* (pp. 216-224). Elsevier. https://doi.org/https://doi.org/10.1016/B0-12-348530-4/00172-7

IUSS. (2002). *World Referance Base for Soil Resources. International soil classification system for naming soils and creating legends for soil maps.* (4 ed.). Vienna, Austria: International Union of Soil Sciences.

Jacques, D., Simunek, J., & van Genuchten, M. T. (2003). The HYDRUS-PHREEQC multicomponent transport model for variably-saturated porous media: Code verification and application. *International Groundwater Modeling Centre, Colorado School of Mines. Conference September 16-19.*

Jalali, M., & Hemati, N. (2013). Chemical fractionation of seven heavy metals (Cd, Cu, Fe, Mn, Ni, Pb, and Zn) in selected paddy soils of Iran. *Paddy Water Environment, 11*, 299-309. https://doi.org/10.1007/s10333-012-0320-8

Job, N. M., le Roux, P. A., Turner, D. P., van der Waals, J. H., Grundling, A. T., van der Walt, M., . . . Paterson, D. G. (2018). *Developing wetland distribution and transfer functions from land type data as a basis for the critical evaluation of wetland delineation guidelines by inclusion of soil water flow dynamics in catchment areas.* Pretoria: Water Research Commission.

Kalbasi, M., Racz, G., & Lewen-Rudgers, L. (1978). Reaction products and solubility of applied zinc compounds in some Manitoba soils. *Soil Science, 125*(1), 55-64.

Kent, D. B., Abrams, R. H., Davis, J. A., Coston, J. A., & Le Blanc, D. R. (2000). Modeling the influence of variable pH on the transport of zinc in a contaminated aquifer using semiemperical surface complexation models. *Water Resources Research, 36*(12), 3411-3425.

Khan, S., Cao, Q., Zheng, Y., Huang, Y. Z., & Zhu, Y. G. (2008). Health risks of heavy metals in contaminated soils and food crops irrigated with wastewater in Beijing, China. *Environmental Pollution, 152*(3), 686-692.

Lindsay, W. L. (1979). *Chemical Equilibria in Soils.* New York: John Wiley & Sons Inc.

MacDonald, J. D., Belanger, N., & Hendershot, W. H. (2004). Column leaching using dry soil to estimate solid-solution partitioning observed in zero-tension lysimeters to trace metals. *Soil and Sediment Contamination, 13*, 375-390. https://doi.org/10.1080/10588330490466021

Mallmann, F. J., Dos Santos, D. R., Ceretta, C. A., Cella, C., Simunek, J., & van Oort, F. (2012). Modeling field-scale vertical movement of zinc and copper in a pig slurry-ammended soil in Brazil. *Journal of Hazardous Materials, 243*, 223-231.

Merva, G. E. (1987). The velocity permeameter technique for rapid determination of hydraulic conductivity in-situ. *Third International Workshop on Land Drainage. 7-11 December 1987*, (pp. G55-G66). Columbus.

Molina, M., Nanquian-Cerda, K., & Escudey, M. (2010). Sorption and selectivity sequesces fo Cd, Cu, Ni, Pb and Zn in single- and multi-component systems in a cultivated Chilean Mollisol. *Soil and Sediment Contamination, 19*, 405-418. https://doi.org/10.1080/15320383.2010.486053

Naiker, K. (2023). Email to Talbot & Talbot Customer Services, 28 September 2023.

Naka, A., Yasutaka, T., Sakanakura, H., Kalebe, U., Watanabe, Y., Inoba, S., . . . Someya, M. (2016). Column percolation test for conaminated soils: Key factors for standardization. *Journal of Hazardous Materials, 320*, 326-340. https://doi.org/10.1016/j.jhazmat.2016.08.046

Noshadi, M., Pavizi, H., & Sepaskhah, A. (2012). Evaluation of different methods for measuring field saturated hydraulic conductivity under high and low water table. *Vadose Zone Journal, 11*. https://doi.org/10.2136/vzj2011.0005

Page, A. L. (Ed.). (1983). *Methods of Soil Analysis: Part 2 Chemical and Microbiological Properties, Agronomy Monograph 9.* American Socieity of Agronomy. https://doi.org/10.2134/agronmonogr9.2.2ed

Panday, S., & Huyakorn, P. S. (2008). MODFLOW SURFACT: A state-of-the-art use of vadose zone flow and transport equations and numerical techniques for environmental evaluations. *Vadose Zone Journal, 7*, 610-631.

Parkhurst, D., & Appello, C. (2013). *Discription of input and examples for PHREEQC version 3: a computer program for speciation, batch-reaction, one-dimentional transport and inverse geochemical calculations.* Denver: US Geological Survey.

PC Progress. (2006). HYDRUS (2D/3D). Version 3.04.0130. (M. Sejna, J. Simunek, & R. van Genuchten, Compilers) Retrieved from www.pc-progress.com

Pepper, I., Gerba, C. P., & Gentry, T. (2014). *Environmental Microbiology.* Amsterdam: Elsevier.

Plum, L. M., Rink, L., & Haase, H. (2010). The essential toxin: impact of zinc on human health. *International Journal of Environmental Research and Public Health, 7*(4), 1342-1365. https://doi.org/10.3390/ijerph7041342

Pourbaix, M. (1974). *Atlas of electrochemical equilibria in aqueous solutions.* Houston: NACE International.

Reynolds, W. D. (1993). Saturated hydraulic conductivity: Laboratory measurement. In M. R. Carter (Ed.), *Soil sampling and methods of analysis* (pp. 589-598). Boca Raton, FL: Canadian Society of Soil Science. Lewis Publications.

Reynolds, W. D., & Elrick, D. E. (1984). *Measurement of field-saturated hydraulic conductivity, sorptivity and the conductivity-pressure head relationship using the "Guelph Permeameter".*

Reynolds, W. D., & Elrick, D. E. (1985). In-Situ measurement of field saturated hydraulc conductivity, sorptivity and the w-parameter using the Guelph Permeameter. *Soil Science, 140*(4), 292-302.

Rice, E. W., Baird, R. B., Eaton, A. D., & Clesceri, L. S. (Eds.). (2012). *Standard Methods for the Examination of Water and Wastewater. 22th Edition.* American Public Health Association.

Rieuwerts, J. S., Thornton, I., Fargo, M. E., & Ashmore, M. R. (1998). Factors influencing metal bioavailability in soils: preliminary investigations for the development of a critical loads approach for metals. *Chemical Speciation and Bioavailability, 10*(2), 61-75. https://doi.org/10.3184/09542

Rogers, J. S., & Carter, C. E. (1987). Auger hole hydraulic conductivity determination in layered soils. *Transactions of the ASAE, 30*, 374-378. Mishigan, USA: American Socieity of Agricultural and Biological Engineers.

RSA. (1998). *Government Gazette No. 19182 Vol. 398. Republic of South Africa National Water Act 36 of 1998.* Cape Town: Republic of South Africa.

RSA. (1998). *Government Gazette No. 19519, Vol. 401, Republic of South Africa National Enviornmental Management Act 107 of 1998.* Cape Town: Republic of South Africa.

RSA. (2009). *Government Gazette No.32000 Vol. 525. Republic of South Africa National Environmental Management Waste Act 59 or 2008.* Cape Town: Government Gazette.

RSA. (2010). *Republic of South Africa Framework for the Management of Contaminated Land.* Pretoria: Department of Environmental Affairs.

Rutkowska, B., Szulc, W., Bomze, K., Gozdowski, D., & Spychaj-Fabisiak, E. (2015). Soil factors affecting solubility and mobility of zinc in contaminated soils. *International Journal of Enviornmnental Science and Technology, 12*, 1687-1694. https://doi.org/10.1007/s13762-014-0546-7

Simunek, J. J., Jacques, D., Langergraber, G., Bradford, S. A., Sejna, M., & van Genuchten, M. T. (2013). Numerical modeling of contaminant transport using HYDRUS and its specialized modules. *Journal of the Indian Institute of Science, 92*(2), 265-284.

Simunek, J., & Bradford, S. A. (2008). Vadose Zone Modeling: Introduction and Importance. *Vadose Zone Journal, 7*(2), 581-586. https://doi.org/10.2136/vzj2008.0012

Simunek, J., van Genuchten, M. T., & Sejna, M. (2008). Development and applications of the HYDRUS and STANMOD software packages, and related codes. *Vadose Zone Journal, 7*(Special Issue "Vadose Zone Modeling" 2), 587-600. https://doi.org/10.2136/VZJ2007.0077

Simunek, J., van Genuchten, M. T., Sejna, M., Toride, N., & Leij, F. J. (1999). *The STANMOD computer software for evaluating solute transport in porous media using analytical solutions of convection-dispersion equation. Versions 1.0 and 2.0*

*IGWMC-TPS-71.* Golden, Colorado: International Groundwater Modeling Centre. Colorado School of Mines.

SRK. (2016). *Groundwater Plume and Phytoremediation Assessment in SiteA.* Johannesburg: SRK Consulting.

SRK. (2018). *Site A 2016-2017 Site Monitoring.* Johannesburg: SRK Consulting.

Steefel, C., & Yabusaki, S. (1996). *OS3D/GIMRT, Software for multicomponent-multidimentional reactive transport, user manual and programmers guide. PNL-11166.* Richland: Pacific North West Laboratory.

Stephan, C. H., Courchesne, F., Hendershot, W. H., McGrath, S. P., Chaudri, A. M., Sappin-Didier, V., & Sauve, S. (2008). Speciation of zinc in contaminated soils. *Environmental Pollution, 155*(2), 208-216. https://doi.org/10.1016/j.envpol.2007.12.006

Stephens, D. B. (2019). *Vadose Zone Hydrology.* New York: CRC Press.

Svendsen, M. L., Steinnes, E., & blom, H. A. (2011). Partitioning of Zn, Cd, Pb, and Cu in organic-rich soil profiles in the vicinity of a zinc smelter. *Chemical Speciation and Bioavailablity, 3*(4), 189-200. https://doi.org/10:3184/0954222911X13103862613085

Tan, K. H. (2005). *Soil Sampling, Preparation, and Analysis (2nd Edition).* Boca Raton: CRC Press. https://doi.org/10.1201/9781482274769

Tanchuling, M. A., Khan, M. R., & Kusakabe, O. (2003). Zinc sorption in clay using batch equilibrium and column leaching tests. *Materials and Geoenvironment, 50*(1), 381-384.

The Non-affiliated Soil Analysis Work Committee. (1990). *Handbook of Standard Soil Testing Methods for Advisory Purposes.* Pretoria: Soil Science Society of South Africa.

Toride, N., Leij, F. J., & van Genuchten, M. T. (1995). *The CXTFIT code for estimating transport parameters from laboratory or field tracer experiments. Version 2.0, Research Report No. 137.* Riverside, CA: U.S. Salinity Laboratory. USDA.

US Army Corps of Engineers. (2012). *Environmental Quality. Conceptual Site Models.* Washinton DC: USACE.

USDA. (1987). *Soil Mechanics Level 1, Module 1. Unified Soil Classification System Study Guide (Revised March 1987).* Soil Conservation Service. Washington DC: Unitied States Department of Agriculture.

USEPA. (1987). *Summary review of health effects associated with zinc and zinc oxide. Health issue assessment.* Environmental Criteria and Assessment Office, Office of Health and Environmental Assessment, Office of Research and Development. Durham: United States Environmental Protection Agency.

USEPA. (1999). *Understanding variation in partition coefficient, Kd, values.* Office of Air and Radiation. Washington: United States Environmental Protection Agency.

Vallee, B. L., & Falchuk, K. H. (1993). The Biochemical Basis of Zinc Physiology. *Physiological Reviews, 73*(1), 79-118. https://doi.org/10.1152/physrev.1993.73.1.79

van Dam, J. C., Groendendijk, P., Hendriks, R. F., & Kroes, J. G. (2008). Advances of medling water flow in variable saturated soils with SWAMP. *Vadose Zone Journal, 7*, 640-653.

van Genuchten, M. T. (1980). A closed-form equation for predicting the hydraulic conductivity of unsaturated soils. *Soil Science Socieity of America Journal*, 892-898.

van Genuchten, M. T., Leij, F. J., & Yates, S. R. (1991). *The RETC Code for Quantifying the Hydraulic Functions of Unsaturated Soils, Version 1.0. EPA Report 600/2-91/065.* Riverside, Ca: U.S. Salinity Laboratory.

Van Tol, J., & Le Roux, P. (2019). Hydropedoloical grouping of South African soil forms. *South African Journal of Plant and Soil, 36*(3), 233-235. https://doi.org/10.1080/02571862.2018.1537012

White, M. D., Oostrom, M., Rockhold, M. L., & Rosing, M. (2008). Scalable modleing of carbon tetracholoride migration at the Hanford site using the STOMP simulator. *Vadose Zone Journal*, 654-666.

Wischmeier, W., Johnson, C., & Cross, B. (1971). A soil erodibility nomograph for farmland and construction sites. *Journal of Soil and Water Conservation, 26*, 189-193.

Wuana, R. A., & Okeiemen, F. E. (2012). Heavy metals in contaminated soils: A review of sources, chemistry, risks and best available strategies for remediation. *International Scholarly Research Network - Ecology*. https://doi.org/10.5402/2011/402647

# APPENDIX A: SOIL COLUMN PACKING

The setup details for soil column leaching experiment as described in Section 3.6, are detailed in Table A.1.

Table A.1 Soil column setup details

| | Column 1&2 UHS | Column 3&4 MHS200 | Column 5&6 WET1 | Column 7&8 MHS360 | Column 9 & 10 WET_UP |
|---|---|---|---|---|---|
| Bulk density | 1.44 | 1.53 | 0.87 | 1.58 | 1.87 |
| Particle density | 2.35 | 2.41 | 2.08 | 2.46 | 2.53 |
| Porosity | 0.384 | 0.366 | 0.584 | 0.356 | 0.26 |
| Column diameter (cm) | 13.9 | 13.9 | 13.9 | 13.9 | 13.9 |
| Column height (cm) | 33.5 | 30.5 | 34 | 33.8 | 33.5 |
| Column volume ($cm^3$) | 5 083.52 | 4 628.28 | 5 159.39 | 5 129.04 | 5 083.52 |
| Weight soil per column (g) | 11 946.26 | 11 154.14 | 10 731.53 | 12 617.44 | 12 861.30 |
| $K_{sat}$ (m/s) | 1.87E-06 | 4.24E-06 | 6.76E-06 | 4.12E-06 | 3.01E-06 |
| Flow @ 50% $K_{sat}$ ($cm^3$/min) | 0.853 | 1.928 | 3.077 | 1.876 | 1.370 |
| Pump setting flow rate (ml/min) | 0.663 | 0.20 | 0.66 | 0.66 | 0.20 |
| 1 pore volume ($cm^3$) | 1952 | 1694 | 3013 | 1826 | 1322 |
| Initial water mass KBr solution | 951.634 | 849.752 | 1571.034 | 972.466 | 760.494 |
| Conc KBr per column @ 2000 mg/l | 1903.27 | 1699.50 | 3142.07 | 1944.93 | 1520.99 |
| Initial saturation % | 48.8% | 50.2% | 52.1% | 53.3% | 57.5% |

# APPENDIX B: ZINC CHLORIDE LEACHING SOLUTION DETAILS

Laboratory measurements taken of the zinc chloride leaching solution for the duration of the experiment are provided in Table B.1. ORP measurements have been converted to reference the standard hydrogen electrode.

Table B.1 ZnCl leaching solution measurements (pH, EC, Temp, Eh)

| Date | pH | EC mS/cm | Temp (°C) | Eh (V) |
|---|---|---|---|---|
| 08-Feb | 3.89 | 3.98 | 16.4 | 0.5258 |
| 15-Feb | 3.86 | 1.56 | 16.4 | 0.5008 |
| 16-Feb | 3.12 | 1.78 | 16.5 | 0.5728 |
| 22-Feb | 3.18 | 1.64 | 18.1 | 0.5645 |
| 23-Feb | 3.34 | 1.57 | 20.3 | 0.5321 |
| 01-Mar | 3.23 | 1.12 | 19.4 | 0.6353 |
| 16-Mar | 3.33 | 1.10 | 18.0 | 0.5435 |

# APPENDIX C: MEASUREMENTS TAKEN DURING COLUMN EXPERIMENTS

Laboratory measurements taken from the leachate during ZnCl column leach experiments. The data has been graphed for ease of discussion.

Figure C.1 shows the redox measurements taken on the leachate during ZnCl column experiments.

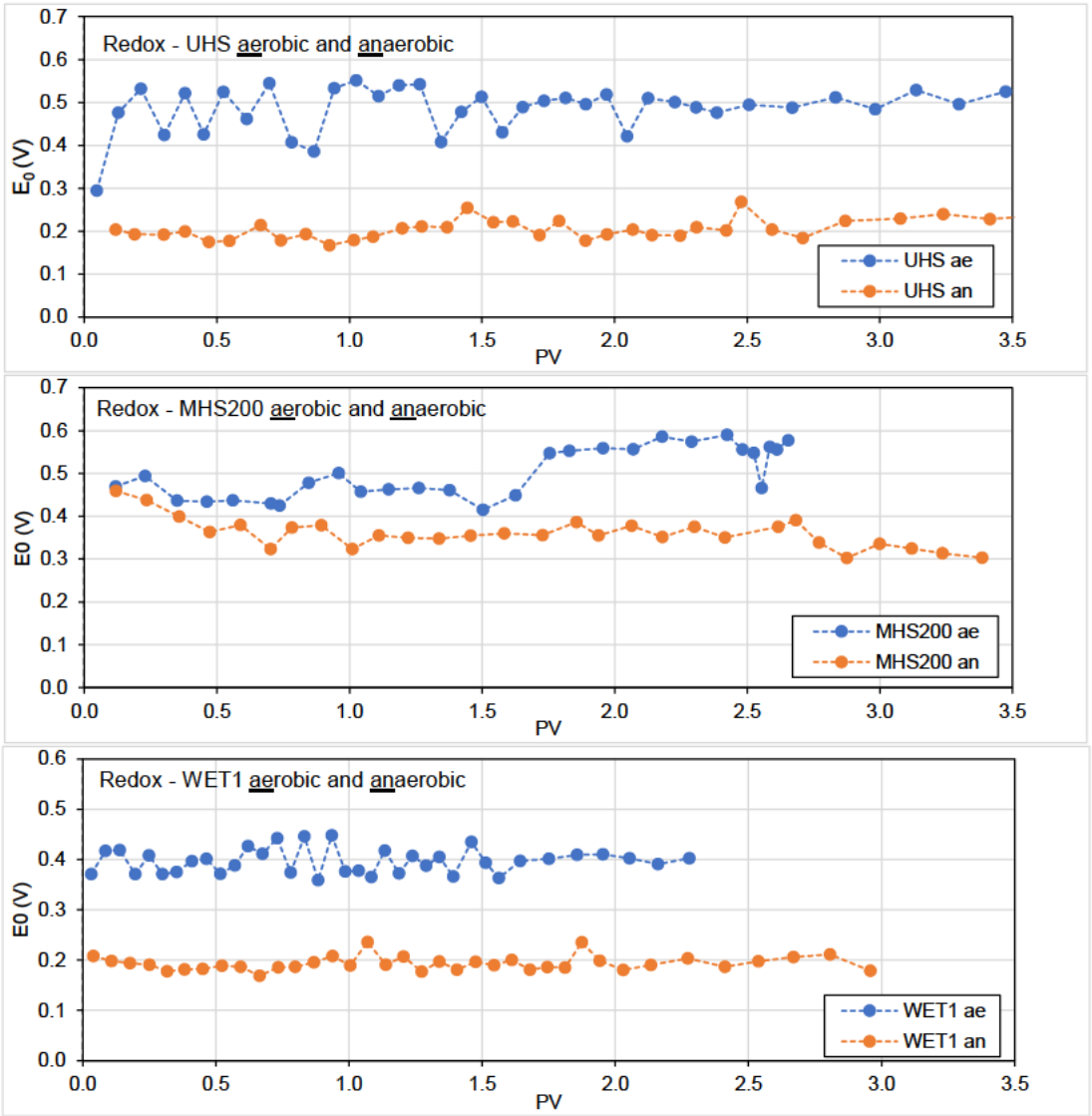

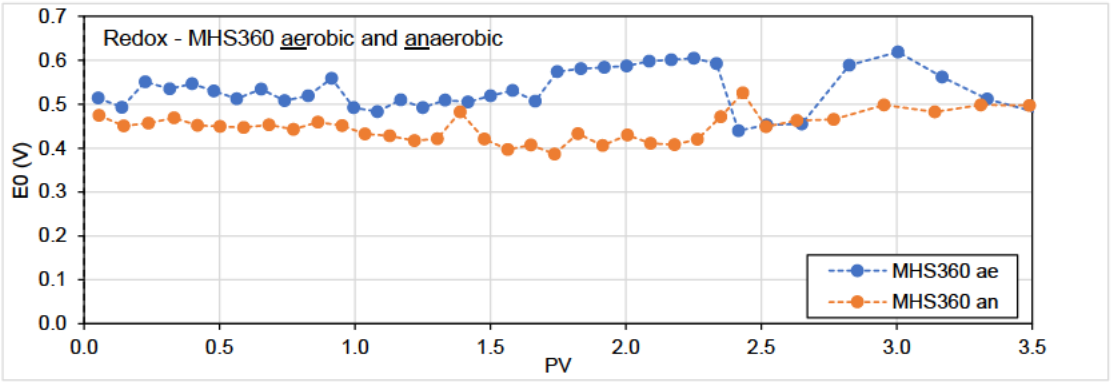


Figure C.1 Graphs of redox measurements vs pV from soil column leachate samples

Figure C.2 shows the comparison of EC datasets from measurements taken during the leaching experiment vs samples submitted to a laboratory for analysis. It also shows which samples were selected for additional analysis based in pore volumes and inflections in the EC data.

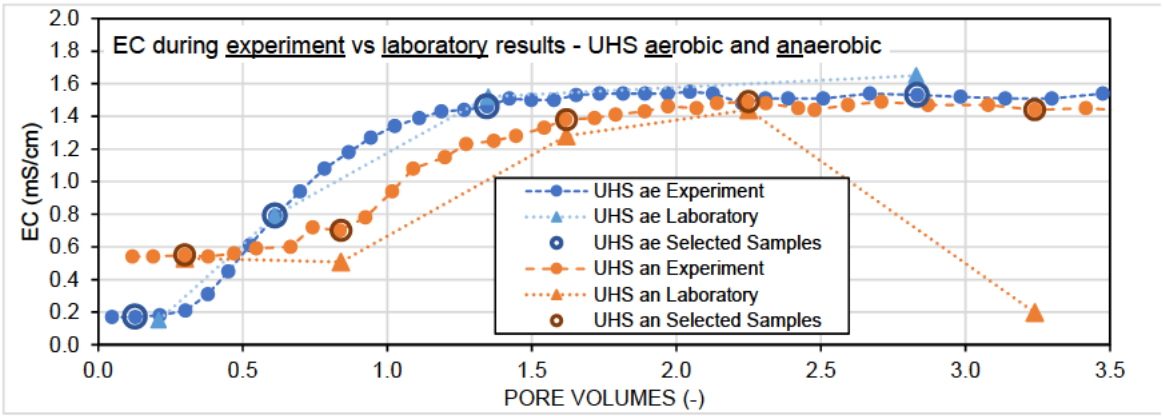


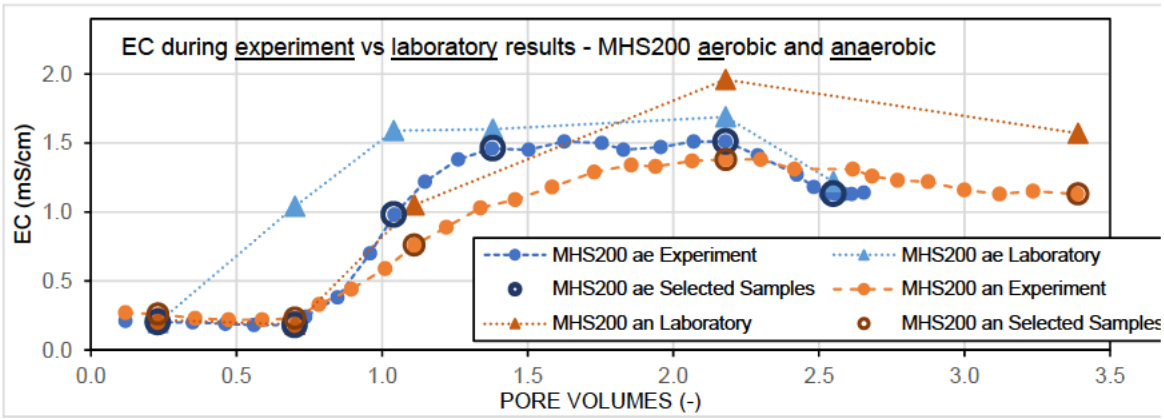


(continued on next page)

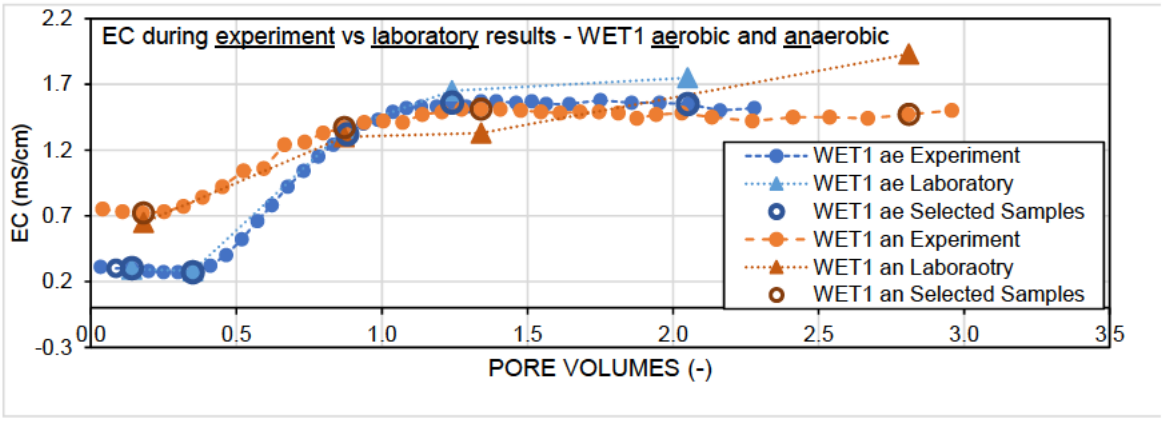


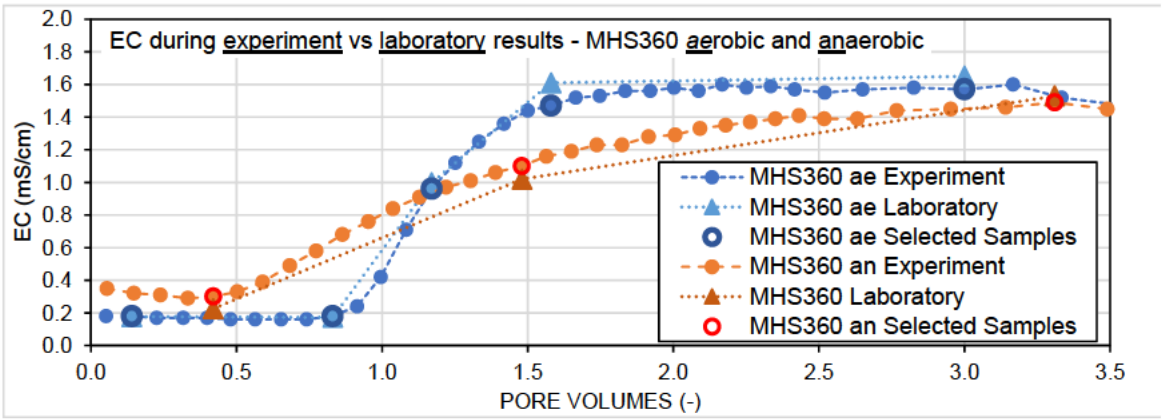


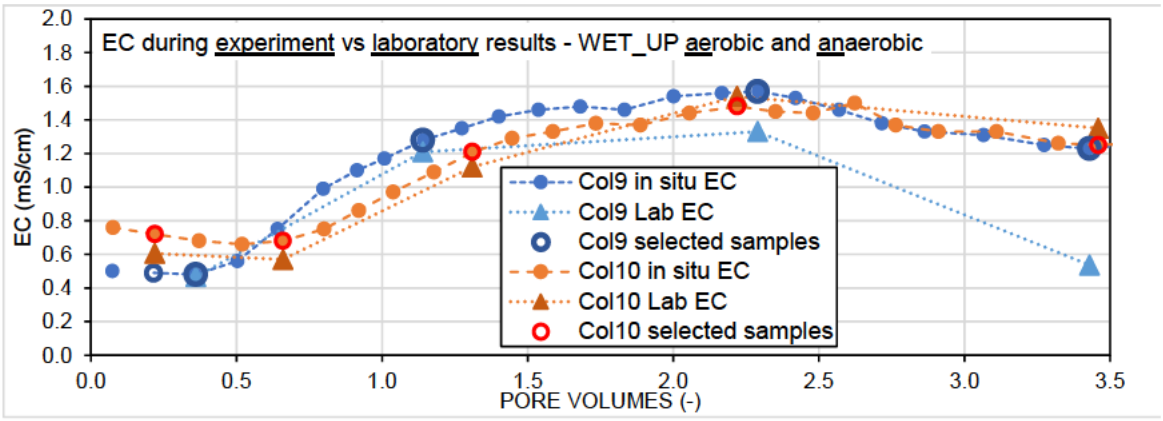


Figure C.2 Graphs of EC measurements vs pV from soil columns leachate samples

Figure C.3 show the concentration of major ions in selected samples from ZnCl column breakthrough curves.

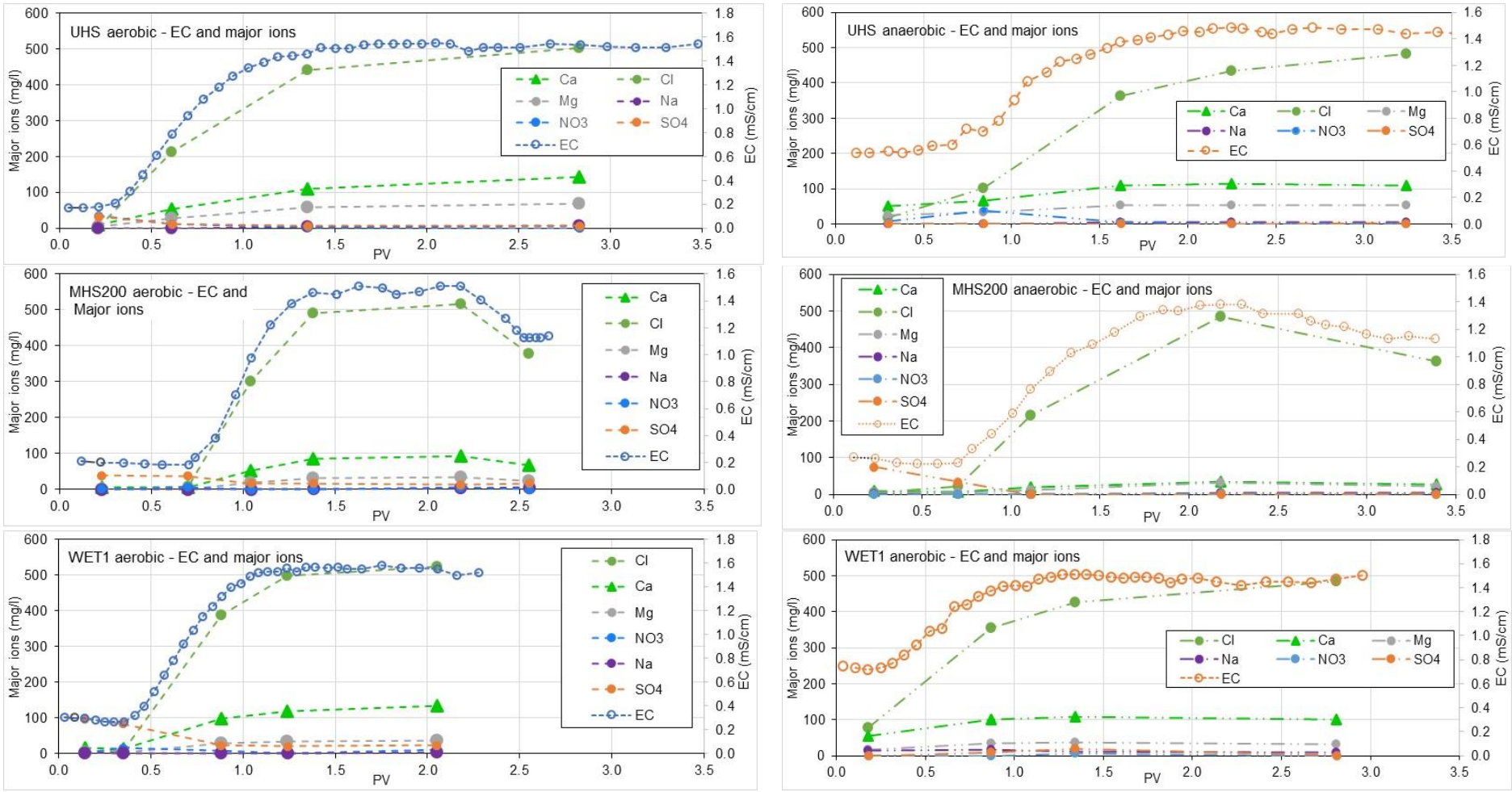


(Continued on next page)

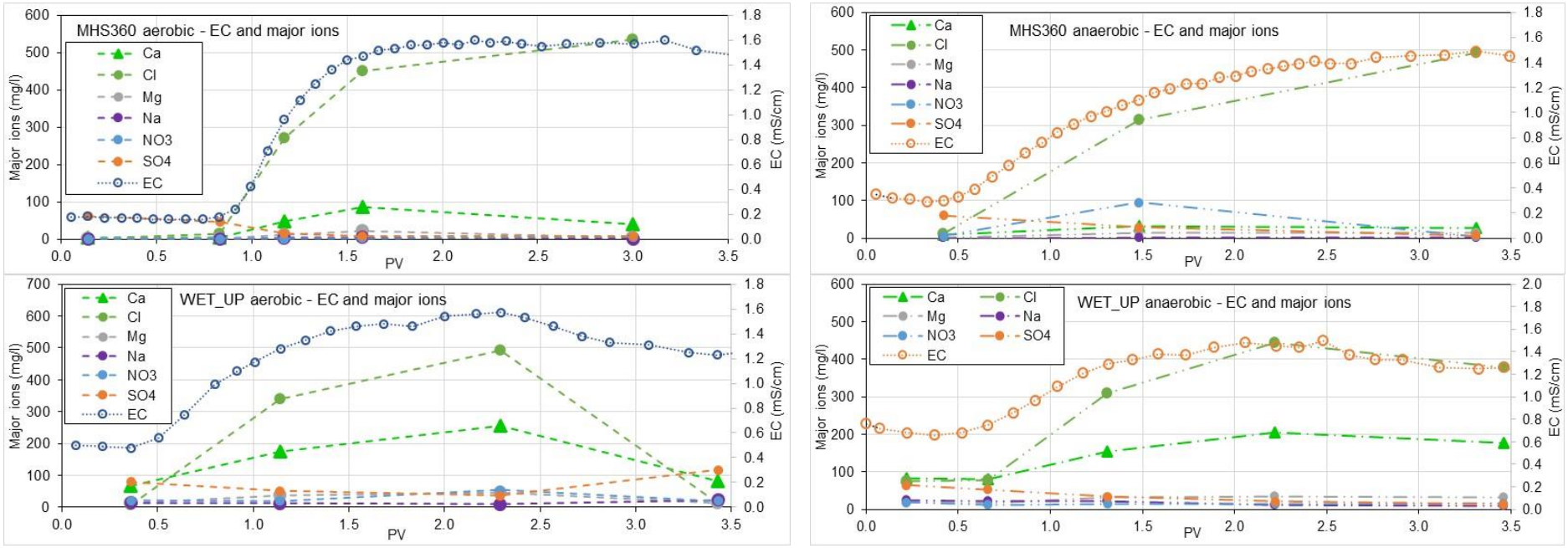


Figure C.3 Graphs of major ions (Ca, Cl, Mg, Na, $NO_3$, $SO_4$) and EC in selected samples from soil column leachate

Figure C.4 graphs the concentrations of selected metals, namely Al, Cu, Mn, Pb, Zn and Fe in selected samples from the ZnCl soil columns experiment leachate.

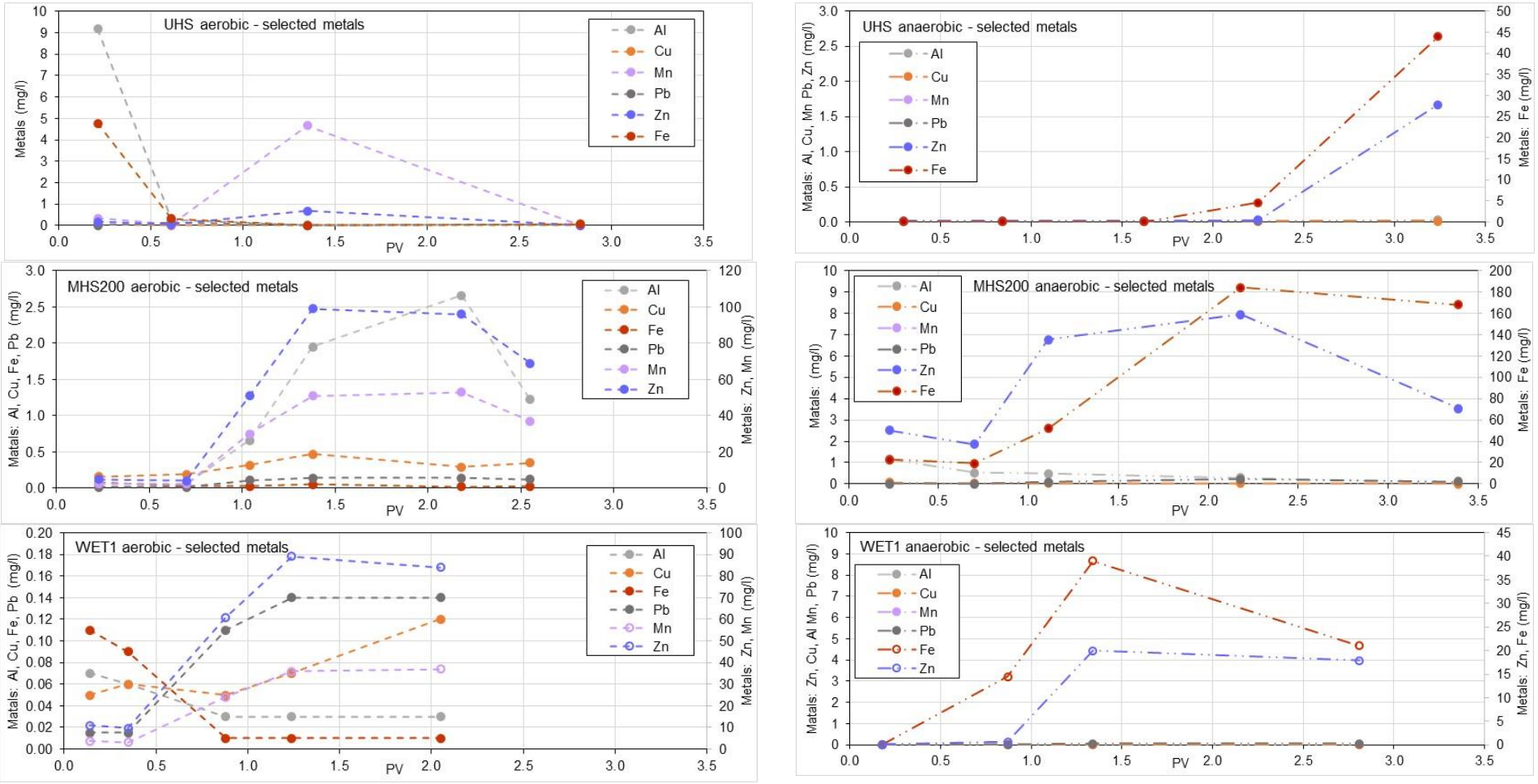

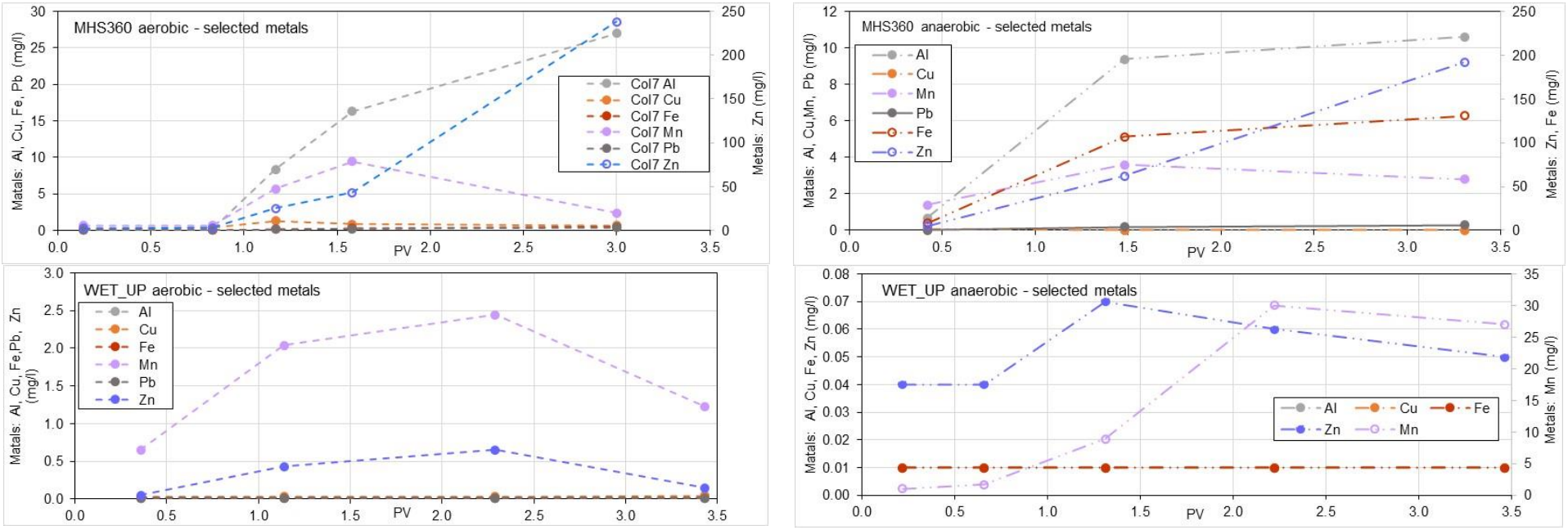


Figure C.4 Graphs of selected metals (Al, Cu, Fe, Mn, Pb, Zn) in soil column leachate samples

# APPENDIX D: NUMERICAL MODEL SETUP

Details of the numerical model setup using Hydrus 2D/3D.

Figure D.1 displays the finite element grid with observation nodes, which were used for calibration purposes to align with existing site data water levels and water chemistry records. The horizontal plane represents 460 m, with the view stretched vertically by a factor of 4. Figure D.2 shows the graphical outputs of the pressure heads of these observation points, together with a table for comparison with the median water levels for each of the associated piezometers.

Domain properties applied to the grid are displayed in Figure D.3, as interpreted from the CSM for the site. Table D.1 provides greater details as to the assigned properties for each of the domains/soils as per the site characterisation and soil transport parameters for zinc.

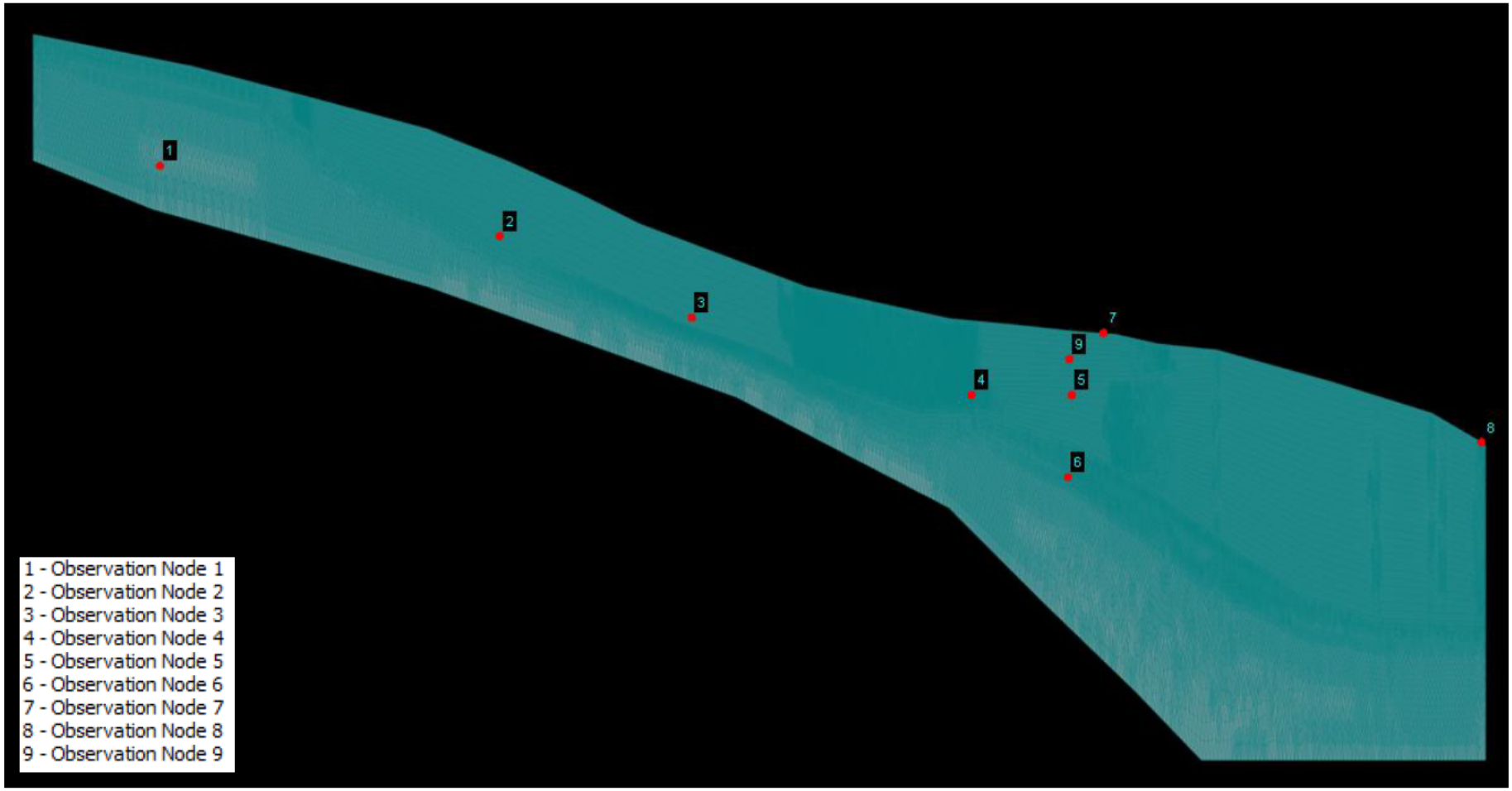


Figure D.1 Hydrus model setup showing finite element grid and location of observation nodes

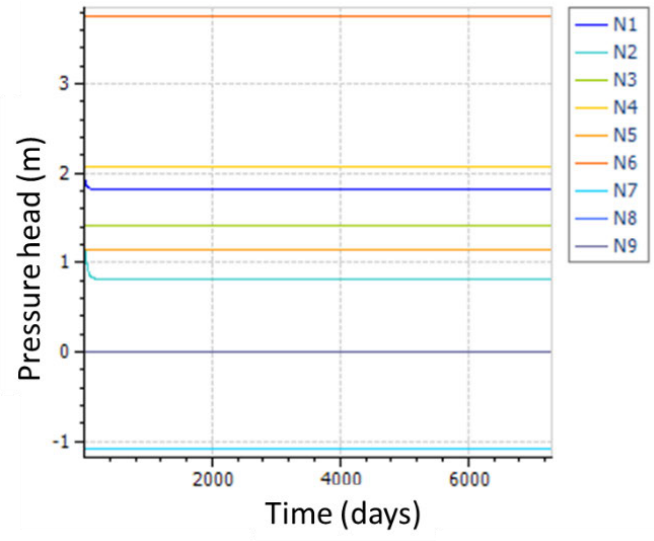


| Observation Node | Modelled pressure head (m)(1) | Measured water level (mbgl)(2) | Modelled water level (mbgl)(3) | Discrepancy (4) |
|---|---|---|---|---|
| Node 1 | 1.8 | 3.1 | 2.3 | 0.8 |
| Node 2 | 0.8 | 1.4 | 1.61 | -0.21 |
| Node 3 | 1.4 | 1 | 0.86 | 0.14 |
| Node 4 | 2.1 | 0.92 | 0.26 | 0.66 |
| Node 5 | 1.17 | 0.47 | 0.89 | -0.42 |
| Node 6 | 3.78 | - | - | contact boundary |
| Node 7 | -1.1 | 0 | 1.1 | Surface seepage |
| Node 8 | | 0 | 0 | Wetland ponded water |
| Node 9 | 0 | 0.1 | 0.9 | -0.8 |

Notes: (1) Data as per stead state mode for each observation node. (2) median water level for actual site piezometer, based on a 12 year spread of water level data. (3) modelled pressure head converted to water level for each monitoring point. This differs from the pressure head as the data is reported as meters below ground level. (4) Refers to the difference between the measured vs the modelled water levels.

Figure D.2 Modelled pressure heads at observation points at stead state conditions, with comparison table showing median water levels at these points.

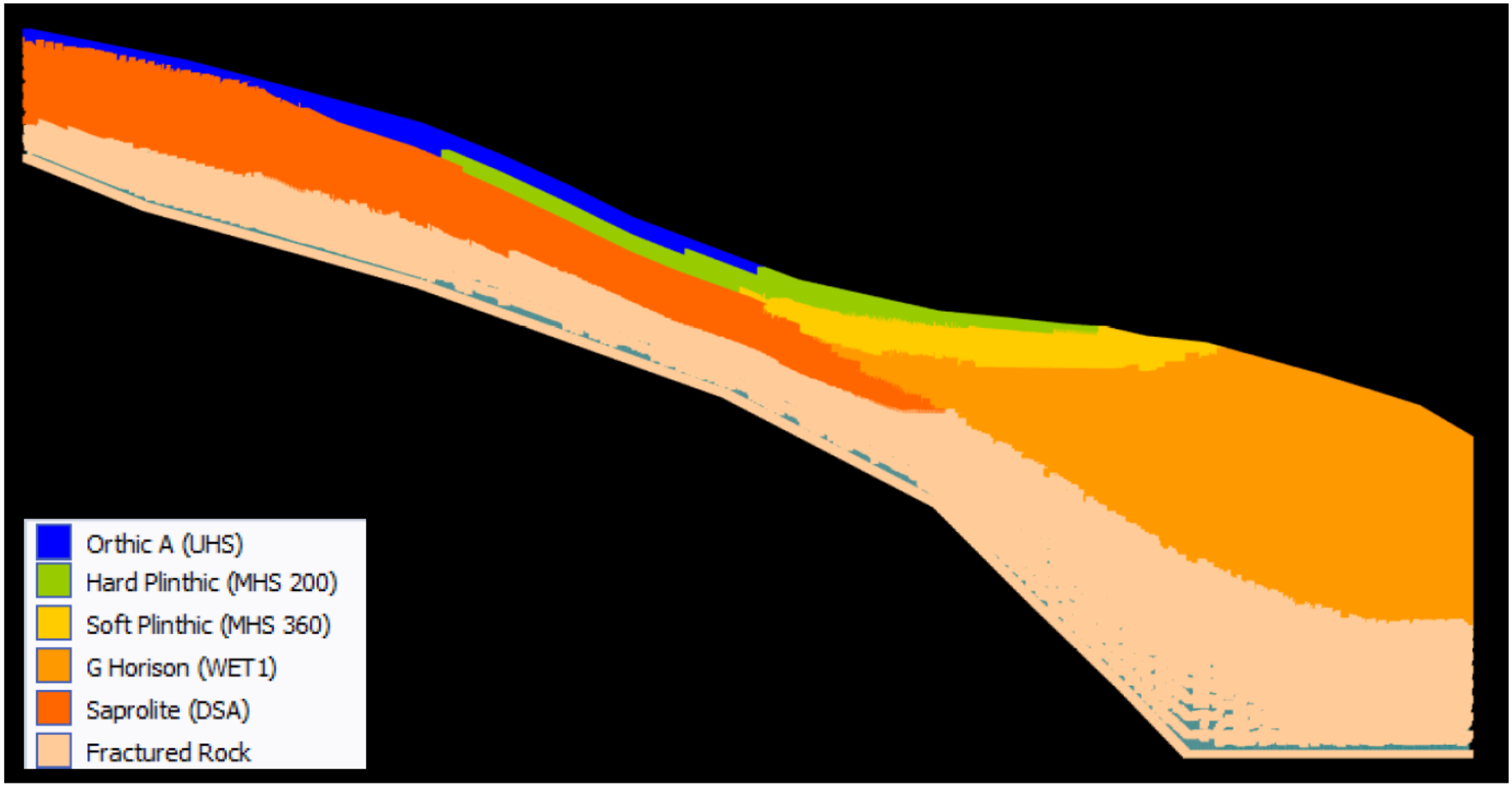


Figure D.3 Hydrus model setup showing distribution of domain properties assigned to finite element grid

Table D.1 Water and solute parameters assigned to domain properties in Hydrus model

| Water flow parameters | Orthic A (UHS) | Hard plinthic (MHS200) | Soft plinthic (MHS360) | G Horizon (WET1) | Saprolite | Fractured rock |
|---|---|---|---|---|---|---|
| Residual water content ($\theta_r$) | 0.00 | 0.215 | 0.205 | 0.414 | 0.067 | 0.067 |
| Saturated water content ($\theta_s$) | 0.524 | 0.425 | 0.424 | 0.728 | 0.460 | 0.460 |
| $\alpha$ | 0.153 | 4.175 | 1.879 | 3.695 | 0.002 | 0.002 |
| n | 2.971 | 2.639 | 2.620 | 3.513 | 1.459 | 1.459 |
| $K_{sat}$ (m/d) | 2.135 | 1.389 | 0.138 | 0.141 | 0.514 | 0.01 |
| Solute transport and reaction parameters | | | | | | |
| Bulk density M/m$^3$ | 1.44 | 1.53 | 1.58 | 0.87 | 1.5 | 1.5 |
| Longitudinal dispersivity (m) | 0.225 | 0.214 | 0.470 | 0.411 | 0.305 | 0.305 |
| Transverse dispersivity (m) | 0.023 | 0.021 | 0.05 | 0.041 | 0.031 | 0.031 |
| $K_d$ | 13.056 | 1.122 | 2.533 | 4.437 | 0 | 0 |